Report No. FHWA-RD-75-51

PB244486

EVALUATION OF FLOOD RISK FACTORS IN THE DESIGN OF HIGHWAY STREAM CROSSINGS

Vol. I. Experimental Determination of Channel Resistance for Large Scale Roughness

M.T. Tseng, G.K. Young, and M.R. Childrey

August 1974
Final Report

This document is available to the public through the National Technical Information Service, Springfield, Virginia 22161

Prepared for

FEDERAL HIGHWAY ADMINISTRATION
Offices of Research & Development
Washington, D.C. 20590

TECHNICAL REPORT STAN[illegible]

1. Report No.	2. Government Accession No.	3. Re[illegible]
FHWA-RD-75-51		PB 244 486

4. Title and Subtitle	5. Report Date
EVALUATION OF FLOOD RISK FACTORS IN THE DESIGN OF HIGHWAY STREAM CROSSINGS. Vol. I. Experimental Determination of Channel Resistance for Large Scale Roughness	August 1974
	6. Performing Organization Code
7. Author(s) M. T. Tseng, G. K. Young, M. R. Childrey	8. Performing Organization Report No. WRE 20810
9. Performing Organization Name and Address Water Resources Engineers 8001 Forbes Place Springfield, Virginia 22151	10. Work Unit No.
	11. Contract or Grant No. DOT-FH-11-7669
12. Sponsoring Agency Name and Address Offices of Research and Development Federal Highway Administration U.S. Department of Transportation Washington, D.C. 20590	13. Type of Report and Period Covered Final Report
	14. Sponsoring Agency Code E0101

15. Supplementary Notes

FHWA Administrator: Gilbert Trainer
FHWA Contract Manager: J. Sterling Jones
FHWA Project Manager: Roy E. Trent
FHWA Implementation Manager: Milo O. Cress

16. Abstract

The overall objective of the study is to develop an engineering systems analysis method to enhance the decision-making process in the design of highway stream crossings. This method applies economic risk techniques as well as standard hydraulic and hydrologic factors in the design of bridge waterways.

Volume I presents the results of experiments to determine channel resistance coefficients from artificial roughness elements representative of heavily vegetated flood plains. These coefficients are used to define the roughness field for use in bridge backwater experiments and calculations reported in Volumes II and III.

The other volumes of this study are:

- II Analysis of Bridge Backwater Experiments
- III Finite Element Model for Bridge Backwater Computation
- IV Economic Risk Analysis for Design of Bridge Waterways
- V Data Report on Spur Dike Experiments

PRICES SUBJECT TO CHANGE

17. Key Words	18. Distribution Statement
Channel Resistance, Large Scale Roughness, Roughness Coefficients	No Restrictions. This document is available to the public through the National Technical Information Service, Springfield, Virginia 22161
19. Security Classif. (of this report) Unclassified	20. Security Classif. (of this page) Unclassified

Form DOT F 1700.7 (8-69)

891-522

ACKNOWLEDGEMENTS

The data collection for this study was undertaken jointly by the personnel of Water Resources Engineers and the Environmental Control Group of the Federal Highway Administration. The study has received a great deal of support and cooperation from the staff of the Environmental Control Group, especially from H. W. Parker, J. M. Normann, R. E. Trent, and J. S. Jones. Mr. Jones performed the final FHWA review of this report. John Matticks, Bert Black and Hugo Bonucelli of WRE assisted the data analysis of this study, Joe Wagner was responsible for the graphics and illustrations, and Phyllis Weiner edited the text.

Preceding page blank

TABLE OF CONTENTS

Preceding page blank

TABLE OF CONTENTS
(Continued)

LIST OF FIGURES

LIST OF TABLES

I. INTRODUCTION

This report is the first in a series of five volumes comprising the final report for the study entitled *Evaluation of Flood Risk Factors in the Design of Highway Stream Crossings*, authorized by the Federal Highway Administration (FHWA) under Contract No. DOT-FH-11-7669. The overall objective of the study is to develop an engineering systems analysis method to enhance the decision-making process in the design of highway stream crossings. This method applies economic risk techniques as well as standard hydraulic and hydrologic factors in the design of bridge waterways.

Volume I presents the results of experiments to determine channel resistance coefficients from artificial roughness elements representative of heavily vegetated flood plains. These coefficients are used to define the roughness field for use in bridge backwater experiments and calculations reported in Volumes II and III.

GOALS AND OBJECTIVES

The major task of this phase of the total study is to determine, by experiment, the configurations of artificial roughness elements that produce in a large flume a resistance sufficiently high to simulate the effect of heavily vegetated flood plains. The degree of artificial roughness produced in the large flume must be relatively high since (1) densely forested flood plains are characterized by high resistance, and (2) the distortion of the scale model requires additional roughness to satisfy the law of dynamic similarity between the model and the prototype.

The conceptual scheme is to treat the roughness elements as acting on the whole body of the flow rather than on their individual flow perimeters in order to obtain a more prototype-like flow behavior. The specific objectives are to:

1. Experimentally determine the resistance coefficients for a series of artificial roughness elements, placed at various distribution patterns, in gradually-varied open channel subcritical flows, and

2. Determine those roughness patterns which produce sufficiently high resistance in a large test flume to simulate the flow characteristics in heavily vegetated flood plains.

BACKGROUND

Recent field verification of current methods for backwater prediction has demonstrated that existing methods tend to underpredict the magnitude of backwater in many cases, particularly when bridges extend over wide valleys with heavily vegetated flood plains. In recognition of this problem, the FHWA directed that one of the principal objectives of this study would be to develop a more accurate method to predict backwater levels. The method to be developed would include the following factors, which have generally not been previously applied to the problem:

1. Use of realistic resistance elements to simulate vegetated flood plains,
2. Analysis of the effect on backwater of large scale roughness and flow characteristics over wide flood plains,
3. Effect of width-depth ratio on bridge backwater for wide channels on flood plains, and
4. Effect of dynamic similitude between model and prototype.

The only means of considering all these factors in backwater prediction would be to conduct field measurements of water surface elevation at flood stage. However, in light of the impracticality of such a program in the time and budget available, the strategy adopted in this study was to:

1. Use to the maximum extent possible all available information and data related to the bridge backwater problem,
2. Develop otherwise unavailable data from hydraulic experiments in the laboratory to determine flow characteristics in the vicinity of the bridge opening, and
3. Use all data acquired in (1) and (2) to develop a two-dimensional mathematical model to simulate flood plain flow and bridge backwater. This computer model is then verified as far as possible by field data obtained from state highway agencies.

In other words, the WRE approach was to maximize the use of existing technology to model, both physically and mathematically, the prototype behavior in such a way as to minimize the uncertainty associated with bridge waterway hydraulics. It is not only uneconomical but practically impossible to physically model the entire river reach under the influence of bridge backwater, mainly due to the wide variation in the width-depth ratio existing in natural streams. A physical model, however, may be used with confidence to study the flow patterns adjacent to the bridge opening. Away from the opening, the flow conditions may vary markedly from site to site, depending upon the variations of roughness distribution and the topographic features of the stream. It is this area which the physical model is not able to reproduce accurately and which must be simulated by other means, in our case by a finite element model. The use of this computer model may be further expanded once the model is verified or calibrated.

In the prototype condition of densely forested flood plains, the energy losses of the flow are due to bed roughness, bank roughness and the resistance of bushes, plants and trees in the flood plains. These roughness elements either are submerged or extend up through the free surface during floods. Their distribution is invariably random, making it impracticable to scale size and distribution patterns in the model flume. Nevertheless, these roughness components produce one common effect: energy dissipation of the flow. This effect is the focal point of the study.

Traditionally, roughness element studies have been conducted with bottom roughness elements that are completely submerged. The bridge backwater problem, on the other hand, is influenced by trees and brush that penetrate the water surface and are spaced randomly. It was not considered feasible to use model trees for the experiment, so attention concentrates on achieving various levels of channel resistance and relating that resistance to statistical representations of spacing parameters where roughness elements are spaced randomly as well as on a regular pattern.

The hydraulic experiments for this study were conducted in a 22-foot wide flume with large scale roughness to simulate the densely vegetated flood plains in the prototype. The roughness fields to be installed in the large flume were determined by performing preliminary testing and screening experiments in a 9-inch wide flume. The small flume experiments, which are the subject of this volume, isolated the effects of various shapes and densities of roughness patterns.

Altogether there were seven different shapes of roughness element tested in this study. Three types of element distribution, random, rectangular and staggered (or diamond), were tested for flow rates ranging from 0.1 to 0.6 cfs. For each roughness element shape and pattern, the elements were attached to the channel bed and were of sufficient length to protrude through the water surface. The density (number of elements per square foot of the channel bed) of the roughness elements was determined for each configuration. All tests were performed for a steady, nonuniform flow condition. Resistance coefficients for each roughness configuration were determined from the test data.

LITERATURE REVIEW

Although research on the flow of water in open channels with finite artificial roughness was conducted by Bazin (1) between 1855 and 1860, the rigorous definition of the flow phenomena involving boundary roughness was not possible until the advent of Prandtl's boundary layer theory in 1904 (2). Since then the work of Von Karman (3) and Prandtl and the experimental measurements of Nikuradse (4) have contributed to the development of rational formulas for hydraulic resistance in pipe flow and an artificial standard for sand grain roughness. In all of these investigations, the logarithmic law of velocity distribution was assumed.

Keulegan (1) and others have successfully applied the Nikuradse roughness standard to open channels in describing grain-type roughness in wide open channels. However, it has been found inadequate for describing certain other types of roughness, such as dune and ripple patterns on the beds of alluvial channels, in which relative spacing as well as relative size of the roughness elements is an important boundary characteristic.

Sayre and Albertson (5) have conducted a series of experiments to determine the effect of roughness spacing on open channel flow. These experiments were performed in an eight-foot wide by 72-foot long tilting flume. Roughness elements consisting of sheet metal baffles measuring six inches wide and 1-1/2 inches in height were placed in symmetric patterns on the bed of the flume at various longitudinal and transverse spacings. Experiments were performed over a range of discharge, slope and roughness densities; the normal depth varied between 0.254 and 0.983 feet. Thus, the ratio of element height to water depth varied from 0.13 to 0.5.

Test data were analyzed in terms of the Von Karman-Prandtl concepts of turbulent flow near a rough boundary. The data are described by the equations:

$$\frac{C}{\sqrt{g}} = 6.06 \log \frac{y_n}{t} + C_1 \tag{1}$$

and

$$\frac{C}{\sqrt{g}} = 6.06 \log \frac{y_n}{\chi} \tag{2}$$

where C = Chézy coefficient,

y_n = normal depth,

t = height of roughness element,

C_1 = a constant, a function of the longitudinal and transverse roughness spacing, and

χ = a roughness parameter dependent on the size, shape and spacing of the roughness elements.

From an analysis of the experimental data, it is concluded that:

1. Equation 1 is considerably more accurate than the Manning formula over the range of roughness and flow tested;

2. The roughness density may be adequately defined as the ratio of (a) the combined area of all roughness elements projected perpendicularly to the direction of flow to (b) the total area of the channel bed; and

3. The general resistance diagram, in which the resistance function is plotted against the Reynolds number and the Colebrook-White type transition function, is applicable to problems of uniform flow in wide, rigid-boundary open channels.

Subsequent experiments were made by Robinson and Albertson (6) in which the size of geometrically similar roughness elements was varied, but the ratios of longitudinal and transverse spacing to element height were held constant. For a particular roughness pattern, they demonstrated that the Chézy resistance function depends only on the relative roughness (ratio of flow depth to element height), assuming rough boundary conditions.

Einstein and Banks (7) studied the composite resistance of different types of roughness opposing the flow of water through an open channel, using the Salinas River as a case study. In the Salinas River vegetation and sand bars exert resistance to the flow. In this case the total force opposing the flow consists of:

1. The resistance caused by the particles composing the river bed and sides,

2. The geometrical or form resistance of the bars; and

3. The resistance caused by the vegetation.

In their laboratory simulation, Einstein and Banks studied four types of resistance:

1. Blocks without offset and without pegs,

2. Blocks without block offset, combined with various peg densities and patterns,

3. Blocks with alternate blocks offset, without pegs, and

4. Blocks with alternate blocks offset, combined with various peg densities and patterns.

Type 1 was set as a standard level of resistance for the channel bottom. Comparison of Types 1 and 2 showed the influence of pegs, and comparison of Types 1 and 3 showed that of the offset. Results of experiments with Type 4 permit comparison of the sum of the individual resistances with their composite resistance. The ratio of element height to flow depth is in the range of 0.06 to 0.09.

Within the range of the variables tested, the study showed that the total resistance exerted by combined types of roughness is equal to the sum of the resistance forces exerted by each type individually, as long as the component roughness elements do not have any mutual interference.

Information on resistance coefficients in highly vegetated open channel flows has been particularly lacking. One way of estimating resistance factors on such flow regimes is from the high water marks of historic floods. High water marks, however, are not generally available along flood plains for which water surface profiles must be computed.

A report by Barnes (8) gives roughness coefficients for 50 stream channels. For each field site color photographs and descriptive data are presented. The report provides a general idea of the appearance, geometry and roughness characteristics of these channels, thus improving the engineer's ability to select roughness coefficients for other channels.

Barnes used the Manning equation as the basis for computing the reach properties and roughness coefficients. Although the 50 sites cover a wide range of hydraulic conditions from the boulder-strewn mountain streams of the western conterminous United States to the heavily vegetated flat-sloped streams of the southern conterminous United States, all computations but one are for the flood discharges within the channel banks. At that one particular site, Rooling Fork at Boston, Kentucky, the n value is reported to be 0.046 in the main channel and 0.097 in the right overflow channel.

Chow (9) also gives roughness data on a number of typical channels including natural waterways having n value as high as 0.150.

Herbich and Schultis (10) conducted laboratory experiments to determine roughness coefficients for critical concrete roughness elements in subcritical open channel flows. Two sizes of elements, 3.75- and 6-inch, were tested for both submerged and protruding elements. Tests were performed for roughness elements placed in symmetric and random distribution of uniform and nonuniform size. The essential purpose of the study was to obtain the roughness coefficients in streams flowing through cobbles and boulders, with particular attention to the reach of the Susquehanna River near Harrisburg, Pennsylvania. The study gives (1) the results of Manning's roughness coefficient n as a function of the Reynolds number and (2) a roughness parameter relating projected area of roughness elements in the direction of mean flow to the horizontal area of the channel. This roughness parameter is, in fact, a factor that describes the size and spacing of roughness elements. A precise definition of this roughness parameter is very important.

Hsieh (11) conducted experiments using circular cylindrical roughness elements one inch in diameter and two feet in length to determine the effect of spacing and relative depth of flow on the resistance coefficients of circular piers. Results of experiments with subcritical flow conditions indicate that:

1. Spacing and relative depth of flow significantly influence the resistance coefficients,

2. Wave drag is very important under relatively shallow conditions, and

3. The surface effect is relatively small at low Froude number, thus yielding resistance coefficients that approach those of two-dimensional flow.

II. THEORETICAL BASIS FOR ANALYSIS OF LARGE SCALE ROUGHNESS

ONE-DIMENSIONAL OPEN CHANNEL FLOW IN LARGE SCALE ROUGHNESS

Consider an open channel of rectangular cross section, in which large roughness elements are placed on the bottom of the channel. The flow in the channel is steady, nonuniform, as shown in Figure 1. It is assumed that the slope of the bottom and the water surface area are both small, so that gradually-varied flow profile prevails. The mean total head at any cross section is expressed as:

$$H = \frac{V^2}{2g} + y + Z_o \tag{3}$$

where H = total head,
V = mean velocity of flow through the section,
y = depth of flow, and
Z_o = elevation of the channel floor.

A single differentiation with respect to x, which is the distance in the direction of flow, yields

$$\frac{dH}{dx} = \frac{d}{dx}\left(\frac{V^2}{2g}\right) + \frac{dy}{dx} + \frac{dZ_o}{dx} \tag{4}$$

In Equation 4, $\frac{dH}{dx}$ represents the rate of energy loss in the flow direction and is expressed by $-S_f$, whereas $dZ_o/dx = -S_o$ is the slope of the channel.

When the flow is turbulent, the energy dissipation of the flow is through the mechanism of surface resistance, form resistance and wave

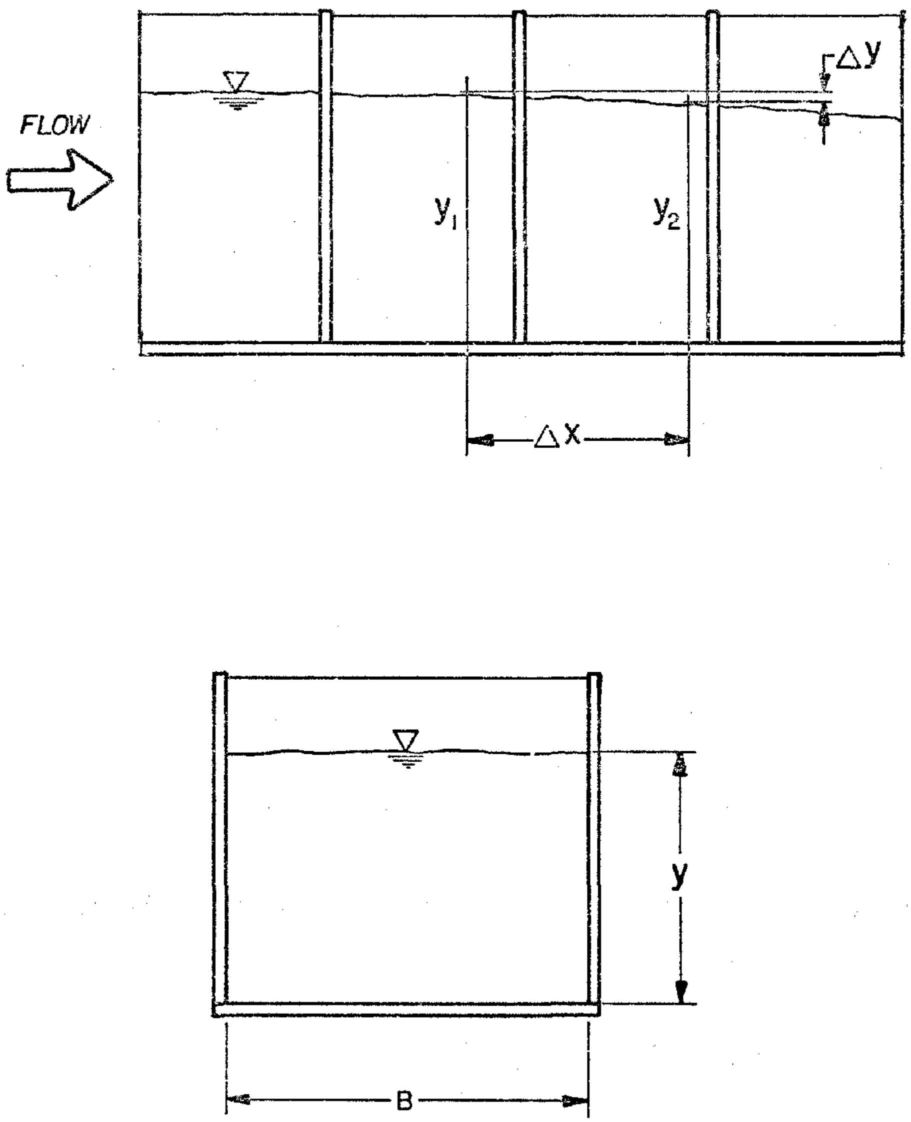

Figure 1. Definition Sketch of the Test Flume

resistance. In a reach length, Δx, the resistance for each type is

Surface resistance $$F_s = \frac{f}{4} \frac{\rho V^2}{2} P \, \Delta x \tag{5}$$

Form resistance $$F_f = C_d \, N \, b \, y \frac{\rho V^2}{2} \tag{6}$$

Wave resistance $$F_w = \phi \, (V^2) \tag{7}$$

where f = Darcy-Weisbach resistance coefficient,
P = wetted perimeter,
ρ = fluid density,
V = mean velocity in x direction,
C_d = drag coefficient for each roughness element,
N = number of elements in the flume area $B \, \Delta x$,
B = width of flume,
b = width of element, and
y = depth.

In steady, nonuniform flow the equation of motion for the elementary volume can be expressed as

$$- \gamma \, B \, y \, \Delta y - \Sigma F = \rho \, B \, y \, \Delta x \, V \frac{dV}{dx} \tag{8}$$

where $\Sigma F = F_s + F_f + F_w$ and
γ = specific weight.

Integration of Equation 8 with respect to x yields the one-dimensional momentum equation

$$\Sigma F = \frac{B}{2} \gamma \, (y_1{}^2 - y_2{}^2) + \rho Q \, (V_1 - V_2) \tag{9}$$

where $$Q = B \, y \, V \tag{10}$$

Equation 8 can be rearranged to yield

$$- \gamma \; B \; y \; \Delta x \left[\frac{\Delta y}{\Delta x} + \frac{V}{g}\frac{dV}{dx}\right] = \Sigma F \tag{11}$$

or

$$- \gamma \; B \; y \; \Delta x \frac{d}{dx}\left(y + \frac{V^2}{2g}\right) = \Sigma F \tag{12}$$

But $$\frac{d}{dx}\left(y + \frac{V^2}{2g}\right) = \frac{dH}{dx} = -S_f$$

Hence $$\gamma \; B \; y \; \Delta x \; S_f = \Sigma F \tag{13}$$

which gives $$S_f = \frac{1}{\gamma \; y}\left(\frac{\Sigma F}{B \; \Delta x}\right) \tag{14}$$

The form of Equation 14 is rather interesting. The expression $\frac{\Sigma F}{B \; \Delta x}$ represents the amount of force expended per unit area of channel bottom, which, in a sense, is the shear stress. This can be demonstrated by letting

$$\Sigma F = \frac{f}{4}\frac{\rho V^2}{2} \; P \; \Delta x \tag{15}$$

which is the case where the boundary resistance plays the dominant role in energy dissipation. Substitution of Equation 15 in Equation 14 yields

$$S_f = \frac{1}{\gamma \; y}\frac{f}{4}\frac{\rho V^2}{2}\frac{P}{B} = \frac{f}{4R}\frac{V^2}{2g} \tag{16}$$

or $$f = \frac{4R \; S_f}{V^2/2g} \tag{17}$$

where R is the hydraulic radius. Equation 17 is the familiar form of resistance equation, where the boundary shear stress is the source of energy dissipation.

If the surface resistance (boundary shear) is small in comparison with form resistance, and the wave resistance and the flow turbulence can be neglected, then Equation 14 takes the form of

$$\gamma \; B \; y \; \Delta x \; S_f = N \; C_d \; b \; y \; \frac{\rho V^2}{2} \tag{18}$$

or

$$\frac{\Sigma F}{B \; x} = \frac{N \; C_d \; b \; y}{B \; \Delta x} \frac{\rho V^2}{2} \tag{19}$$

Equation 19 can be generalized to yield an expression

$$\tau_d = C_f \frac{V^2}{2} \tag{20}$$

where τ_d = equivalent shear stress due to drag, and
C_f = a loss coefficient.

From Equations 19 and 20 it is seen that

$$C_f = \frac{N \; C_d \; b \; y}{B \; \Delta x} \tag{21}$$

In Equation 21 the expression $(N \; b \; y)$ is the total projected area of the roughness elements under water, and $(B \; \Delta x)$ is the area of channel bed in the reach Δx. The ratio of these two is defined as the concentration of roughness elements. Let σ denote the roughness concentration of the channel, then

$$\sigma = \frac{N \; b \; y}{B \; \Delta x} \tag{22}$$

and

$$C_f = \sigma \; C_d$$

Equation 20 then becomes

$$\tau_d = \sigma \; C_d \; \frac{\rho V^2}{2} \tag{23}$$

Since $$\gamma \; y \; S_f = \frac{\Sigma F}{B \; \Delta x}$$

then $$\gamma \; y \; S_f = \sigma \; C_d \; \frac{\rho V^2}{2}$$

or $$C_d = \frac{S_f \; y}{\sigma \; \frac{V^2}{2g}} \tag{24}$$

It is conceivable that under prototype conditions the overall channel resistance is composed of many types of resistance. Formulation of a general expression for each type of resistance is convenient for computational purposes. Since each type of resistance is proportional to the dynamic pressure term, $\rho V^2/2$, of the mean flow and the area of the channel reach, it is reasonable to express the total resistance force as

$$\Sigma F = (C_s + C_f + C_w) \; \frac{\rho V^2}{2} \; B \; \Delta x \tag{25}$$

where C_s is the loss coefficient due to surface resistance, C_f is that due to form drag, and C_w that from surface waves. Among the three loss coefficients, C_w is difficult to define. We therefore incorporate surface wave resistance into the surface and form resistances. Equation 25 thus becomes

$$\Sigma F = (C_s + C_f) \; \frac{\rho V^2}{2} \; B \; \Delta x \tag{26}$$

In Equation 26

$$C_s = \frac{f}{4} \, \frac{P}{B} \tag{27}$$

and $$C_f = \frac{N \; C_d \; b \; y}{B \; \Delta x} \tag{21}$$

Substituting Equations 26, 27 and 21 into Equation 14, we obtain the following expression:

$$4R\ S_f = \frac{V^2}{2g}\left(f + C_d\ \frac{4N\ b\ y}{P\ \Delta x}\right) \qquad (28)$$

If we let $$f_e = f + C_d\ \frac{4N\ b\ y}{P\ \Delta x} \qquad (29)$$

then Equation 28 becomes

$$f_e = \frac{4R\ S_f}{V^2/2g} \qquad (30)$$

Note that Equation 30 resembles Equation 17, the expression for the Darcy-Weisbach resistance coefficient. In the present derivation, f_e may be considered a modified friction factor from the Darcy-Weisbach f. The primary difference between f and f_e is that f represents a resistance coefficient characterized by the boundary shear stress. In the case of submerged elements the value of f can usually be obtained through the integration of the Karman-Prandtl equation for logarithmic velocity distribution to yield

$$\frac{1}{\sqrt{f}} = C_1\ \log \frac{y_n}{k} + C_2 \qquad (31)$$

where C_1 = turbulence coefficient that usually has a value of approximately 2,

C_2 = constant, which is a function of the roughness type, pattern and spacing,

y_n = normal depth, and

k = roughness size.

In the case of flows passing through protruding roughness elements, the overall resistance to the flow is the combined effect of shear stress along the channel bottom and side walls plus the energy dissipation resulting from the eddy formation behind the roughness elements.

A theoretical treatment of this particular type of resistance field is not available in the literature. The difficulty arises from the lack of data for velocity distribution and complex flow characteristics behind the roughness elements. As a result, studies of this type of problem generally rely on physical measurement.

DIMENSIONAL ANALYSIS

Equation 13 can be rearranged to yield

$$S_f = \frac{V}{\gamma Q} \frac{dF}{dx} \tag{32}$$

Thus $\frac{dF}{dx}$ represents the local resisting force per unit length of channel.

In steady nonuniform flow, $\frac{dF}{dx}$ is a function of the following independent variables (see Figure 2):

- the mean depth, d, and the mean velocity, V, at a given section;
- the parameters of roughness elements, b, t, k, L, L_1, ℓ, and a roughness element shape factor, ξ;
- a cross sectional shape factor, η, another factor, θ, describing the channel profile, and another factor, ζ, describing the channel plan; and
- the fluid density, ρ, specific weight, γ, and viscosity, μ.

In the case of the nine-inch test flume used in this study, the channel shape is rectangular, the bottom is horizontal and the width is constant (9 inches); hence the factors η, θ, and ζ may be eliminated. Replacing d with R, the hydraulic radius, we obtain a functional expression

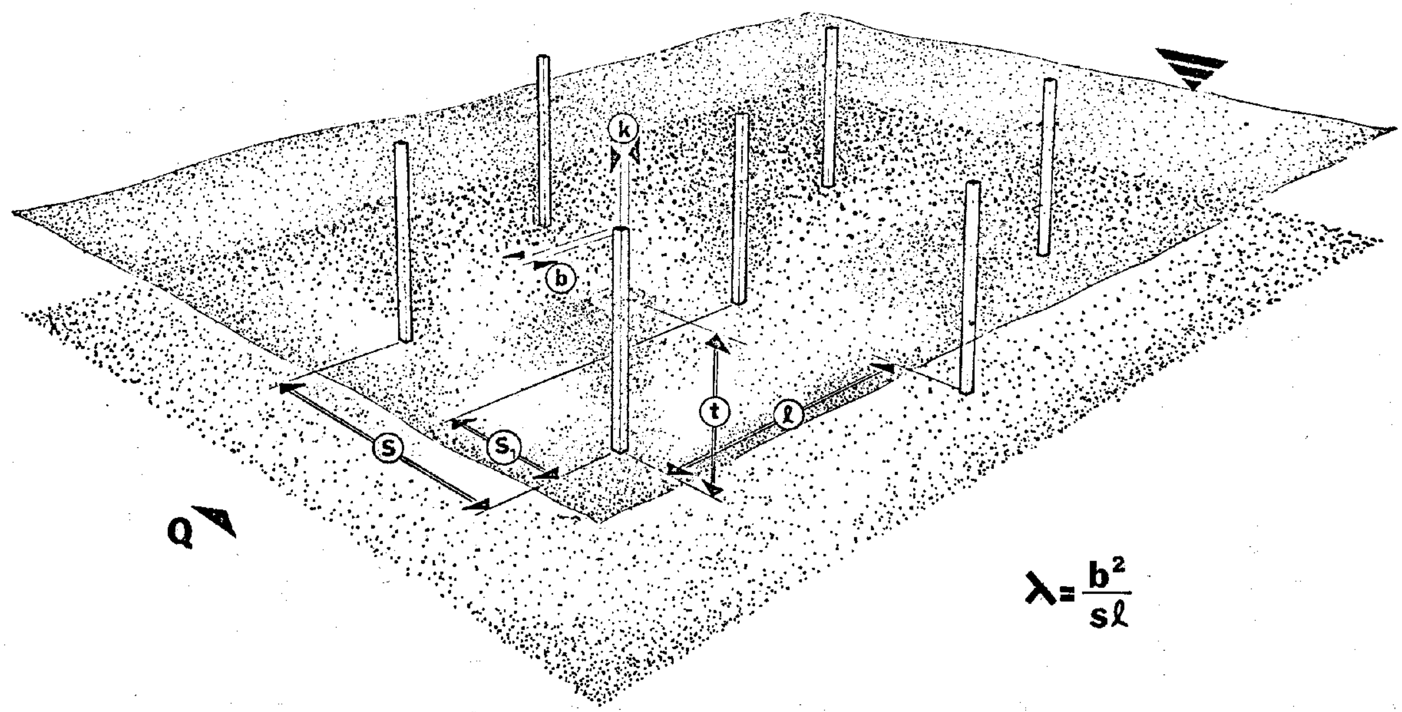

Figure 2. Definition of Roughness Parameters

$$S_f = \phi_1 \ (R, V, b, t, k, L, L_1, \ell, \xi, \rho, \gamma, \mu) \qquad (33)$$

If the hydraulic radius, velocity and density are chosen to be the repeating parameters, the following nondimensional groups will result:

$$f = \phi_2 \ (\mathbf{F}, \mathbf{R}, \frac{b}{R}, \frac{t}{R}, \frac{k}{b}, \frac{L}{b}, \frac{L_1}{s}, \frac{\ell}{b}, \xi) \qquad (34)$$

where
$$f = \frac{4R \ S_f}{V^2/2g}$$

$$\mathbf{F} = \frac{V}{\sqrt{gR}}$$

$$\mathbf{R} = \frac{4V \ R}{\nu} \quad \text{and}$$

$$\nu = \frac{\mu}{\rho}$$

In Equation 34 the term $\frac{k}{b}$ is a parameter describing the aspect ratio of an individual roughness element. For all the types of roughness elements tested, there is a single value of $\frac{k}{b}$ for each type of element; thus, the relationship of f to $\frac{k}{b}$ cannot be determined for each element geometry. The term L_1/L is a parameter describing the offset (or eccentricity) of the elements in the transverse direction. There are three major types of geometric patterns that have been tested. These patterns are the random, rectangular and diamond placement described in Chapter I. It is not possible to determine the value of L_1/L in random patterns. Furthermore, the variation of L_1/L in the rectangular and diamond patterns was not sufficiently wide to examine the effect of L_1/L on f. Dropping $\frac{k}{b}$ and L_1/L, Equation 34 becomes

$$f = \phi_3 \ (\mathbf{F}, \mathbf{R}, \frac{b}{R}, \frac{t}{R}, \frac{L}{b}, \frac{\ell}{b}, \xi) \qquad (35)$$

In Equation 35 the combination of $\frac{b}{R}$, $\frac{L}{b}$ and $\frac{\ell}{b}$ is defined as the concentration of the roughness elements, that is

$$\sigma = \frac{\frac{R}{b}}{\frac{\ell}{b}\frac{L}{b}} = \frac{bR}{L\ell} = \frac{by}{L\ell} \qquad \text{for } R = y \tag{36}$$ [1]

Combining these three terms, Equation 35 becomes

$$f = \phi_4 \left(\mathbf{F}, \mathbf{R}, \frac{t}{R}, \sigma, \xi \right) \tag{37}$$

In the case of flow through protruding roughness elements, the value $\frac{t}{R}$ is a measure of width-depth ratio as can be shown in the following:

$$\frac{t}{R} = \frac{d}{\frac{Bd}{B + 2d}} = \frac{B + 2d}{B} = 1 + 2\frac{d}{B} \tag{38}$$

Equation 37 may therefore be expressed as

$$f = \phi_5 \left(\mathbf{F}, \mathbf{R}, \frac{d}{B}, \sigma, \xi \right) \tag{39}$$

Equation 39 consists of both the Froude number and the Reynolds number. The surface and the form resistances are governed by the roughness elements, boundary characteristics, and the Reynolds number, whereas the wave resistance is a function of the Froude number. The relative significance of $\mathbf{F}$ and $\mathbf{R}$ is mainly determined by the concentration of the roughness elements. When the concentration is high, energy loss of the flow is mainly from form and wave resistance. In cases where $\frac{b}{L}$ approaches unity, the flow is blocked out until the depth upstream is changed. If $\frac{k}{\ell}$ approaches unity, the flow is confined in narrow channels, and assumes the characteristics of slot flow. The Froude number is likely to be the dominant factor for high roughness element concentrations. The Reynolds number may be used to define two characteristics of the flow viscosity: as it relates to bed geometry and to channel obstacles. The effect of these two factors on the flow resistance under the present test conditions is assumed to be minimal because of the flow separation effect at the upstream edges of the obstacles.

[1]For nonsymmetrical distribution patterns, such as the random pattern, Equation 22 is used to determine the value of σ.

In medium to low concentrations, the roughness elements have the effect of isolated obstacles, causing wake interference, and the effect of surface, waves and form resistance on the total flow resistance may be of comparable importance in those cases where F and R are both significant. The relationship of f to F and R is further discussed in Chapter IV.

III. EXPERIMENTAL EQUIPMENT AND PROCEDURE

EQUIPMENT SETUP

The hydraulic models used in this study were constructed and operated on the second floor of the old Bureau of Standards Building 9, located at 4200 Connecticut Avenue, N.W., Washington, D. C. The small flume used for the channel roughness experiments was rectangular and horizontal, nine inches in width, 21-5/8 inches in depth and 198 feet in length, with a wooden floor and plexiglass sides.

The roughness elements were placed along a 50-foot section of the flume, referred to as the test reach. Flow was supplied by either the fire line from the municipal water supply system or a constant head tank above the flume, depending upon the amount of discharge to be tested. A schematic diagram of the setup is shown in Figure 3. The fire line was used only when maximum flow was desired. In most cases the water from the fire line was discharged into a distribution tank and pumped from there into the flume to avoid flow fluctuations which may occur in the fire line. In later experiments, the constant head tank was used exclusively. Flow rates were varied by adjusting the valve opening of the water supply line and measured by diverting the water from the flume into a weighing tank and recording the change in weight over time.

Point gages were used to measure the water surface profile. The point gages were mounted on top of the flume at eight-foot intervals along the upstream portion of the test reach and at four-foot intervals along the downstream portion of the test reach. In order to avoid the marked variation in water surfaces caused by the upstream and downstream transitional

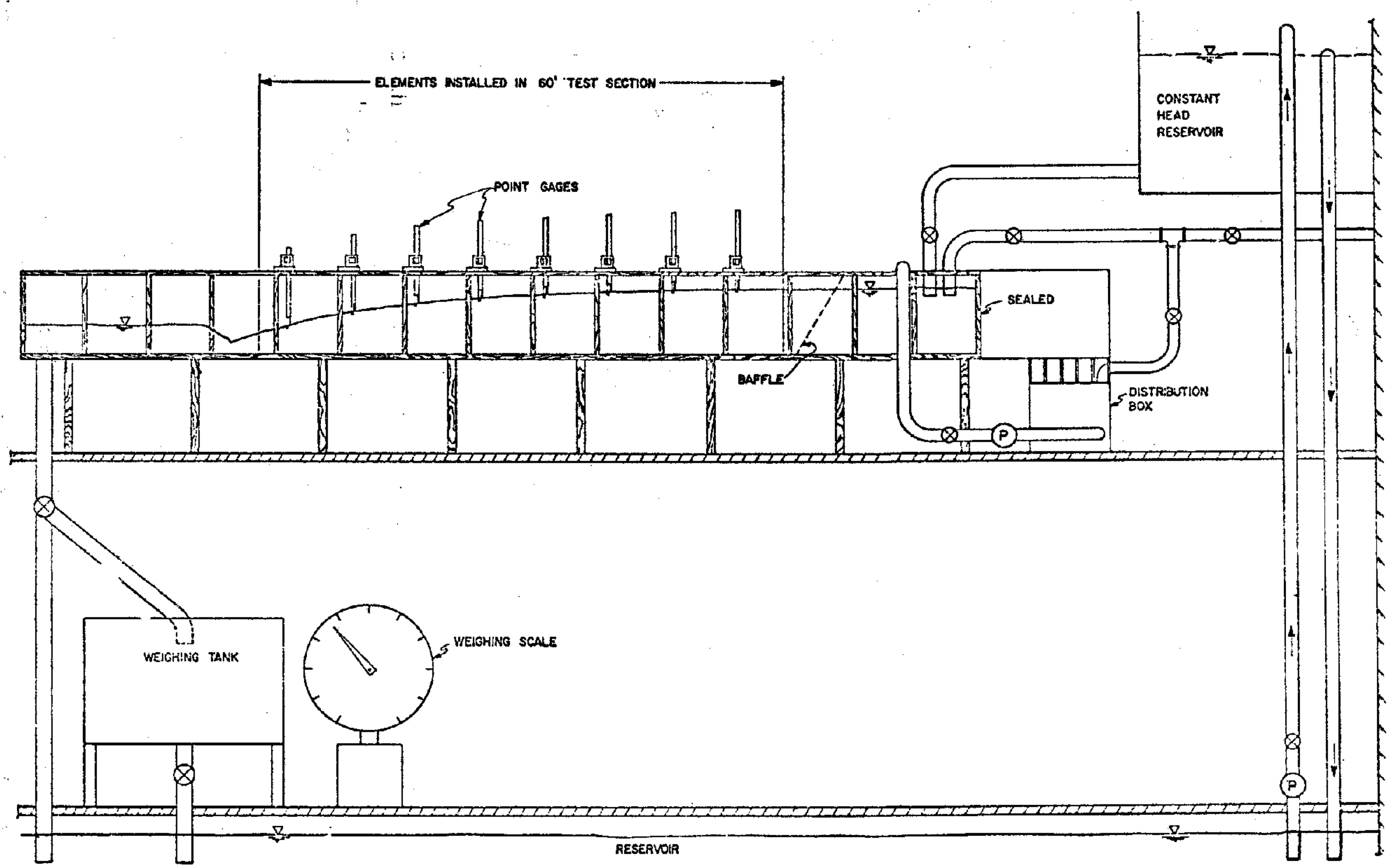

Figure 3. Experimental Setup for Nine-Inch Flume

zones, the point gages were mounted no closer than eight feet from either end of the test section. For most of the experiments, seven point gages were used.

Before testing was begun a common datum, to which all point gages were referenced, was established in the test reach. The flume was first filled with several inches of water and allowed to become still for water surface readings at each point gage. During the testing all surface readings were referred to this datum.

In order to obtain the depth of flow at each section, point gage readings were also taken on the bottom of the flume. Figure 4 shows the elements of the Ott Point Gage and the details of depth measurements. To establish a convention, the flat tip is called the "rod" and the pointed tip the "point." When the point contacts the water surface, an electrical circuit is completed with the rod which is submerged, and the electric indicator turns white. All water surface readings are taken using the point, but it is obvious that the bottom reading cannot be taken in this manner since the rod extends lower than the point. The bottom readings were, therefore, taken using the rod and the resulting depth corrected by adding on the distance from the tip of the point to the tip of the rod. This distance is called the "gage constant" for that point gage. The two readings necessary to obtain this gage constant are illustrated in Figures 4B and 4C. The reading in which the rod contacts the still water surface is called the still rod and the reading in which the point contacts the still water surface is called the still point. The reading in which the rod contacts the flume bottom is called the bottom rod, as shown in Figure 4D.

A dual reference system was used when the point gages were installed along the test reach. Two identification numbers were assigned to each gage, the first indicating position and the second the specific point gage (e.g., 1-3, position 1, gage 3). This system was necessary because the point gages were periodically dismounted for maintenance.

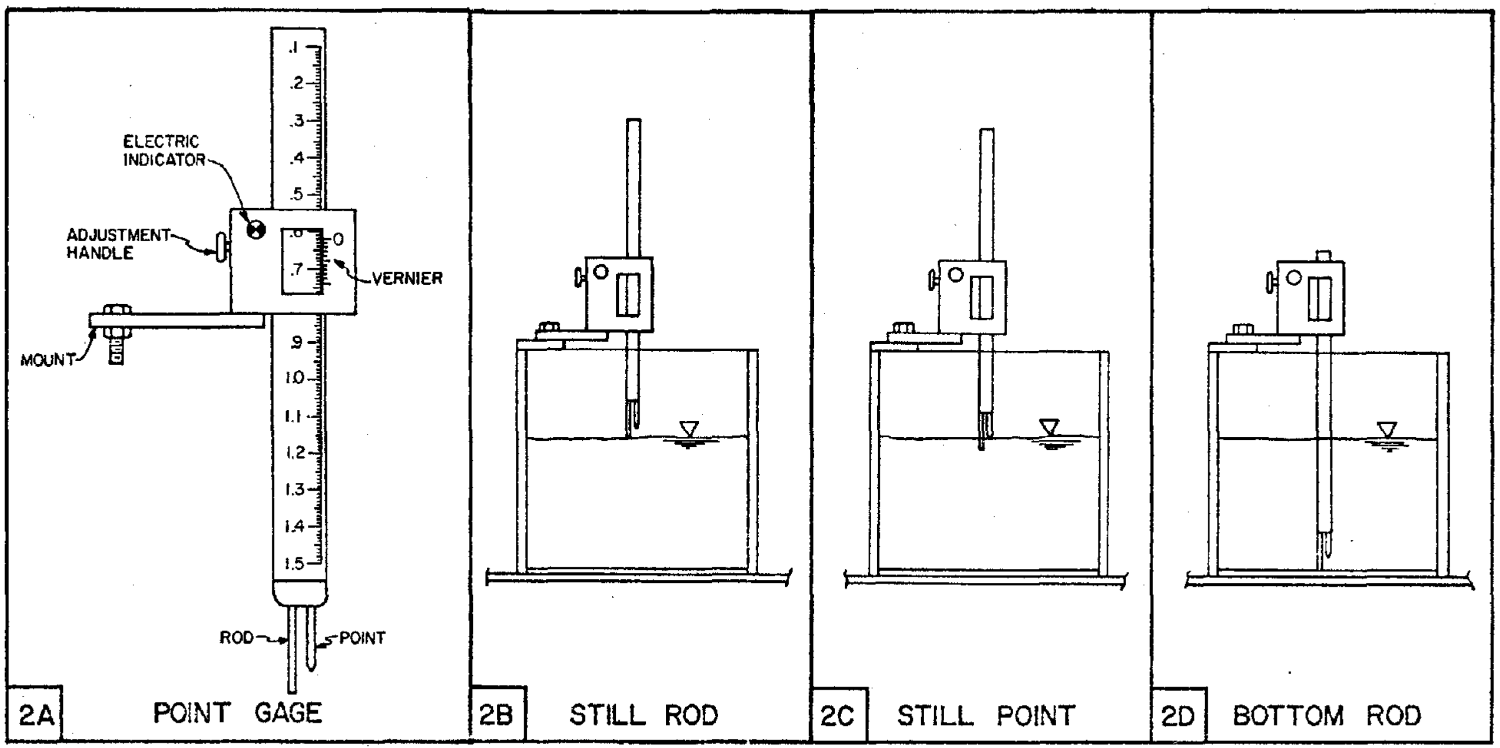

Figure 4. Ott Point Gage and Depth Measurements Procedure

The sequence of the testing procedure is shown in Figure 5. The experiment covered a wide range of flow rates, roughness patterns and concentrations. For each series the water surface data at seven locations were taken for a given roughness element type, pattern, concentration and range of flow rates. Flow rates were determined by a weighing tank and a stop watch. During each run the water temperature was recorded.

ROUGHNESS PATTERNS

Tests were performed on various types of roughness elements with different combinations of patterns and spacings. The various combinations were selected to insure a broad range of values for channel roughness. Since the experiment was intended to simulate the roughness characteristics of forested flood plains, all elements were arranged to protrude from the water surface.

As mentioned previously, three basic patterns of roughness elements were used: random, rectangular and diamond. For each pattern both the longitudinal and lateral spacing was varied to reflect the concentration of elements along the channel bottom. Figure 6 shows in detail the arrangement of roughness patterns.

The random pattern proved to be the most difficult to set up. The procedure used to specify the position of the element was not completely random in that the elements were randomly placed in a preset grid. Grids of 10 X 10 points on 3/4-inch centers were laid out on a four-foot length of plywood. Ten degrees of density[2] (λ) of elements were used for the random pattern. These densities ranged from 5 percent to 50 percent by increments of 5 percent. For the 5 percent density, a set of two-digit numbers was

---

[2] Density is defined as the percentage of grid points in which roughness elements are placed.

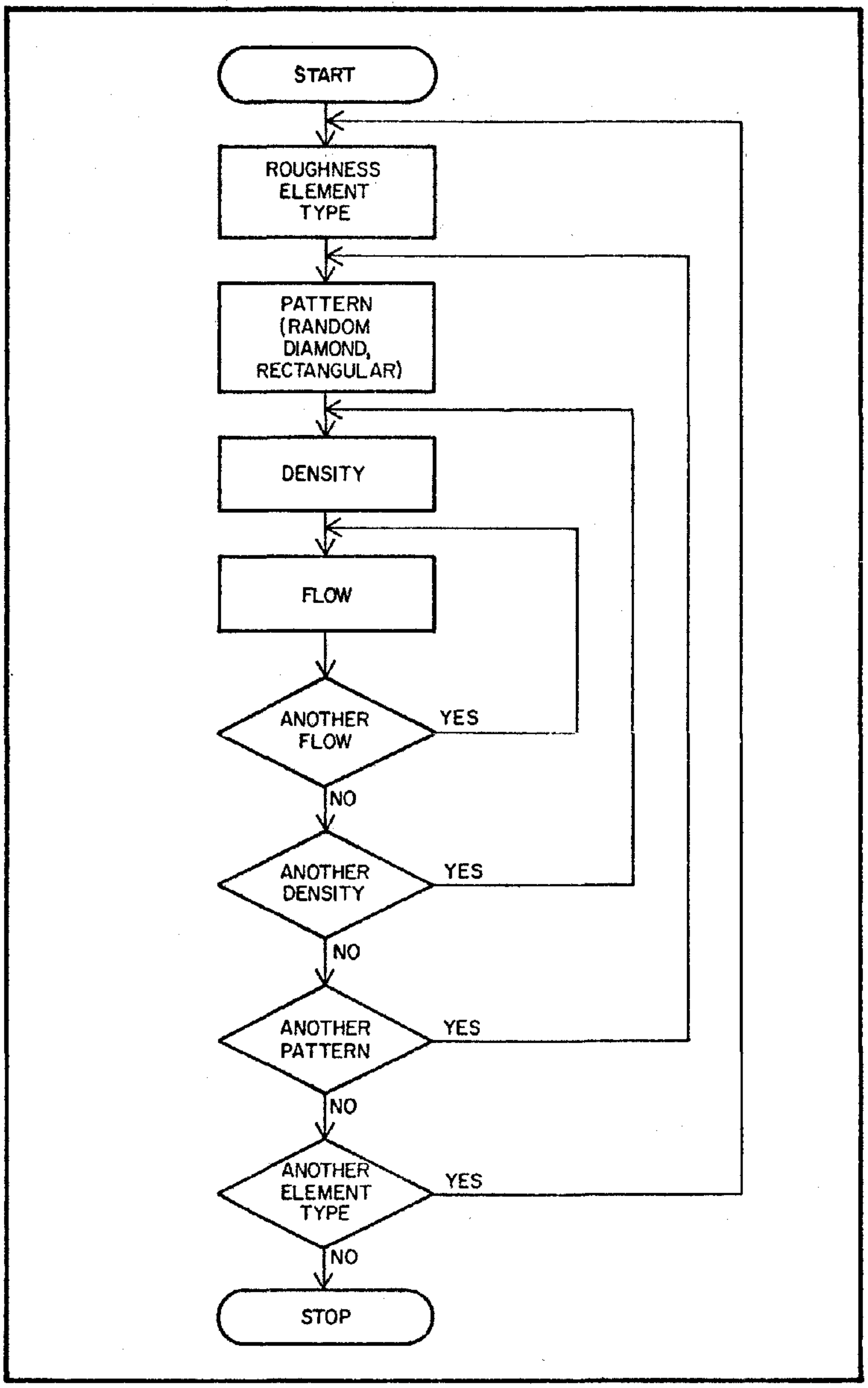

Figure 5. Test Sequence

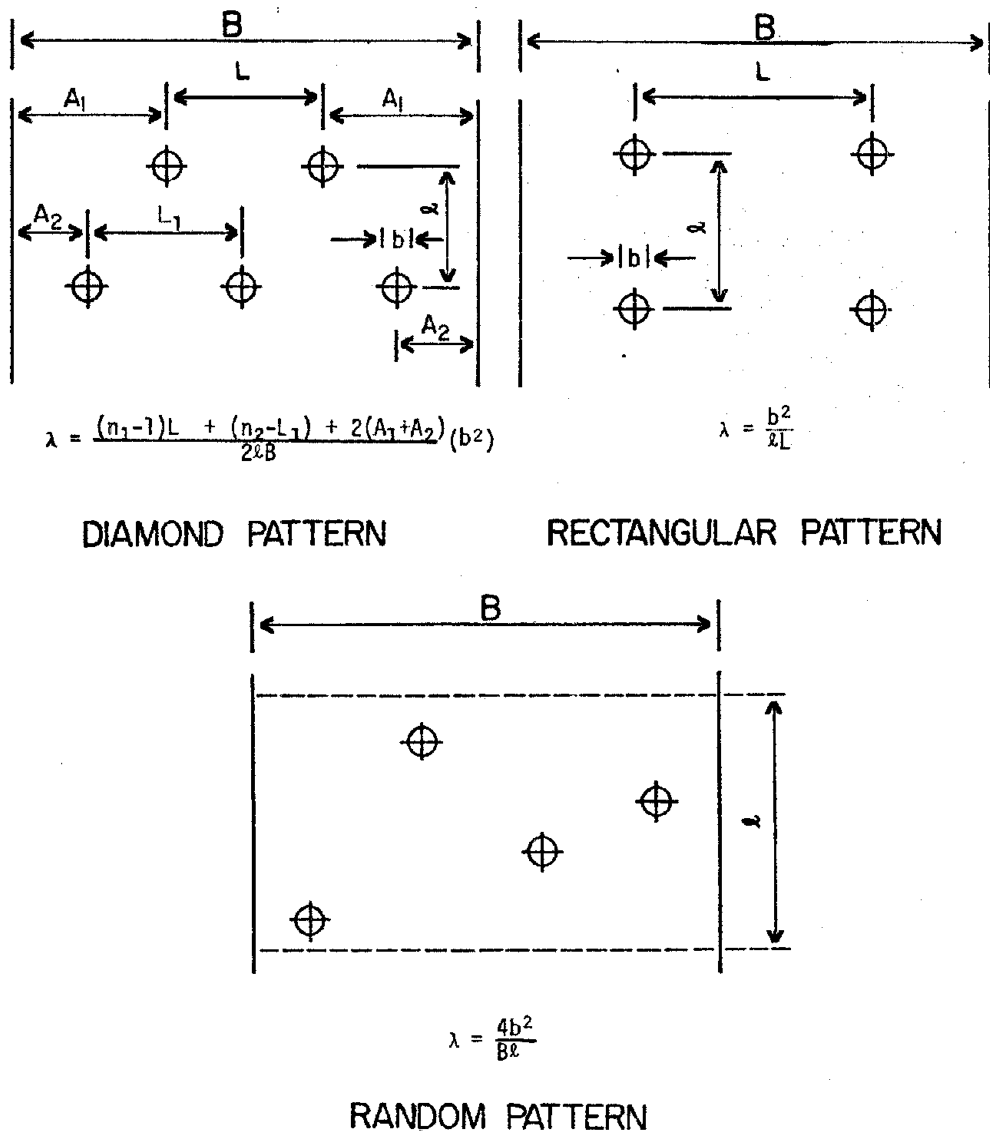

Figure 6. Geometry of Roughness Patterns

taken from random number tables. These two-digit random numbers were used as coordinate points for placing the elements, with the first digit assigned to the ordinate and the second to the abscissa. In order to achieve a 10 percent density, another set of two-digit numbers was taken from the random number tables and placed on the grid as before. For those cases in which a coordinate point was selected more than once, a new coordinate was selected from the random number tables (12).

The above procedure was followed for densities of up to 50 percent. The remaining 10 X 10 grids on the four-foot length of plywood were assigned elements in the same manner. Four pieces of four-foot lengths of plywood were assigned elements using this procedure and this 16-foot section was duplicated until the desired length of test reach was obtained. Figure 7 illustrates a section of the flume in which roughness elements were assigned using the random technique. Due to the amount of effort involved in placing the roughness elements with the random pattern, tests were limited to the circular wooden dowels.

Other patterns tested were the rectangular and diamond patterns. The rectangular pattern was defined as that in which elements are aligned in columns parallel to the direction of flow and rows perpendicular to the direction of flow. The diamond pattern of elements is defined as that in which elements are aligned in columns oblique to the direction of flow. Figure 6 illustrates the parameters necessary to describe the geometry of the patterns.

ROUGHNESS ELEMENT TYPES

The experiments were performed using eight types of roughness elements. All the elements were approximately 18 inches in length. Their projected widths varied from 0.25 inch to 1.06 inches and their cross-

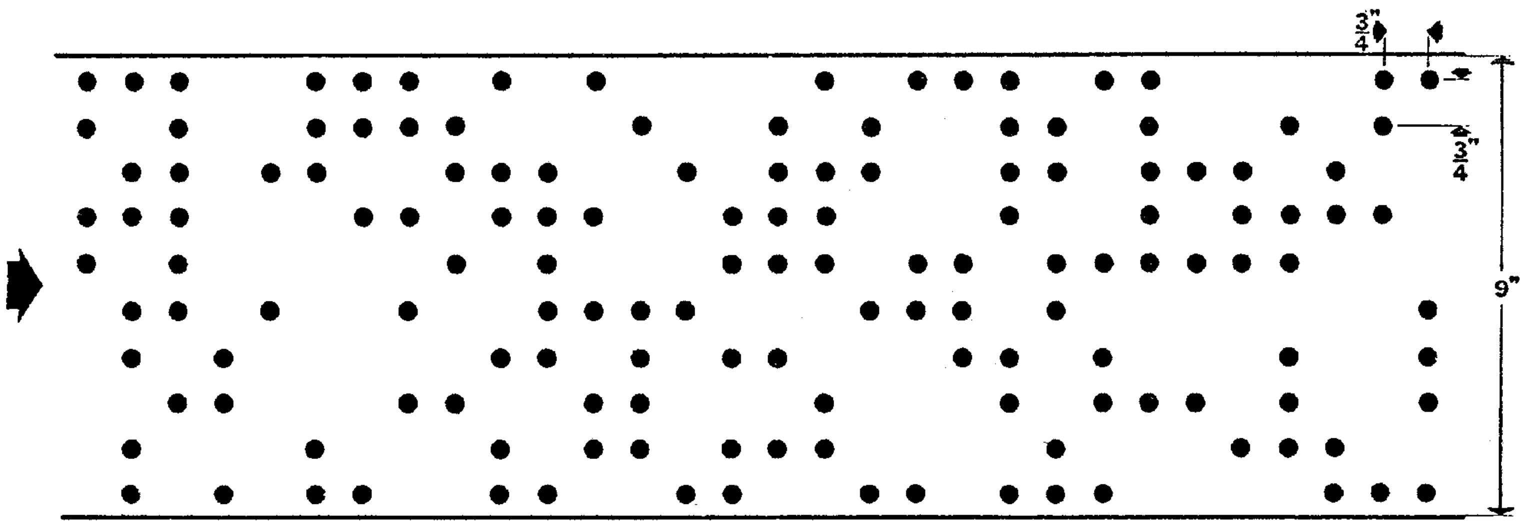

Figure 7. An Example of Random Pattern Roughness Distribution
$\lambda = 0.048$

sectional areas varied from approximately 0.05 square inch to 0.8 square inch. A sketch of these various elements is shown in Figure 8.

Table 1 presents the various parameters needed to describe each series of experiments. The spacing parameters as illustrated in Figure 6 are given in column 4. Column 5 gives an illustration of the cross-sectional area of the elements in relation to the direction of flow. The direction of flow is indicated by an arrow.

While σ is a proper parameter characterizing the roughness concentration of the channel, its determination requires the prior knowledge of depth. Further, in most practical applications depth is a dependent variable which is to be determined, thus the value of σ is not known *a priori*. Without the knowledge of water depth, however, the roughness field can be physically represented by some type of roughness density, such as λ, a parameter used for measuring the number of roughness elements of a typical size per unit area of channel bottom. The value of λ is this case is a constant; hence it is a convenient parameter to characterize the roughness field, though inadequate in a strict sense. The usefulness of λ as a roughness parameter is further discussed in Chapter IV.

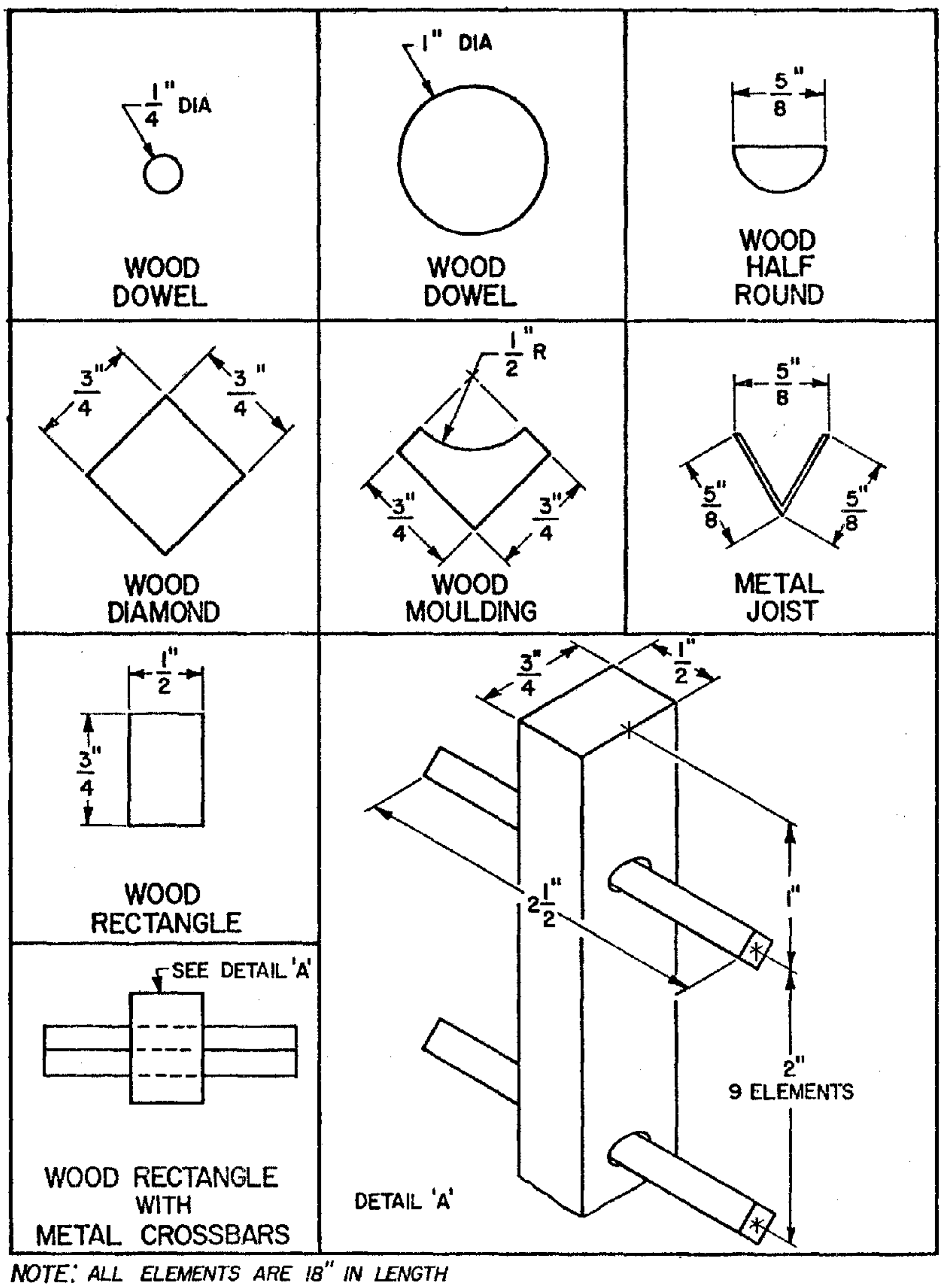

Figure 8. Types of Roughness Elements

Table 1. Configurations of Roughness Elements

Series	Pattern	Density (λ)	Spacing Parameters ℓ	Spacing Parameters L	Element Cross Section	Projected Width of Element (in.)
5	Random	0.0482			→ ○	0.25
6	Random	0.0434			→ ○	0.25
7	Random	0.0386			→ ○	0.25
8	Random	0.0338			→ ○	0.25
9	Random	0.0290			→ ○	0.25
10	Random	0.0241			→ ○	0.25
11	Random	0.0193			→ ○	0.25
12	Random	0.0145			→ ○	0.25
13	Random	0.0096			→ ○	0.25
14	Random	0.0048			→ ○	0.25
15	Rectangular	0.0242	1.50	1.50	→ ○	0.25
16	Rectangular	0.0121	3.00	1.50	→ ○	0.25
17	Rectangular	0.0073	3.00	3.00	→ ○	0.25
18	Rectangular	0.0145	1.50	3.00	→ ○	0.25

Table 1. (Continued)

Series	Pattern	Density (λ)	Spacing Parameters ℓ (in.)	L (in.)	L_1 (in.)	Element Cross Section	Projected Width of Element (in.)
19	Diamond	0.0121	1.50	3.00	3.00		0.25
20	Diamond	0.0218	1.50	3.00	1.50		0.25
25	Diamond	0.0543	6.00	4.50	3.00		1.06
26	Diamond	0.0543	6.00	4.50	3.00		1.06
27	Diamond	0.0543	6.00	4.50	3.00	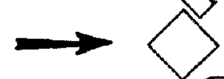	1.06
28	Diamond	0.0463	6.00	4.50	3.00		1.00
29	Rectangular	0.1159	3.00	3.00	3.00		1.00
30	Diamond	0.0556	3.00	4.50	4.50		1.00
31	Diamond	0.0121	6.00	4.50	3.00		0.50
32	Diamond	0.0121	6.00	4.50	3.00		0.50
33	Diamond	0.0189	6.00	4.50	3.00		0.625
34	Diamond	0.0189	6.00	4.50	3.00		0.625
35	Diamond	0.0189	6.00	4.50	3.00		0.625
36	Diamond	0.0113	6.00	4.50	4.50		0.625

IV. DATA ANALYSIS AND RESULTS

GENERAL APPROACH

The main objective of the test data analysis is to establish the functional relationships in Equation 39. In the process of deriving Equation 39, the values of f, F , and R are expressed as functions of the hydraulic radius of the flume. Since the roughness of the glass walls of the test flume is significantly less than that of the elements placed on the flume floor, flows in the flume are essentially two-dimensional. Therefore, the depth of flow is taken as the length parameter in computing f, F and R . Thus

$$f = \frac{8g\ y\ S_f}{V^2} \tag{40}$$

$$\mathsf{F} = \frac{V}{\sqrt{gy}} \tag{41}$$

$$\mathsf{R} = \frac{\Delta V y}{\nu} \tag{42}$$

Additional parameters, including the drag coefficients of various types of roughness elements, Chézy's C and Manning's n, are also computed using the expressions

$$C_d = \frac{2g\ y\ S_f}{V^2} \tag{24}$$

$$C = \left(\frac{8g}{f}\right)^{1/2} \tag{43}$$

Preceding page blank

$$n = \frac{1.49y^{1/6}\sqrt{f}}{\sqrt{8g}} \tag{44}$$

The roughness data as calculated with the above equations are listed in Appendix B.

SURFACE RESISTANCE OF TEST FLUME

In order to determine the surface resistance of the test flume, a series of tests were conducted without roughness elements. These test data are listed in Appendix A. Note that the hydraulic radius has been used as the length parameter for the calculation of f, F and $\mathbf{R}$. This is because the resistance is caused essentially by the shear stress along the wooden bottom and glass walls of the flume. Figure 9 illustrates the relationship of f and $\mathbf{R}$ for this test condition.

Surface resistance data from established sources (13) for a glass surface and a wooden stave are also plotted on Figure 9 . A comparison of these data with the test data indicates that the value of f approximates that of the wooden stave at low Reynolds numbers and that of the glass surface at high Reynolds numbers. This is evident from the fact that for a given channel slope the depth at low Reynolds numbers is shallow; hence, the wooden floor contributes much of the resistance to the flow. At high Reynolds numbers the flow is deep; therefore, the channel resistance is governed by the glass surface. In any event, the surface resistance of the test flume is negligible in comparison with the resistance created by the roughness elements, as is shown in the following section.

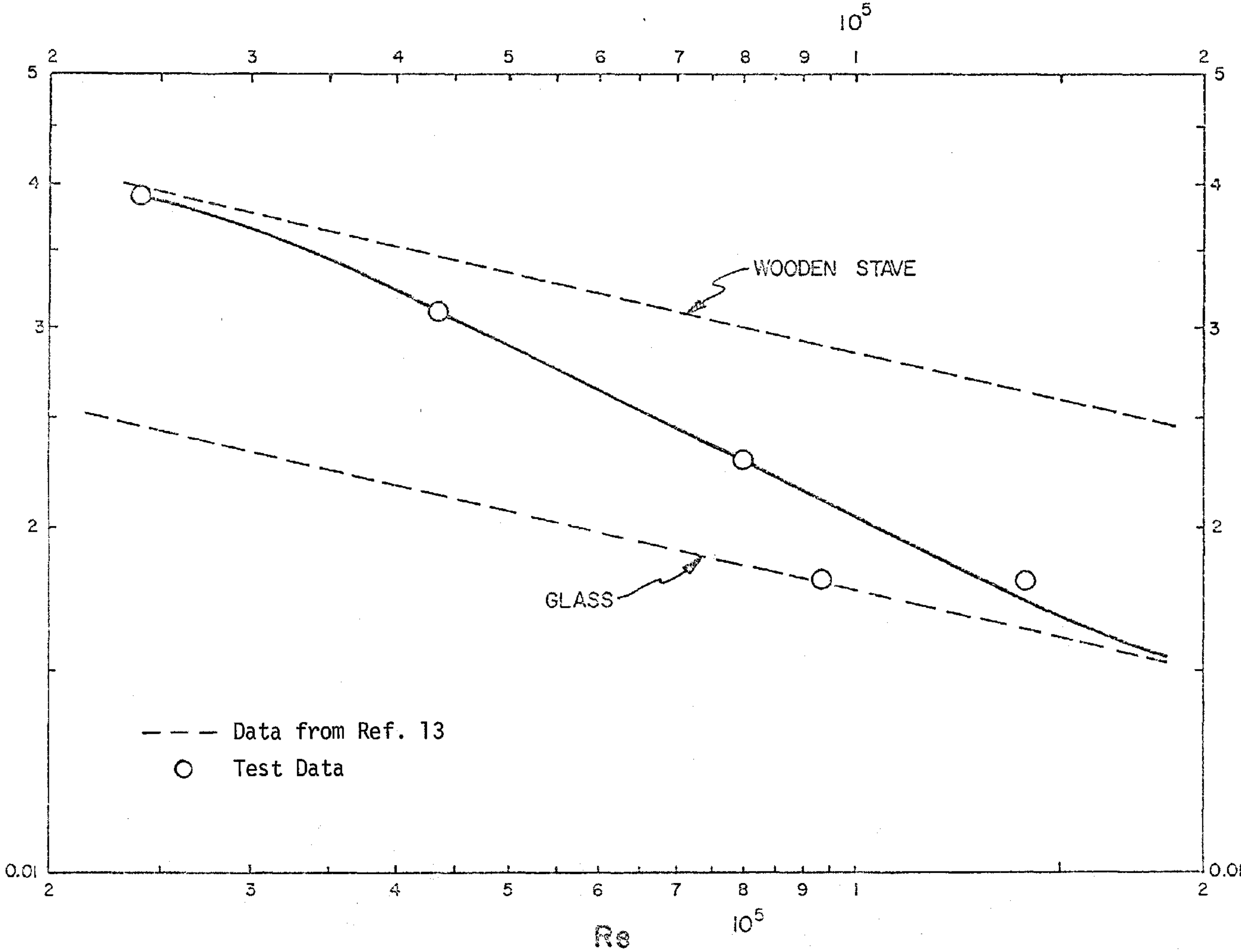

Figure 9. Resistance of Test Flume

CHANNEL RESISTANCE FROM LARGE SCALE ROUGHNESS

$1/\sqrt{f}$ AS A FUNCTION OF ROUGHNESS CONCENTRATION, σ

A common technique for analyzing channel resistance for submerged elements is to plot $1/\sqrt{f}$ against the relative roughness y_n/k to determine their functional relationships in the framework of the Karman-Prandtl concepts. However, since y_n/k is a constant in the case of protruding roughness elements, $1/\sqrt{f}$ is plotted against roughness concentration, σ ($=\lambda y/b$). Figures 10 through 15 show plots of this relationship for all types of roughness elements tested, with Froude number as a parameter. It is interesting to note that the character of the curve is entirely different from the well known Karman-Prandtl equation for roughened pipes. Instead of f decreasing with increasing y, these plots show the opposite. The explanation is that in the case of protruding elements, the flow resistance is proportional to the projected area of the roughness elements which in turn is proportional to the depth of flow.

CHANNEL RESISTANCE AS A FUNCTION OF FROUDE NUMBER

Since it was not possible to tilt the test flume in order to vary its slope, a comprehensive examination of the effect of Froude number on the channel resistance is not possible in this study. However, from Figures 10 through 15, in which the Froude number of each data point is plotted, it appears that channel resistance is slightly dependent on Froude number. The mild dependence of the resistance coefficient on the Froude number for the random pattern in Figure 16 is further demonstrated. Nevertheless, considering the limited range of Froude number tested the true relationship is at best inconclusive.

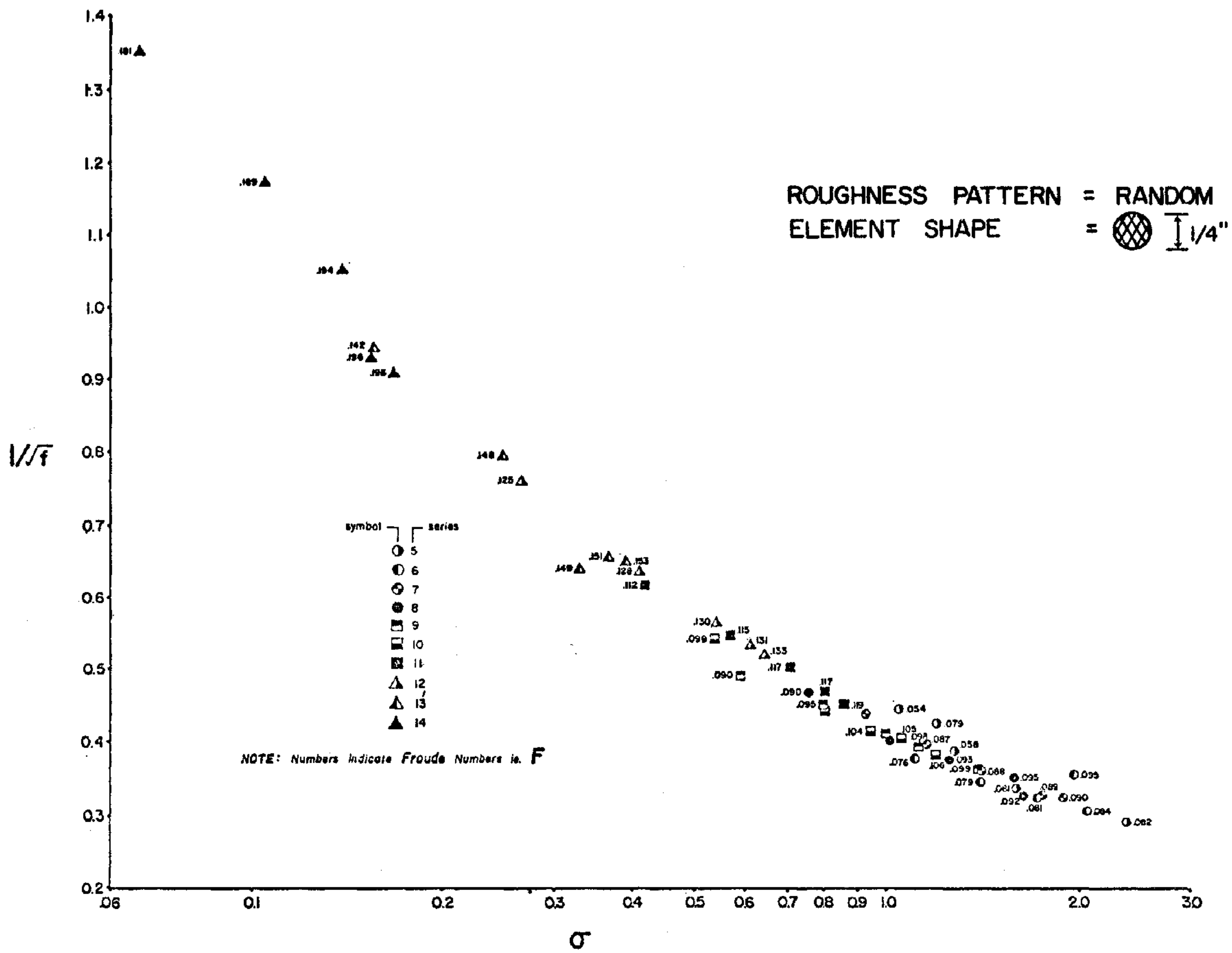

Figure 10. Relationship of Resistance Coefficient to Roughness Concentration with Froude Number as Parameter

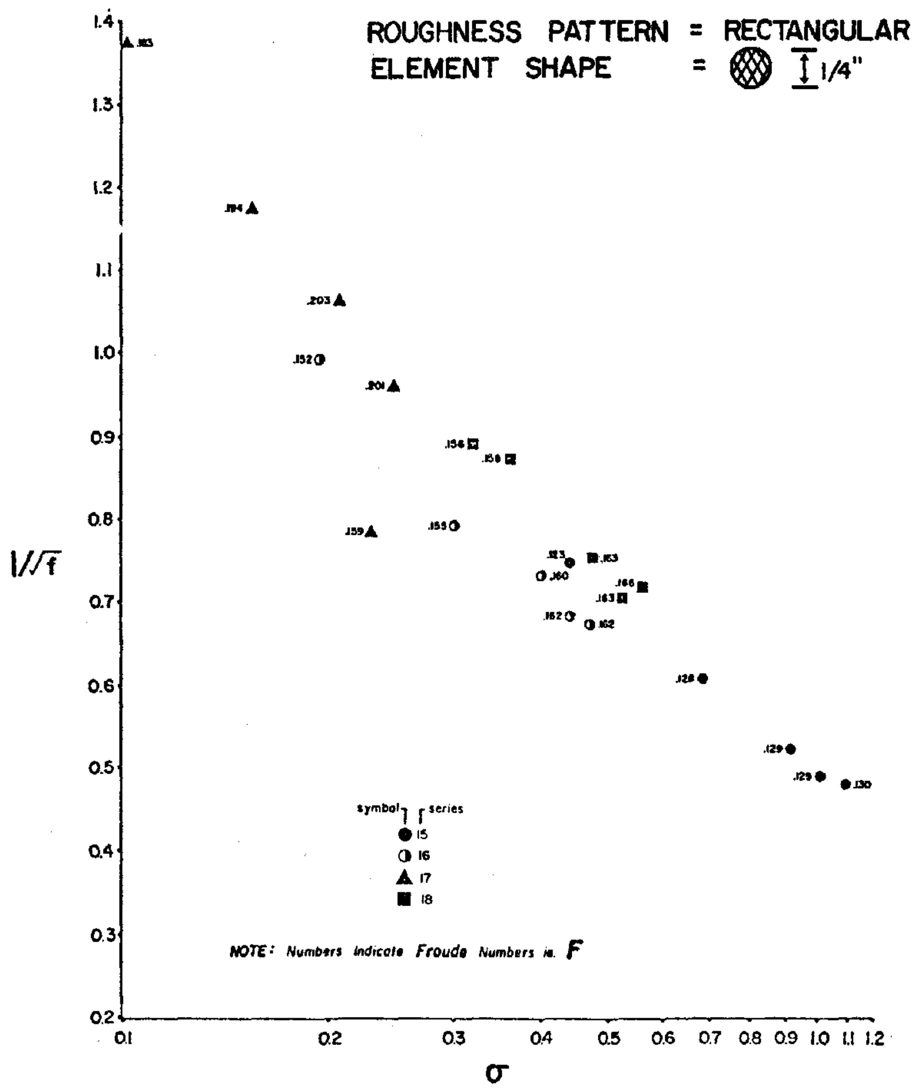

Figure 11. Relationship of Resistance Coefficient to Roughness Concentration with Froude Number as Parameter

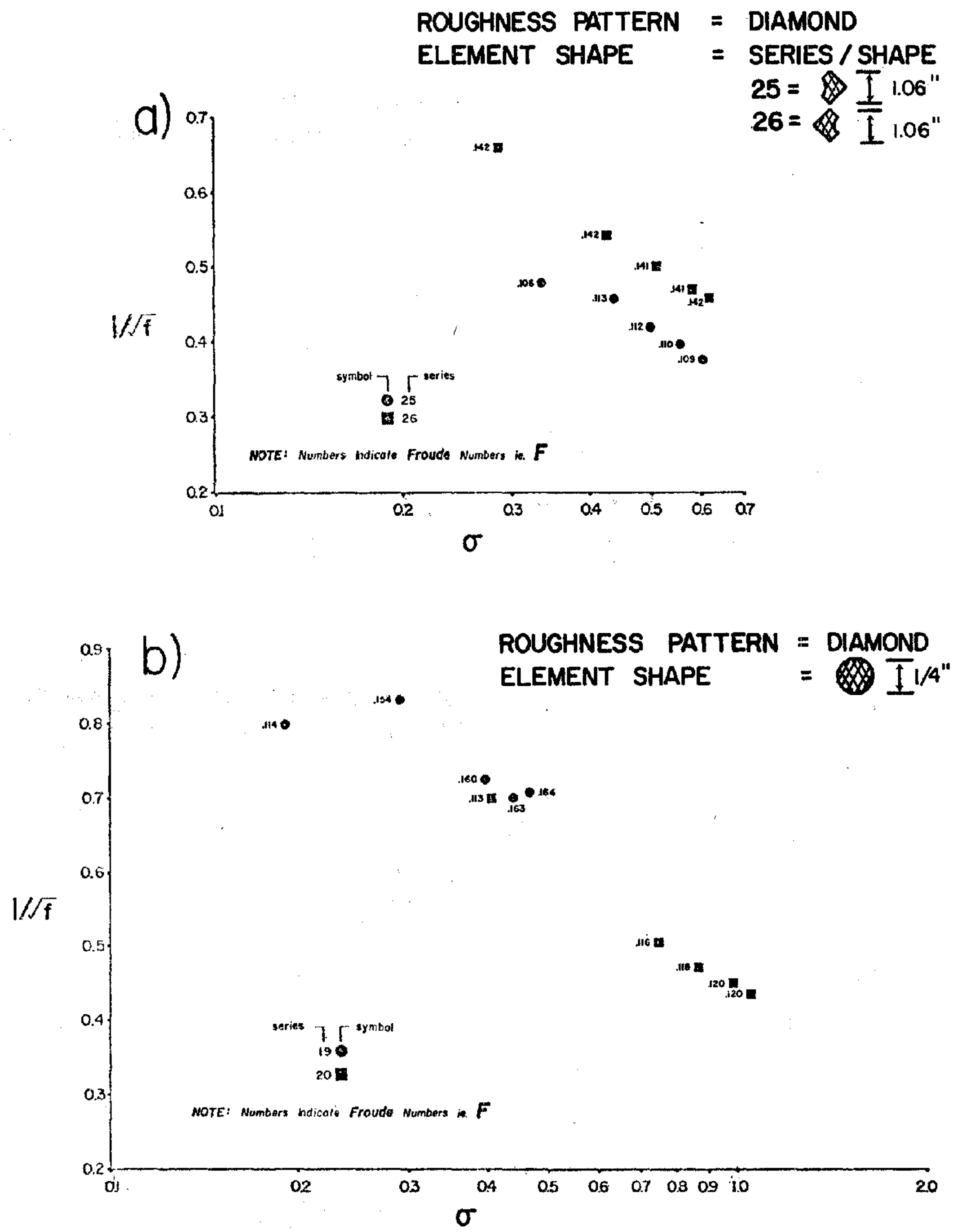

Figure 12. Relationship of Resistance Coefficient to Roughness Concentration with Froude Number as Parameter

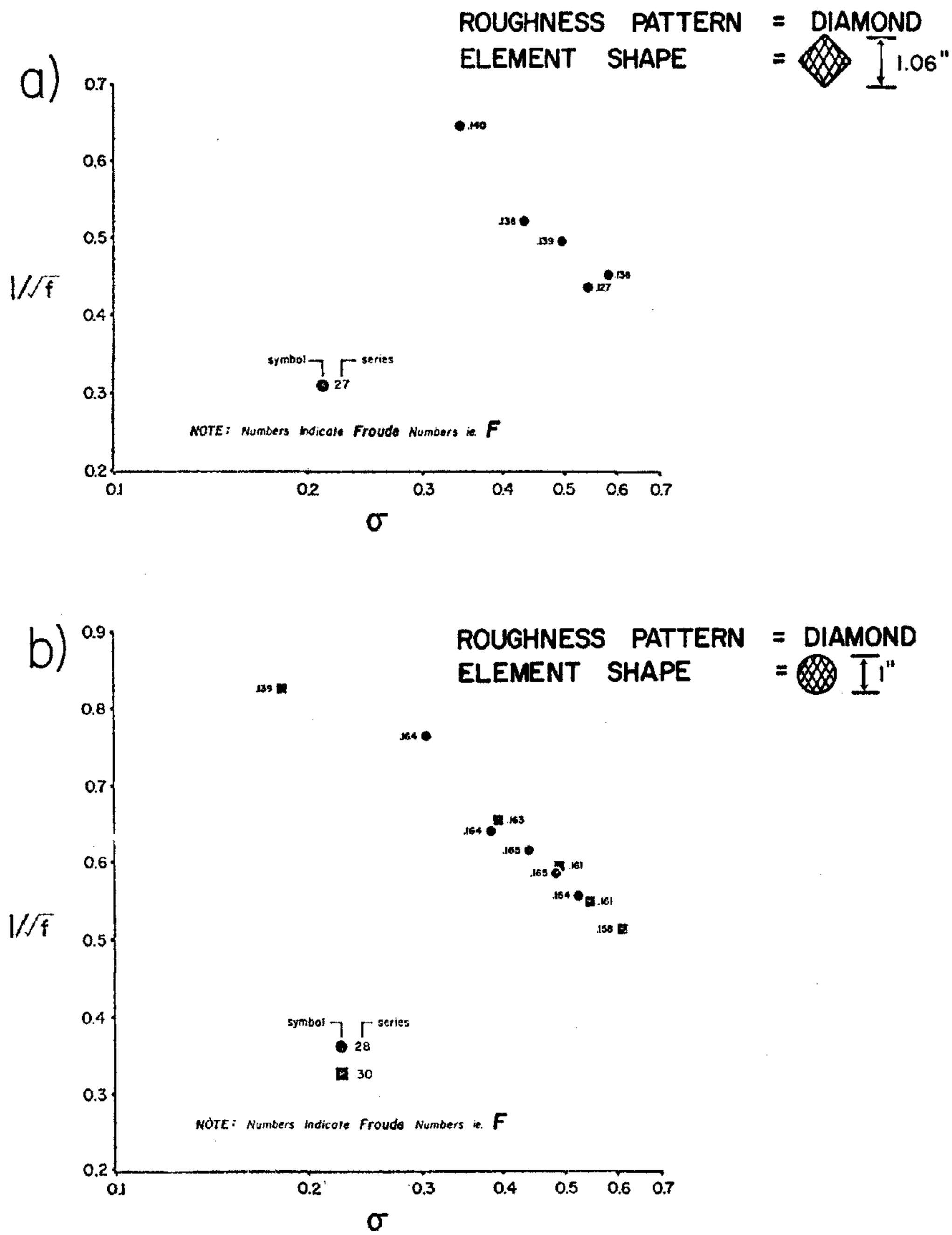

Figure 13. Relationship of Resistance Coefficient to Roughness Concentration with Froude Number as Parameter

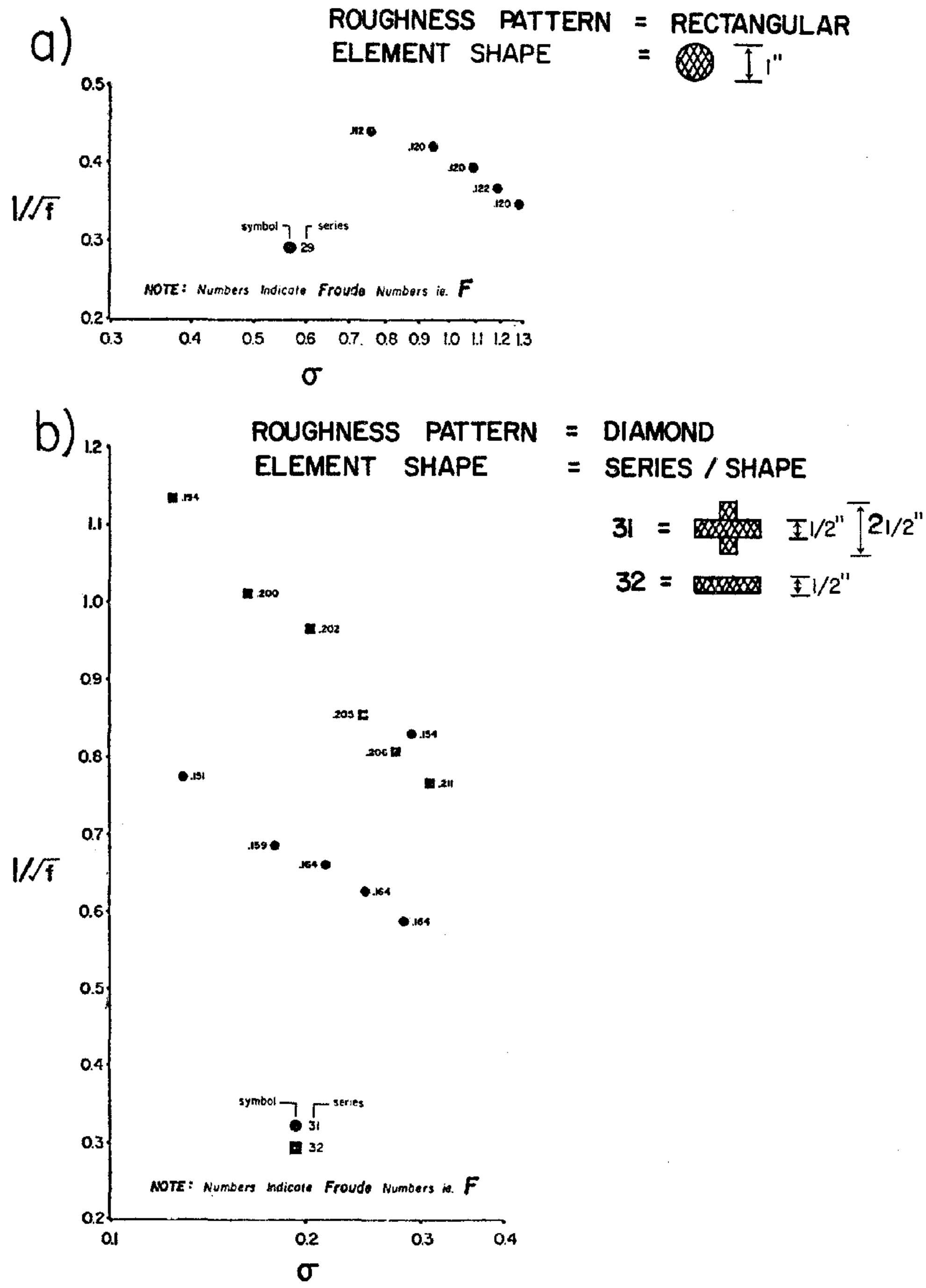

Figure 14. Relationship of Resistance Coefficient to Roughness Concentration with Froude Number as Parameter

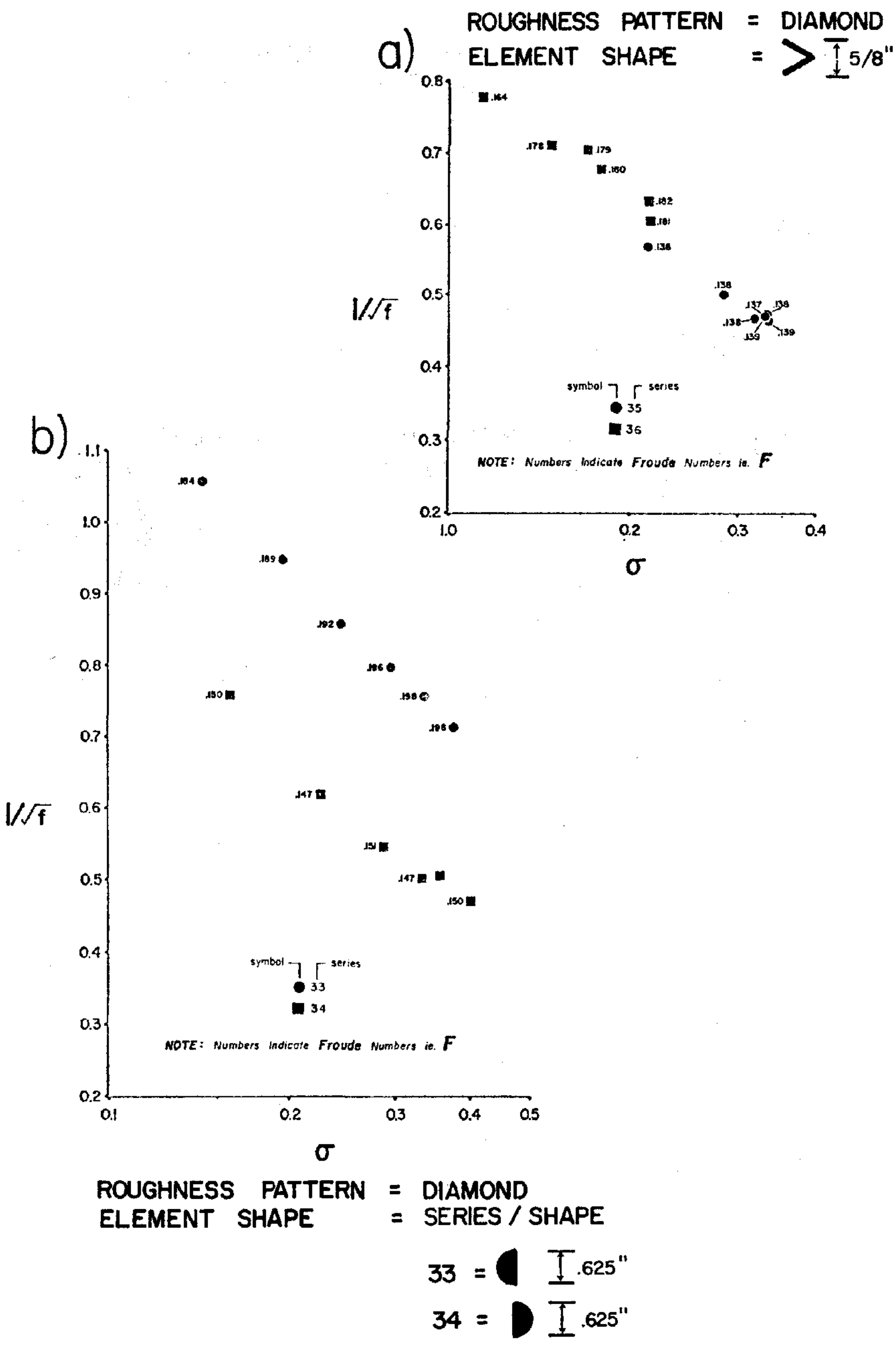

Figure 15. Relationship of Resistance Coefficient to Roughness Concentration with Froude Number as Parameter

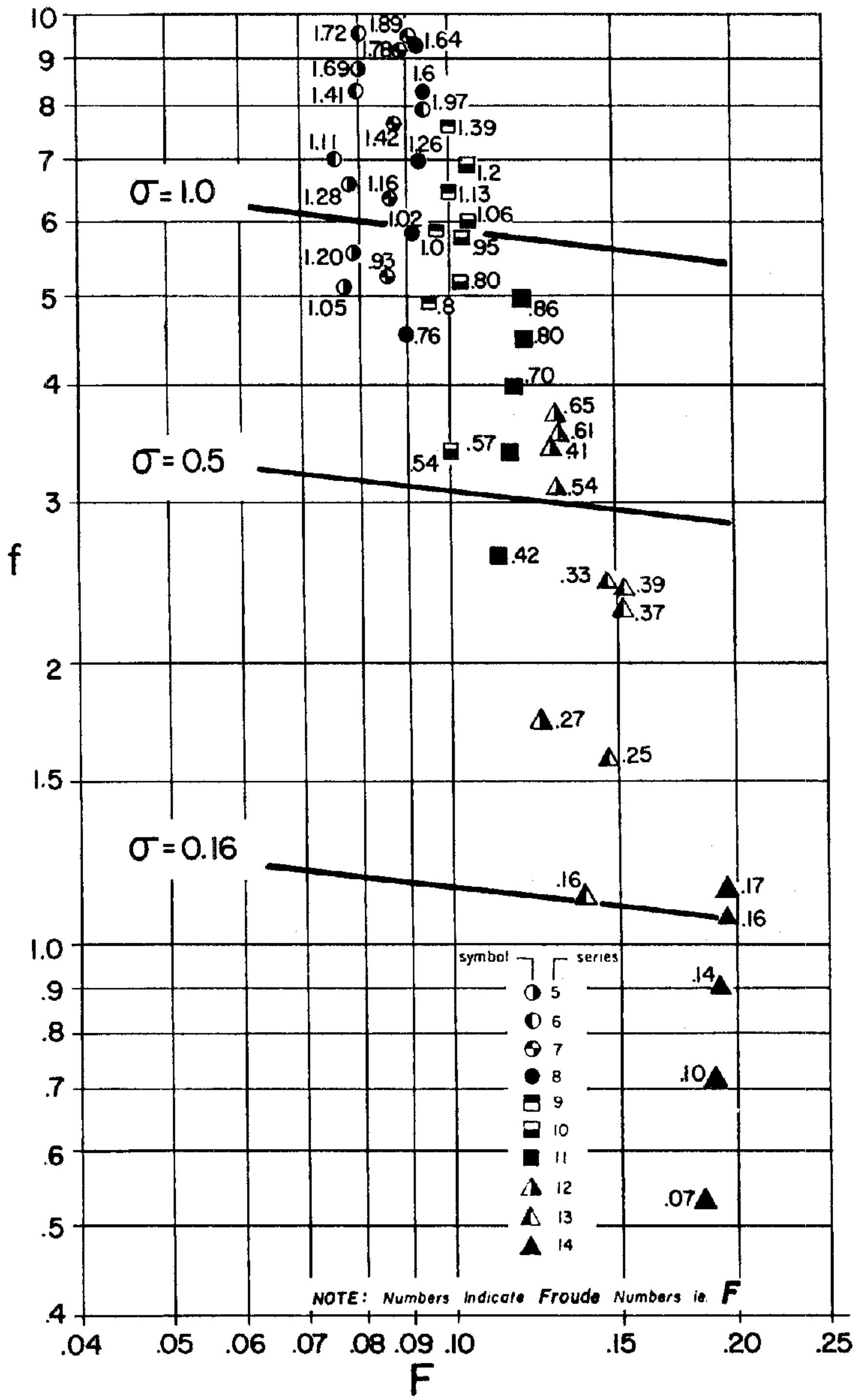

Figure 16. Effect of Froude Number on Resistance Coefficient

CHANNEL RESISTANCE AS A FUNCTION OF REYNOLDS NUMBER

To examine the effect of Reynolds number on the channel resistance the values of $1/\sqrt{f}$ are plotted against the values of σ, with Reynolds number as a parameter. In these plots (Figures 17 through 22) it seems apparent that the Reynolds number has no significant effect on the channel resistance.

To further assess this relationship, a plot of f versus Reynolds number with roughness element concentration as a parameter for the random pattern is shown in Figure 23. From this plot it is clear that for a given concentration f is independent of $\mathbf{R}$. With the magnitude of the Reynolds number in the area of 10^5, the independence of $\mathbf{R}$ from f is expected. This conclusion confirms the results of previous studies.

CHANNEL RESISTANCE AS A FUNCTION OF ROUGHNESS PATTERN

In order to investigate the effect of roughness patterns on the channel resistance, $1/\sqrt{f}$ versus σ curves for the random, diamond and rectangular patterns of the 1/4-inch circular elements were superimposed. The results are shown in Figure 24. It is noted that for a given concentration the random pattern yields higher resistance than that of rectangular and diamond patterns for the concentration range less than one. The resistance curve of the diamond pattern asymtotes to the curve or random pattern at approximately $\sigma = 1$, whereas the resistance curve of the rectangular pattern asymototes to the curve of the random pattern at approximately $\sigma = 2$. This information is significant in the planning of large scale model tests, when a decision must be made whether to use random or regular spacing of roughness elements in the test flume. It is apparent that if the roughness field of regular spacing can adequately reproduce the random spacing (or more prototype-like roughness field), then a considerable economy can be realized for the large scale model test.

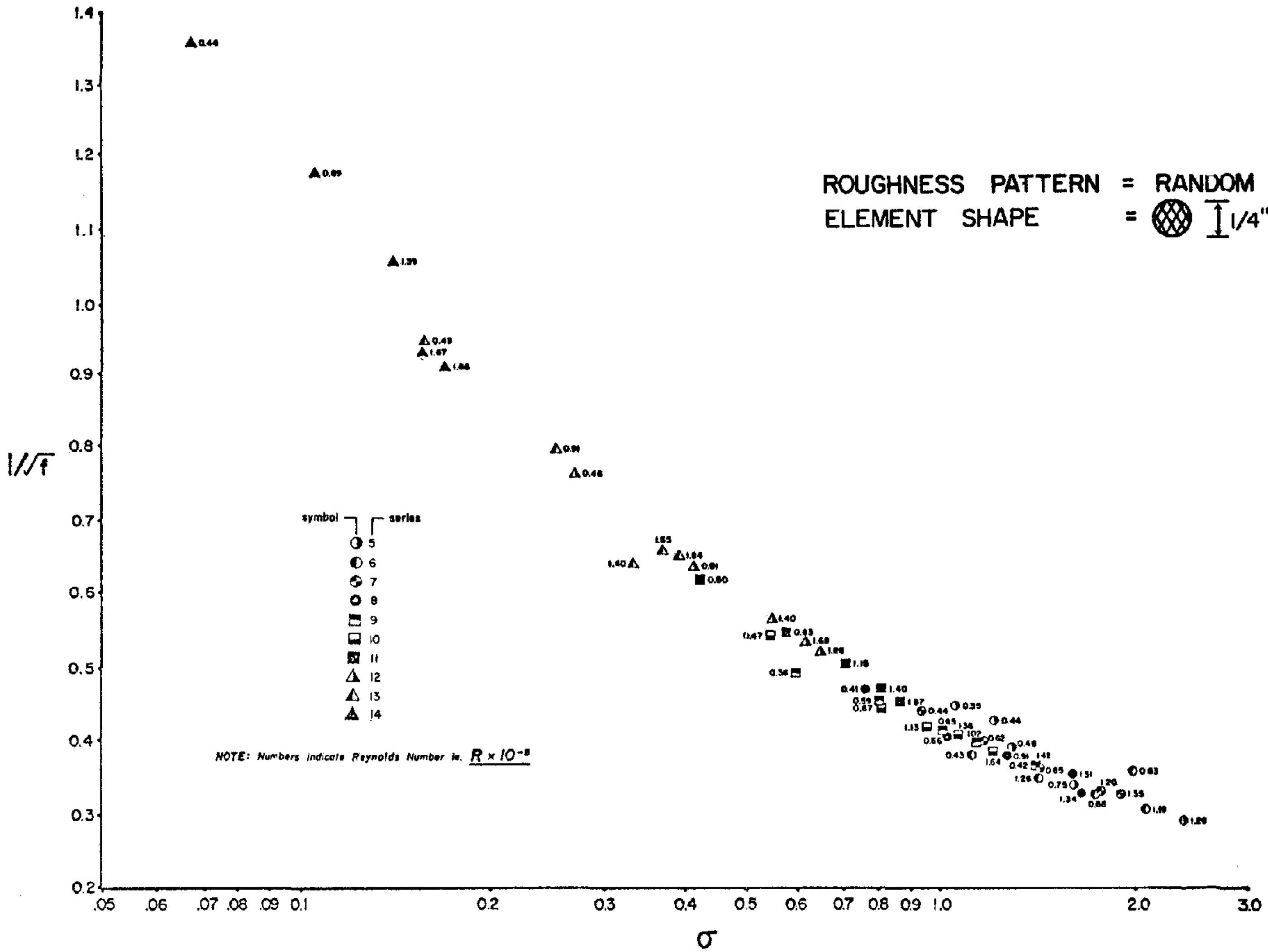

Figure 17. Relationship of Resistance Coefficient to Roughness Concentration with Reynolds Number as Parameter

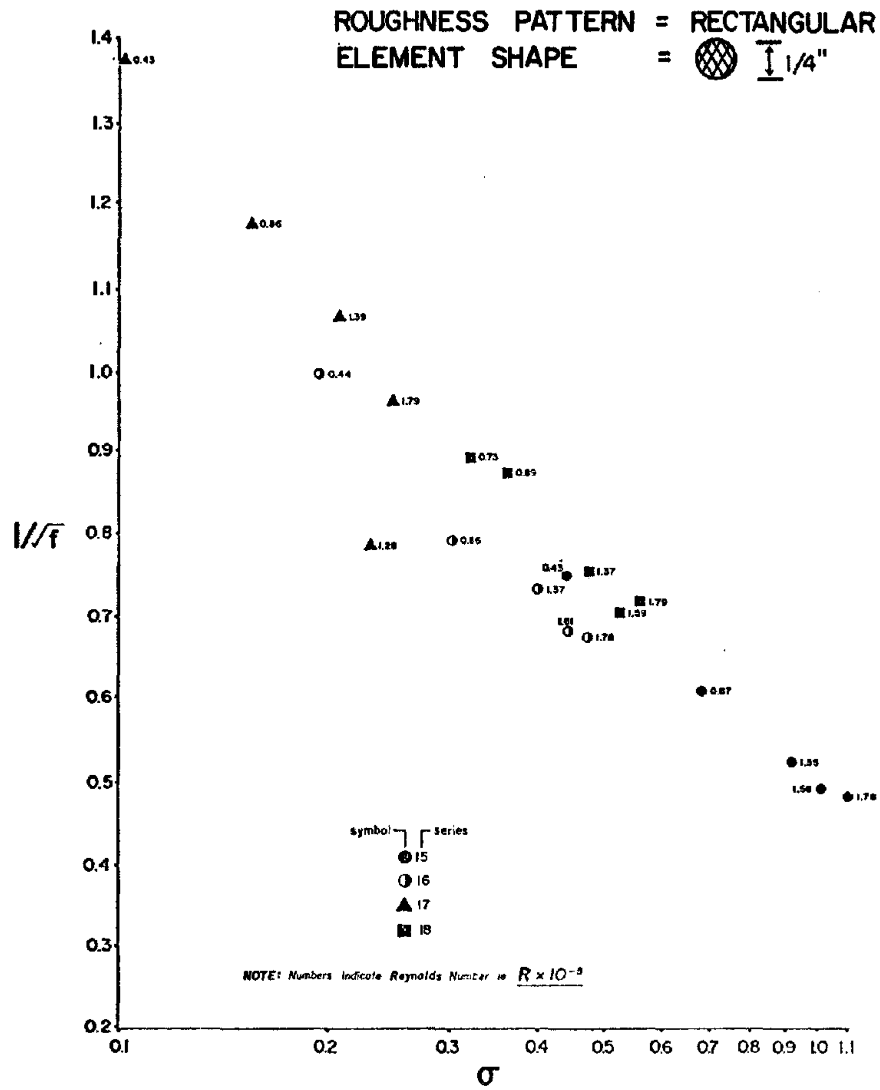

Figure 18. Relationship of Resistance Coefficient to Roughness Concentration with Reynolds Number as Parameter

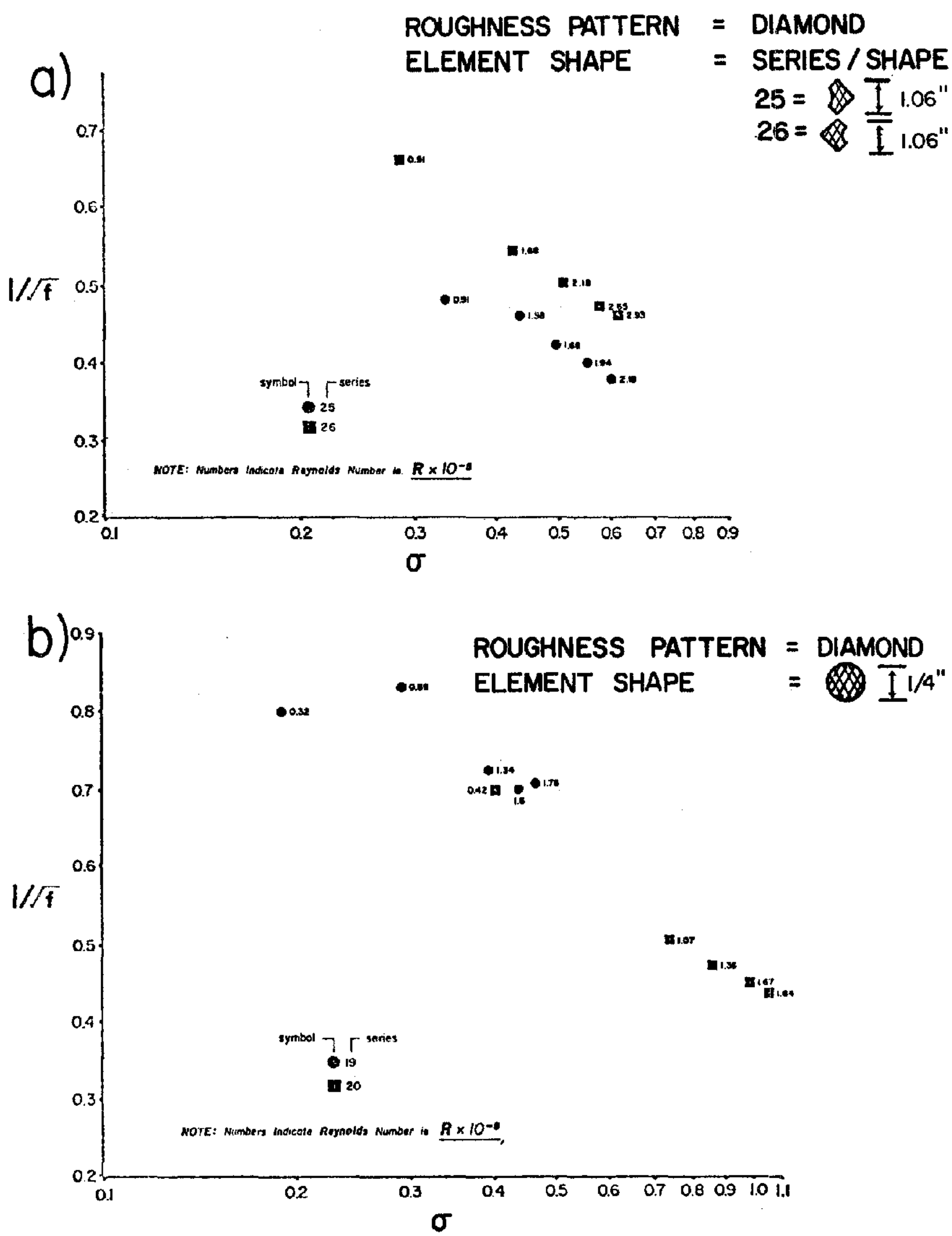

Figure 19. Relationship of Resistance Coefficient to Roughness Concentration with Reynolds Number as Parameter

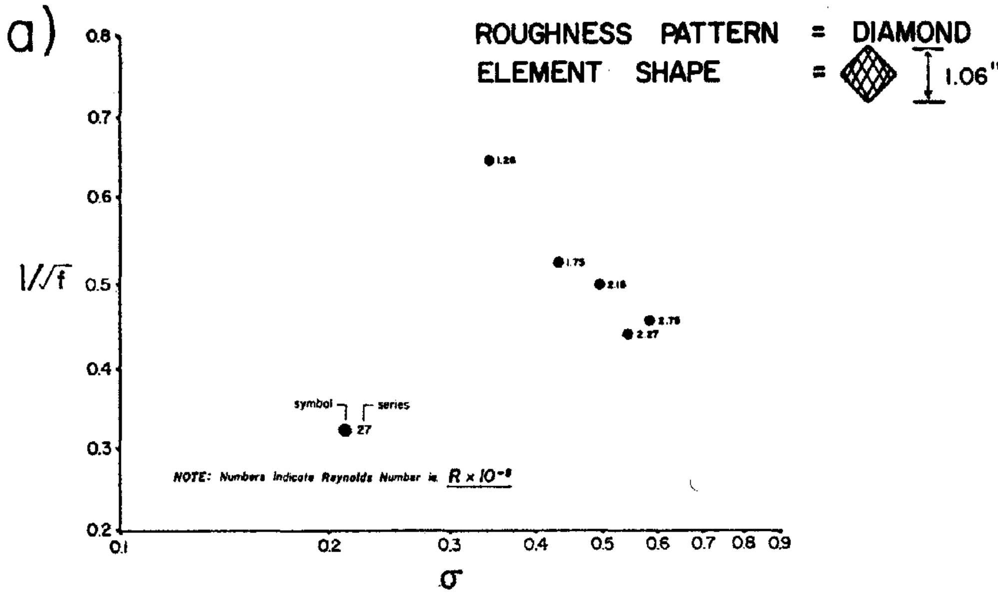

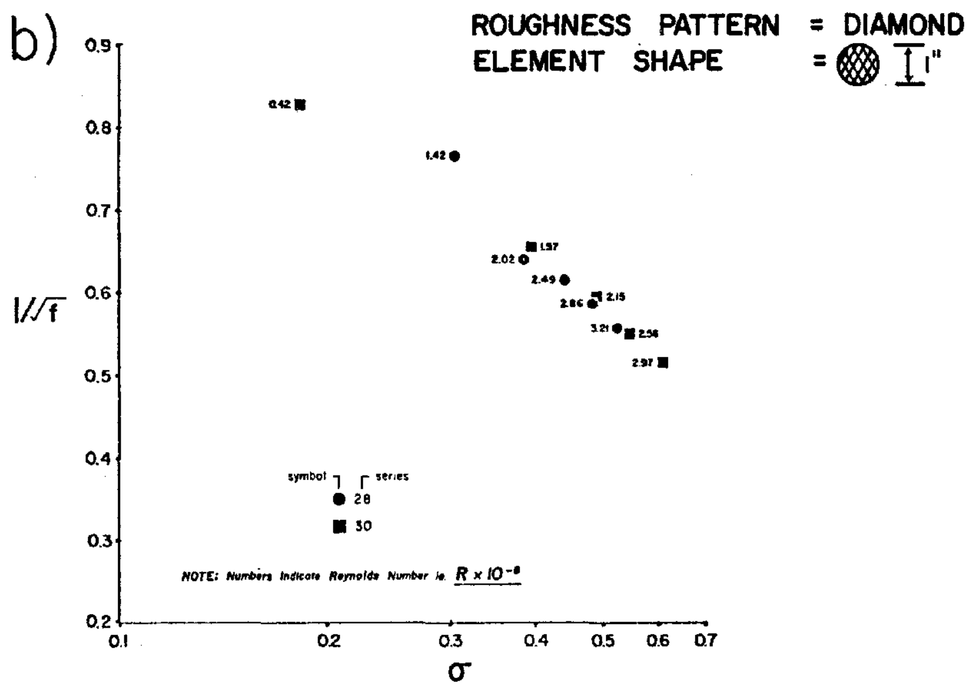

Figure 20. Relationship of Resistance Coefficient to Roughness Concentration with Reynolds Number as Parameter

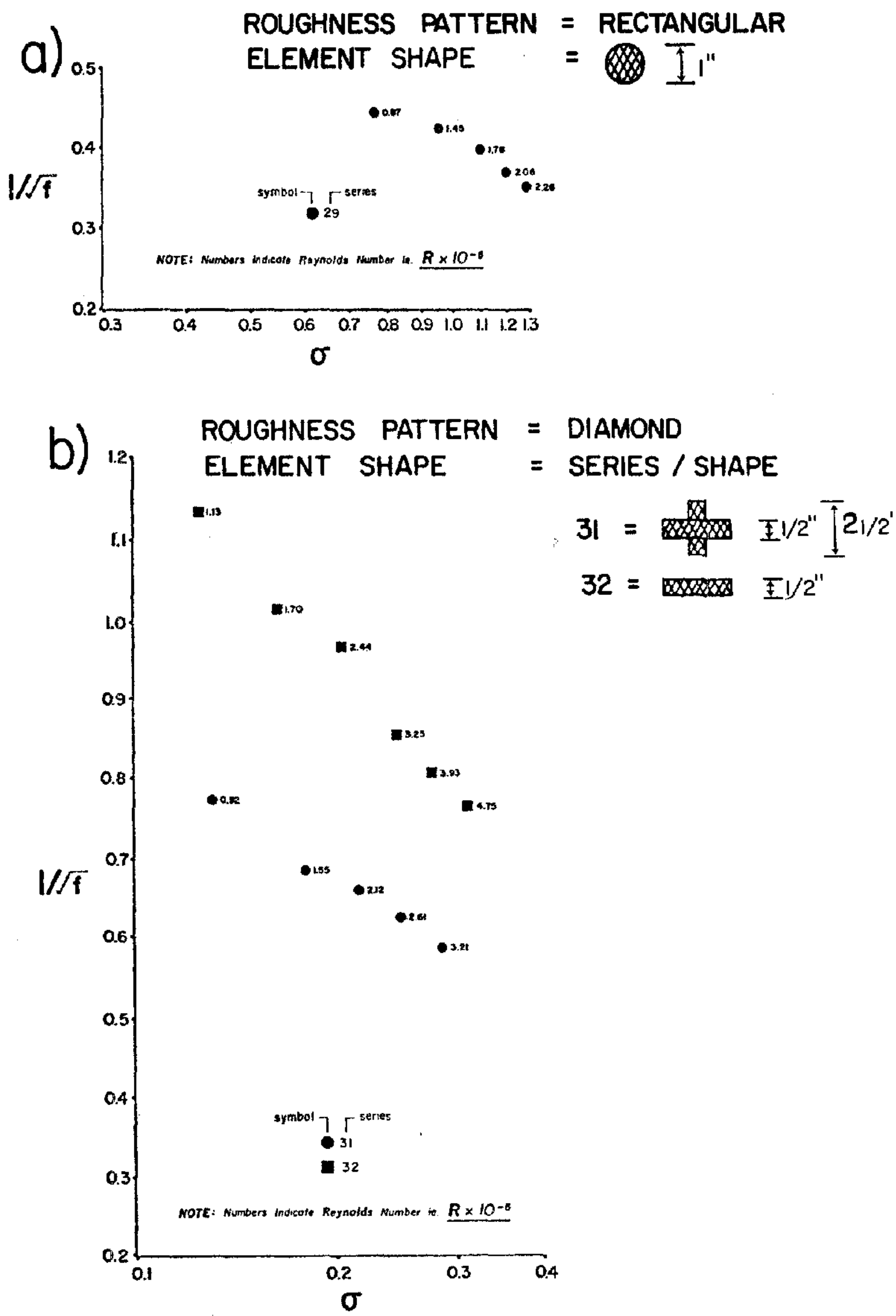

Figure 21. Relationship of Resistance Coefficient to Roughness Concentration with Reynolds Number as Parameter

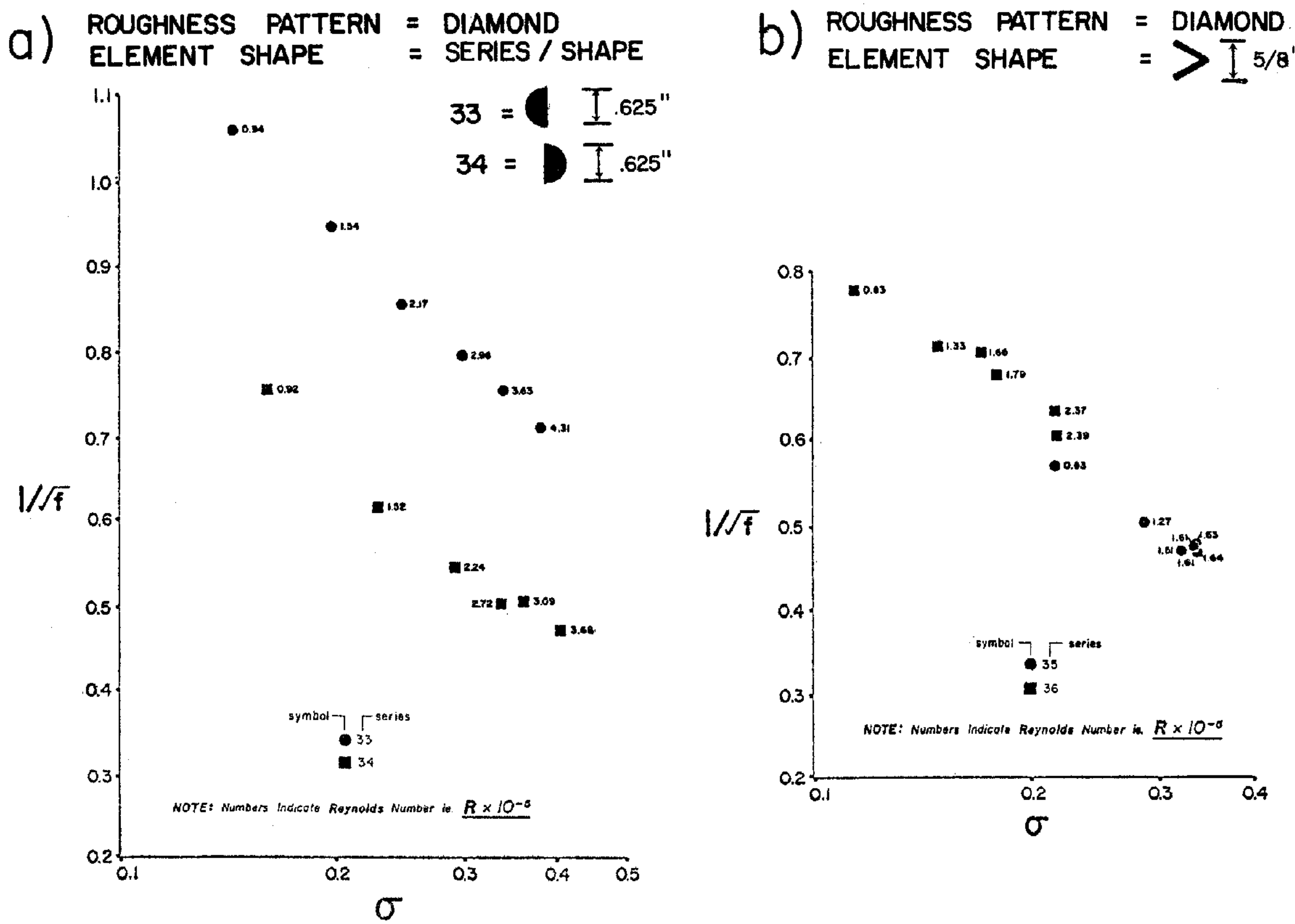

Figure 22. Relationship of Resistance Coefficient to Roughness Concentration with Reynolds Number as Parameter

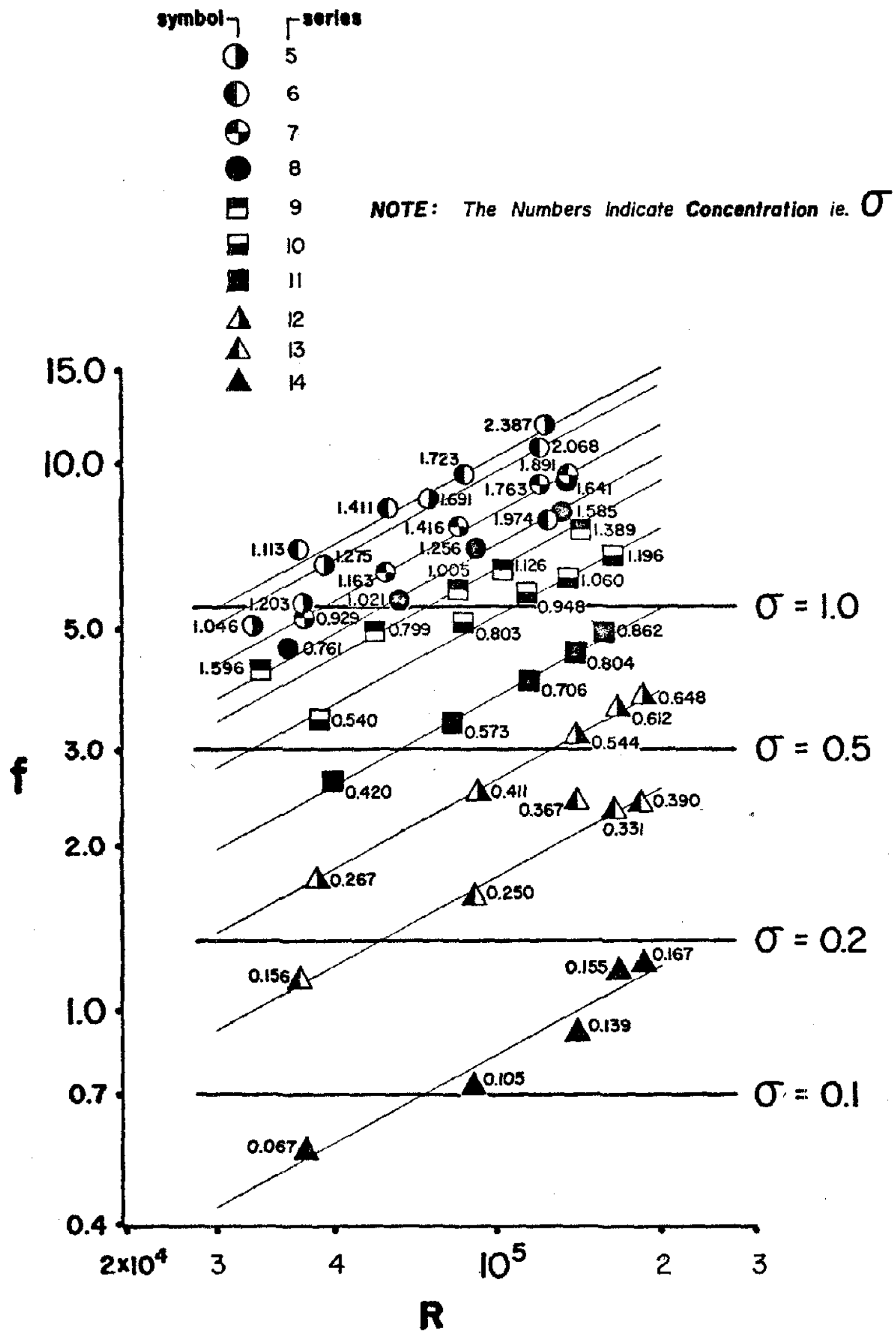

Figure 23. Effect of Reynolds Number (in the order of 10^4- 10^5) on Resistance Coefficient

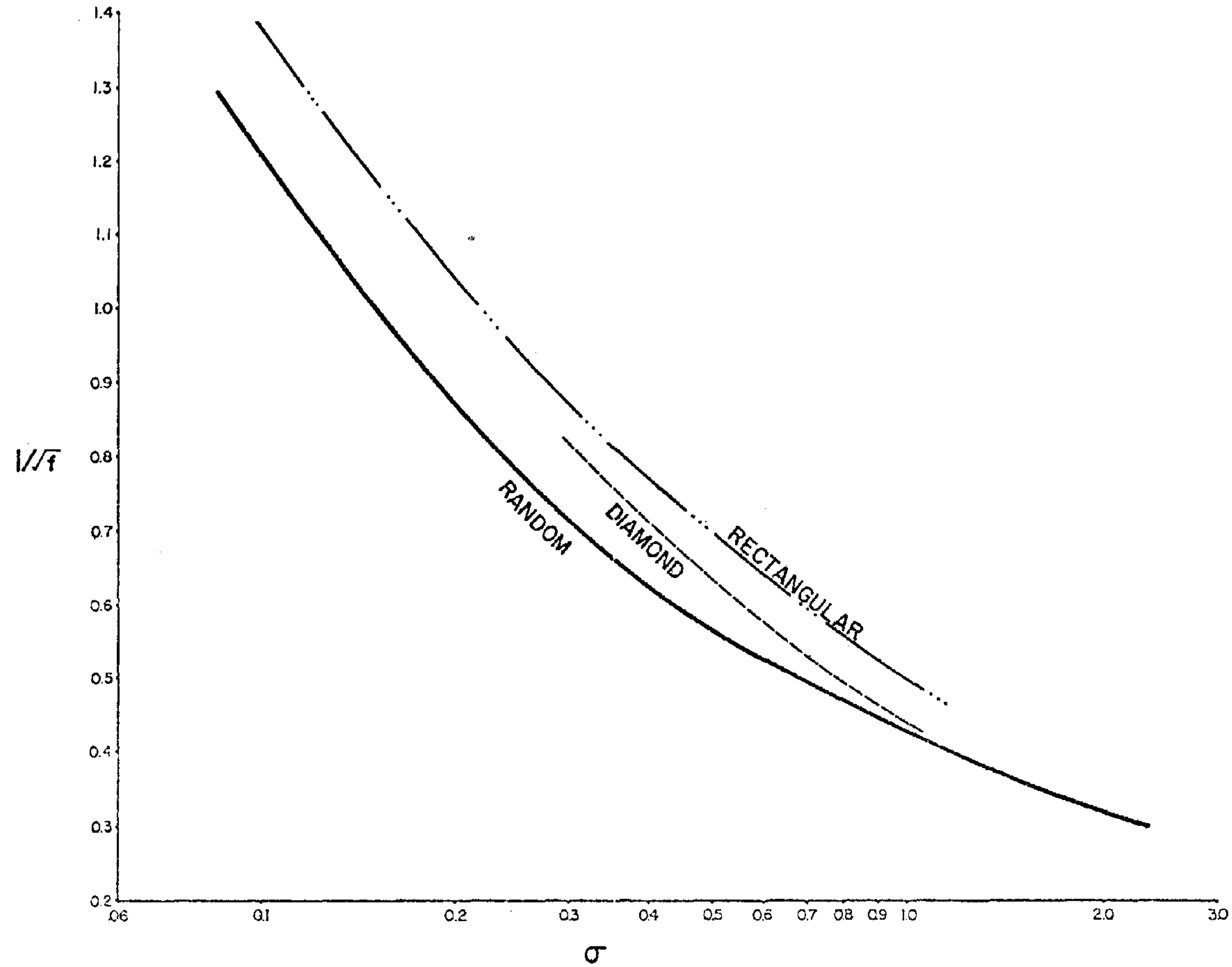

Figure 24. Effect of Roughness Pattern on Channel Resistance

The results shown in Figure 24 suggest that:

1. The regular roughness pattern is capable of producing the kind of roughness field that a random roughness spacing will yield.
2. A diamond pattern of roughness placement more closely reproduces the effects of a random pattern than a rectangular pattern.

These conclusions have been based on a test using 1/4-inch circular roughness elements. It is assumed that other roughness element shapes would obtain similar results, since the basic energy dissipation mechanism associated with the elements remains the same.

CHANNEL RESISTANCE AS A FUNCTION OF CONCENTRATION

The relationships shown in Figures 10 through 15 and 17 through 22 imply that the effect of the depth-width ratio, $\frac{d}{B}$, on the channel resistance is also insignificant. It can then be concluded from Equation 39 that for a given type of roughness element pattern, ξ, the channel resistance, f, is a unique function of the roughness concentration, σ. Thus

$$f = \phi_6(\sigma) \qquad \text{for } \xi = \text{constant.}$$

Such an observation is definitely supported by the results shown in Figures 25 through 34. Figures 25 through 34 also show the relationships of Manning's n to σ. The functional expression for any roughness pattern is

$$f = \alpha\ \sigma^{\beta} \tag{45}$$

or

$$n = \alpha_1\ \sigma^{\beta_1} \tag{46}$$

The values of α, β, α_1 and β_1 are listed in Table 2. These results are considered to be valid for the range of Froude number and Reynold's number tested.

PRACTICAL APPLICATION

In practical application the expressions in Equations 45 and 46 are not sufficiently explicit. It is therefore necessary to use a trial and error method to determine the water depth for a combination of roughness concentration and discharge. This difficulty can be overcome by a plot of y/y_c versus λ (Figures 35 to 37), where y_c is the critical depth and λ is the density of roughness elements. For a given roughness pattern and density the value of λ is determined by

$$\lambda = \frac{N\ b^2}{B\ \Delta x} \tag{47}$$

Entering the value of λ in Figures 35 to 37 yields the value of y/y_c, denoted by ε, for that λ. For a given flow rate and channel geometry

$$y_c = \left(\frac{q^2}{g}\right)^{1/3} \tag{48}$$

where q is the flow rate per unit width of the channel. Finally,

$$y = y_c\ \varepsilon \tag{49}$$

The relationship of Figures 35 to 37 has been derived from test data for a horizontal channel slope. It is recommended that further tests be made in a tilting flume to establish similar relationships for other slopes.

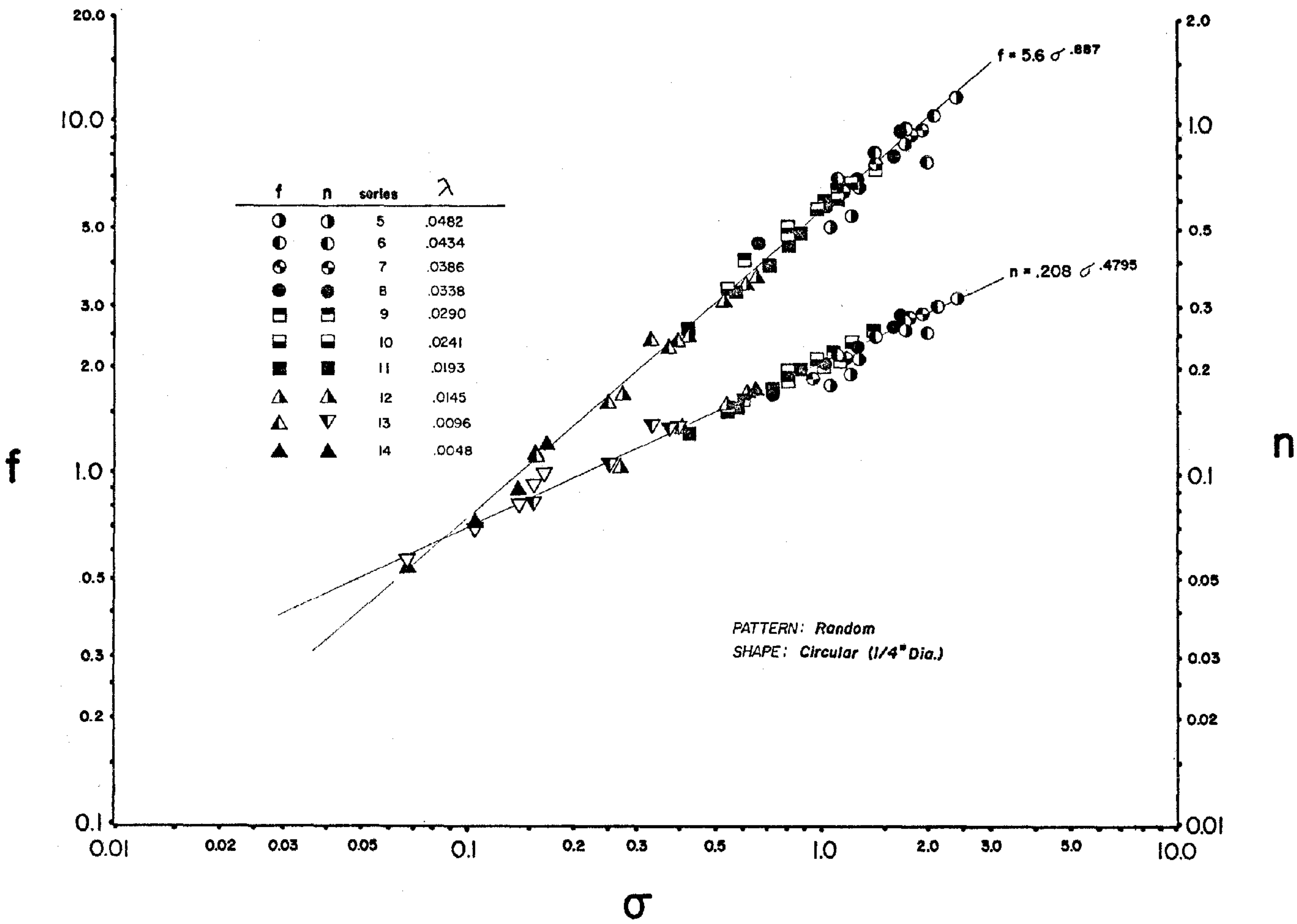

Figure 25. Functional Relationship of Resistance Coefficient to Roughness Concentration (0.08<F<0.21)

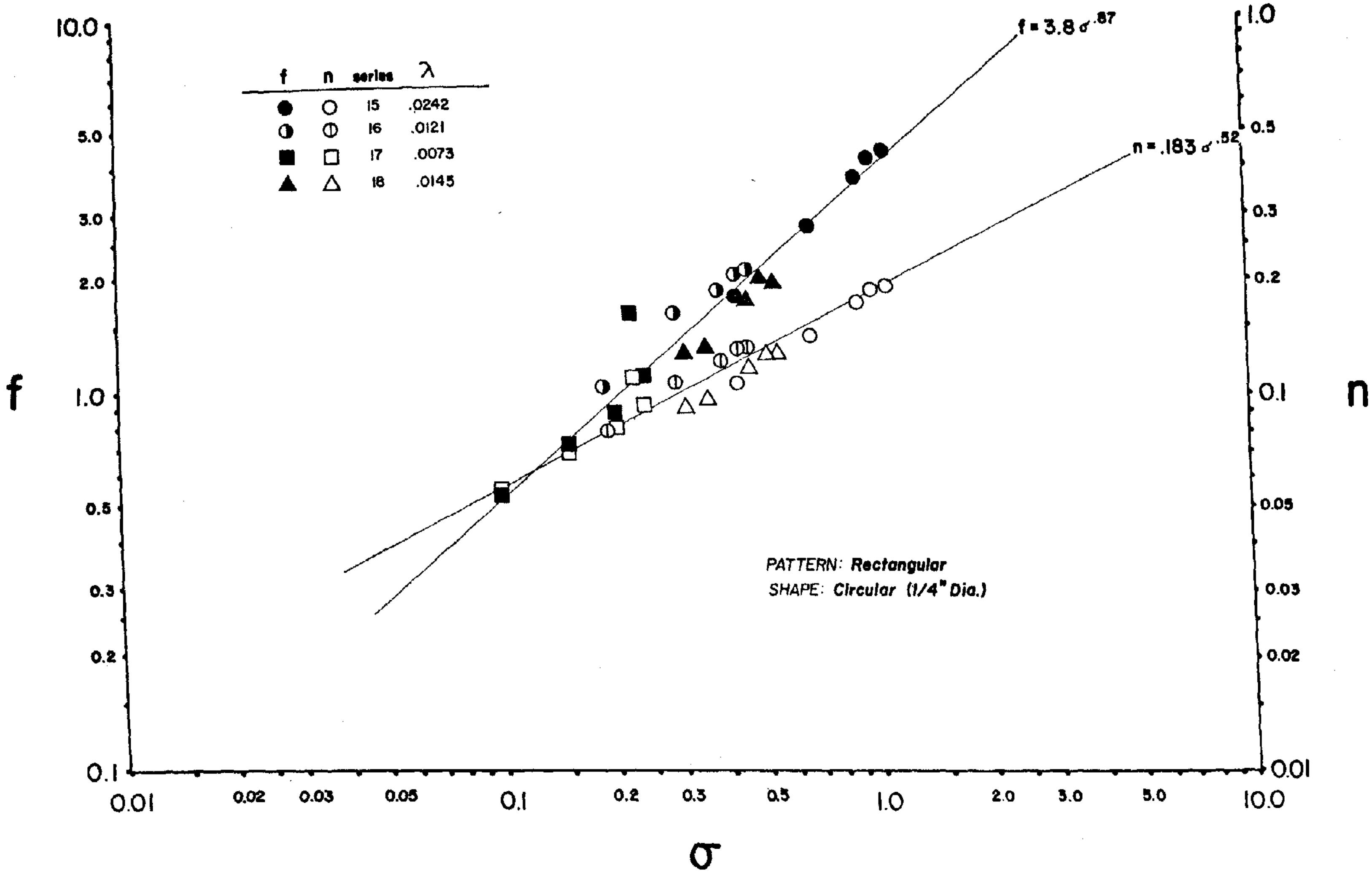

Figure 26. Functional Relationship of Resistance Coefficient to Roughness Concentration (0.08<F<0.21)

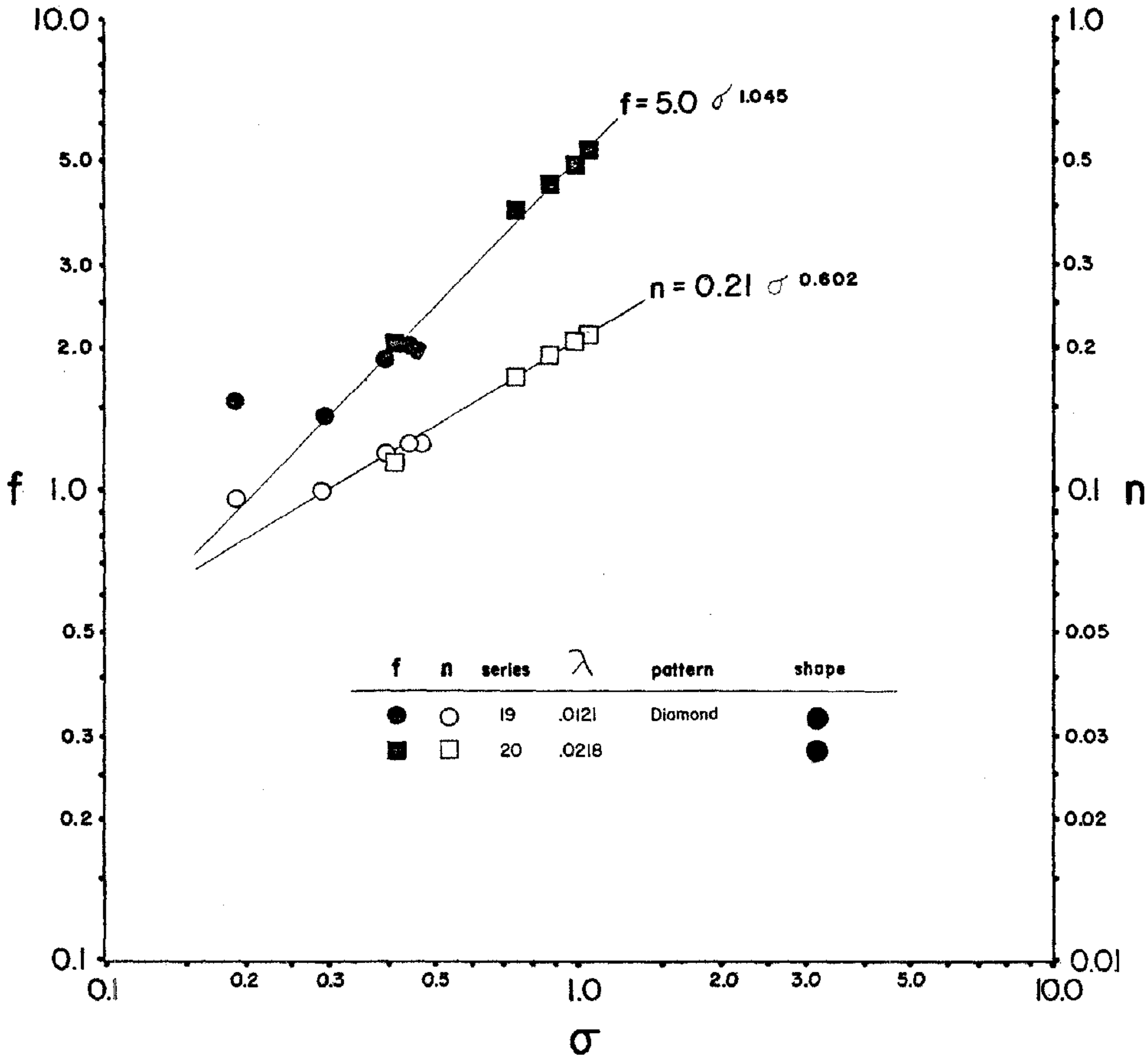

Figure 27. Functional Relationship of Resistance Coefficient to Roughness Concentration (0.08<F<0.21)

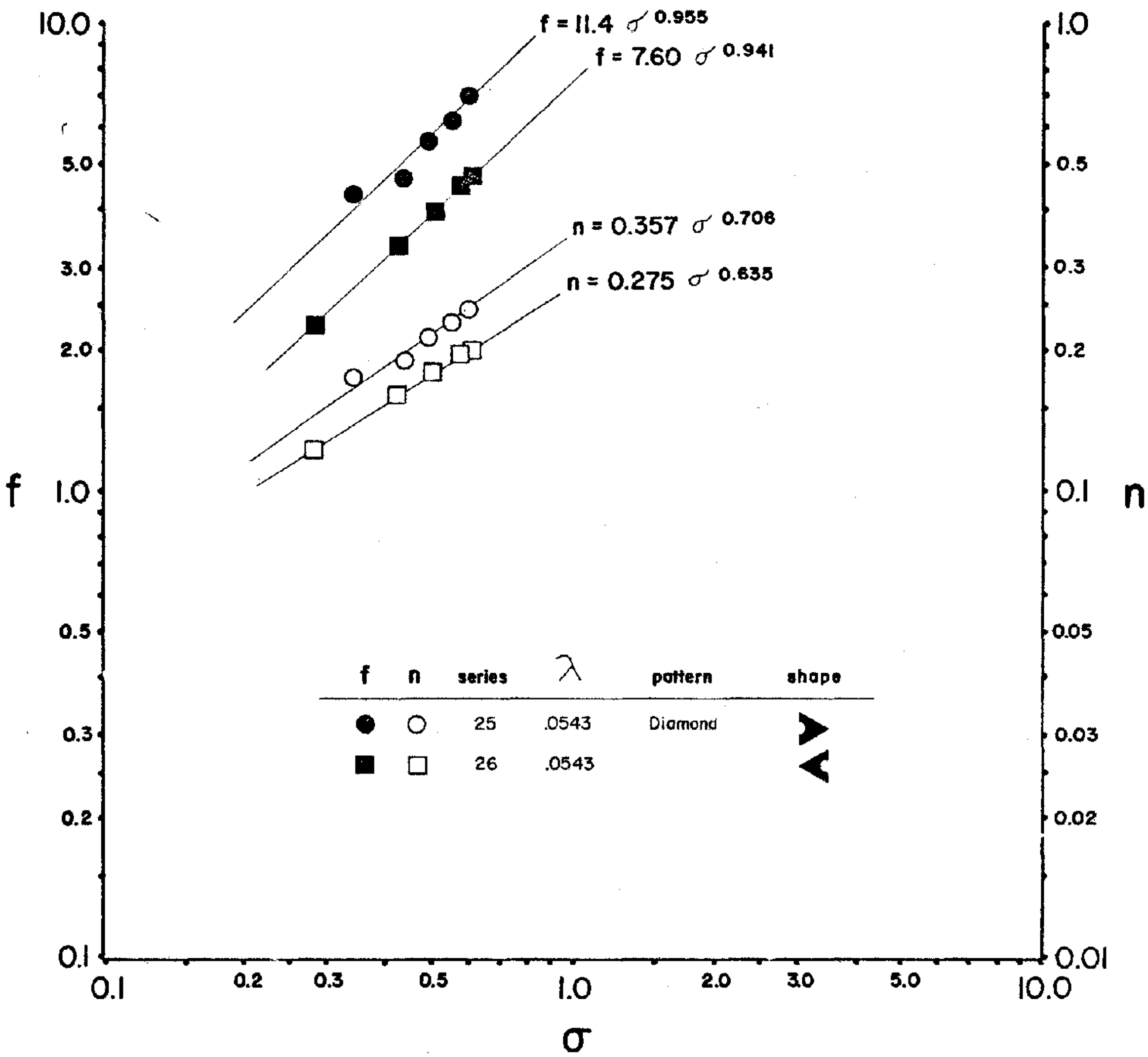

Figure 28. Functional Relationship of Resistance Coefficient to Roughness Concentration (0.08<F<0.21)

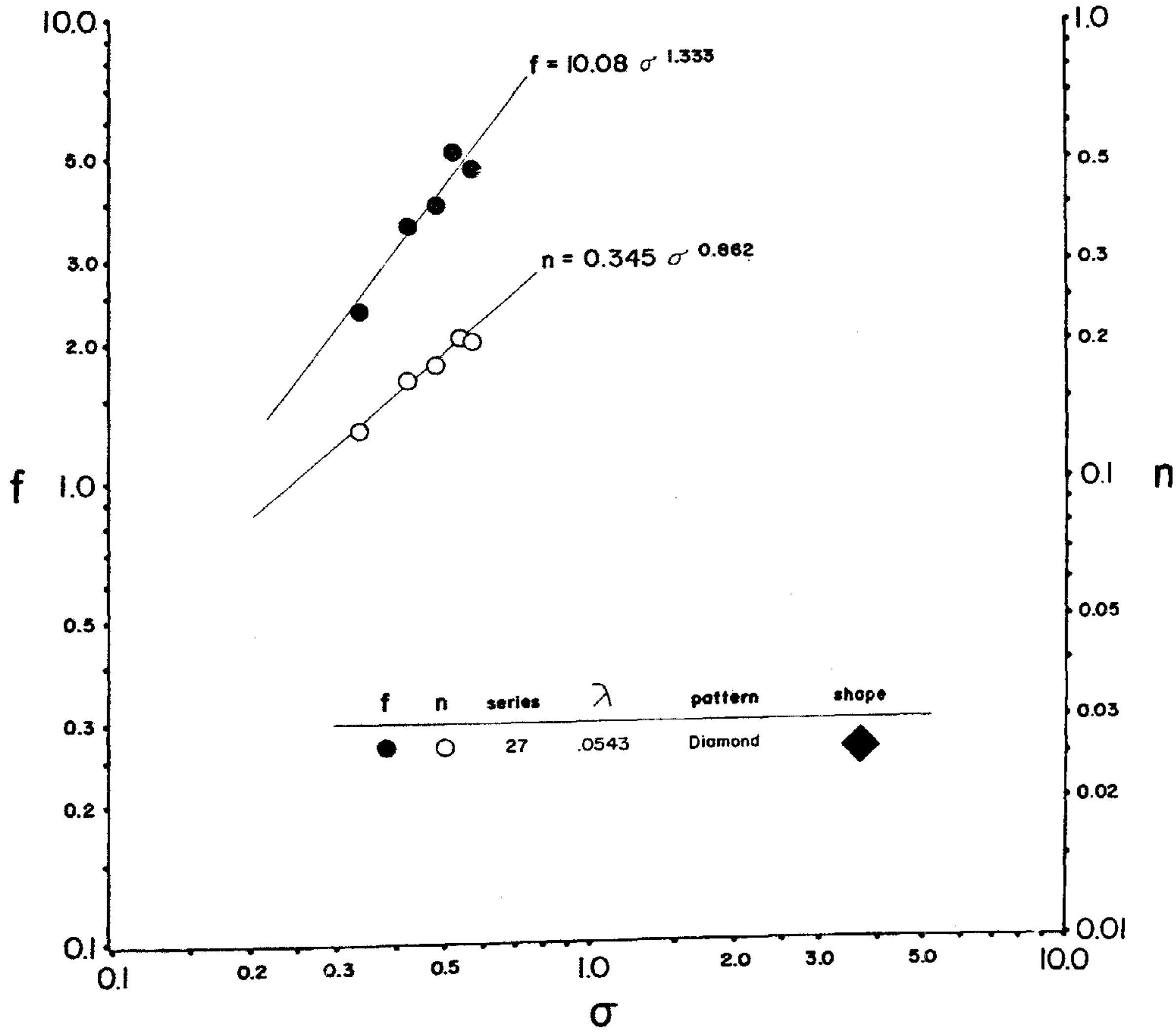

Figure 29. Functional Relationship of Resistance Coefficient to Roughness Concentration (0.08<F<0.21)

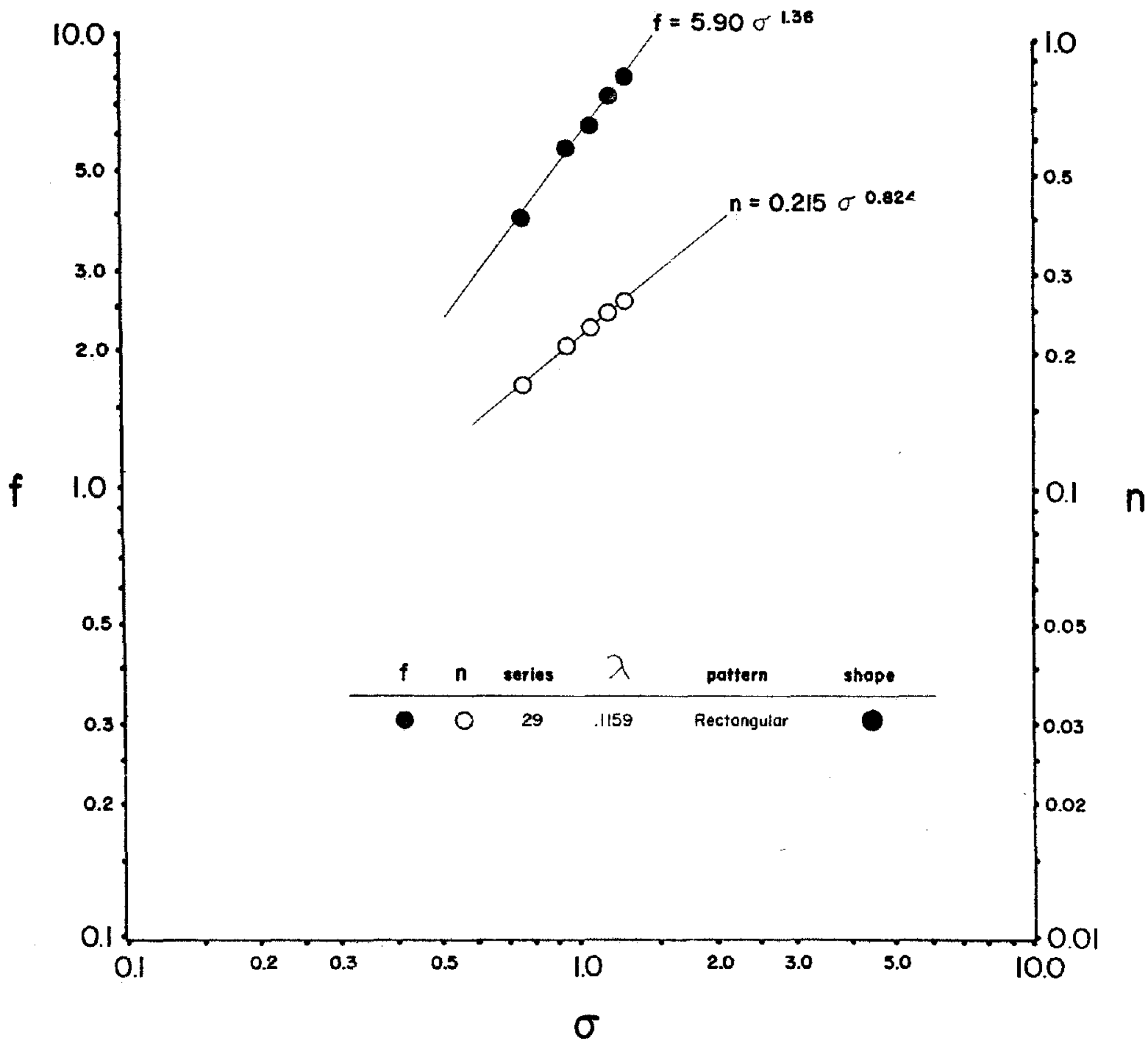

Figure 30. Functional Relationship of Resistance Coefficient to Roughness Concentration (0.08<F<0.21)

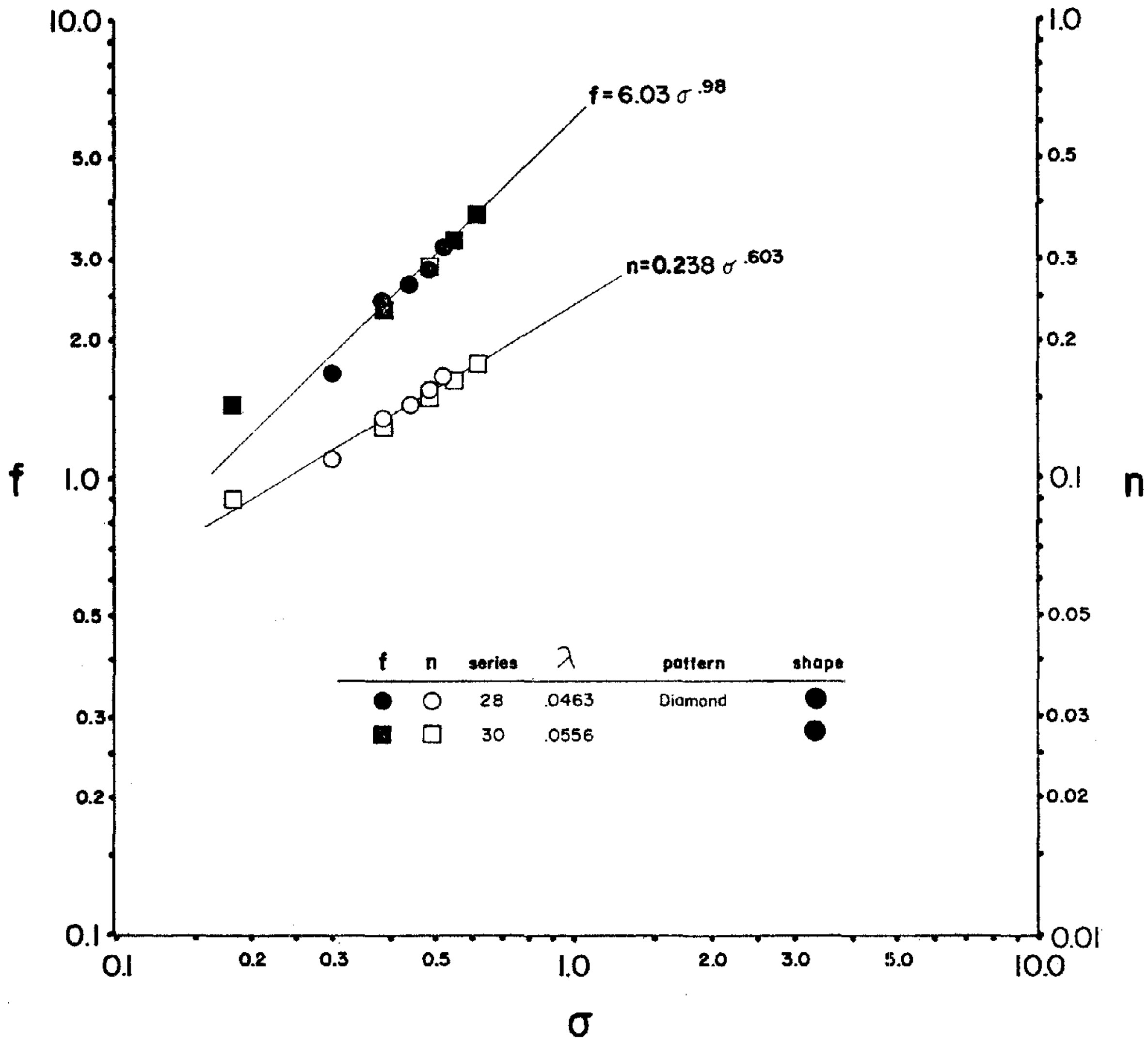

Figure 31. Functional Relationship of Resistance Coefficient to Roughness Concentration (0.08<F<0.21)

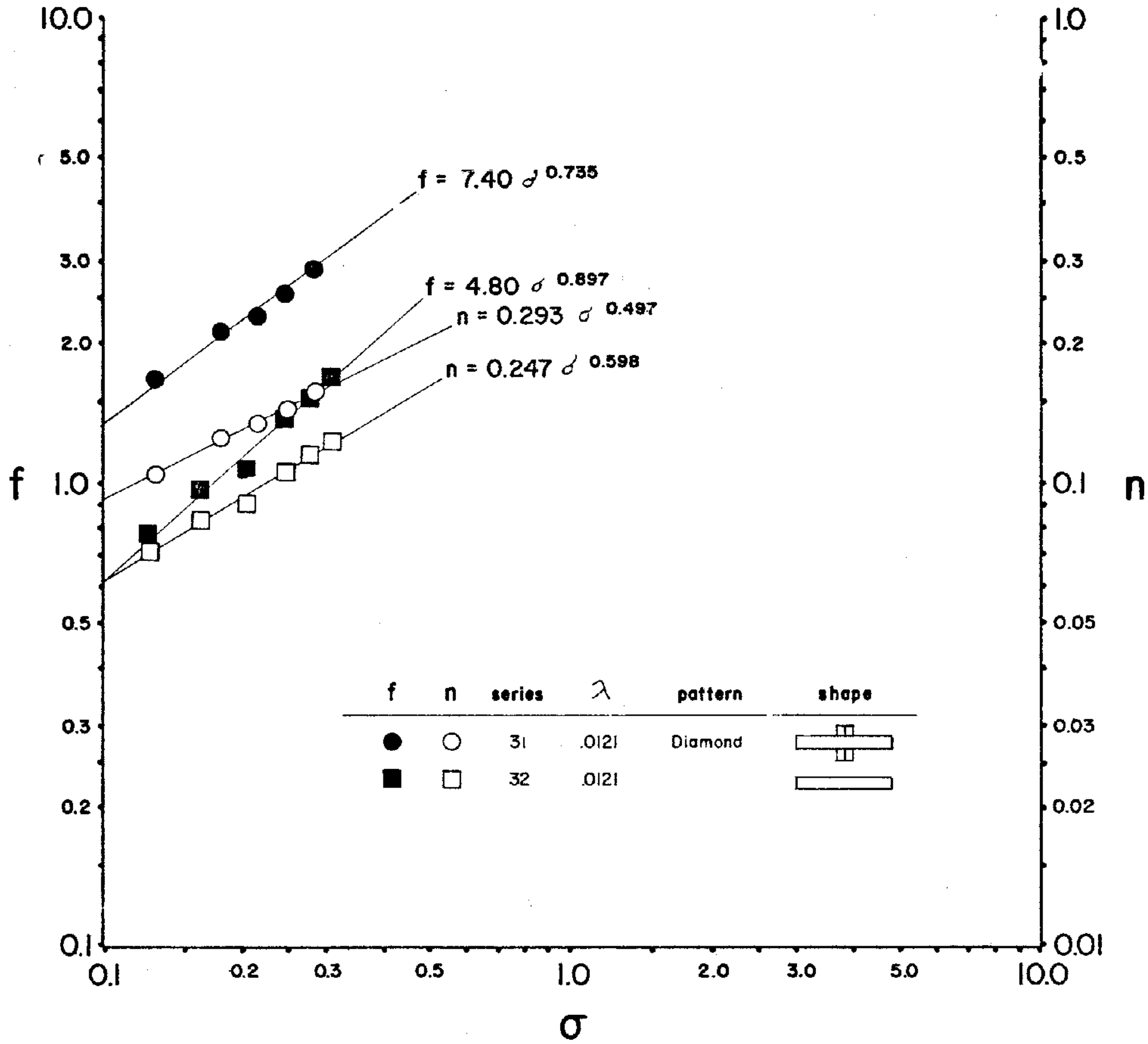

Figure 32. Functional Relationship of Resistance Coefficient to Roughness Concentration (0.08<F<0.21)

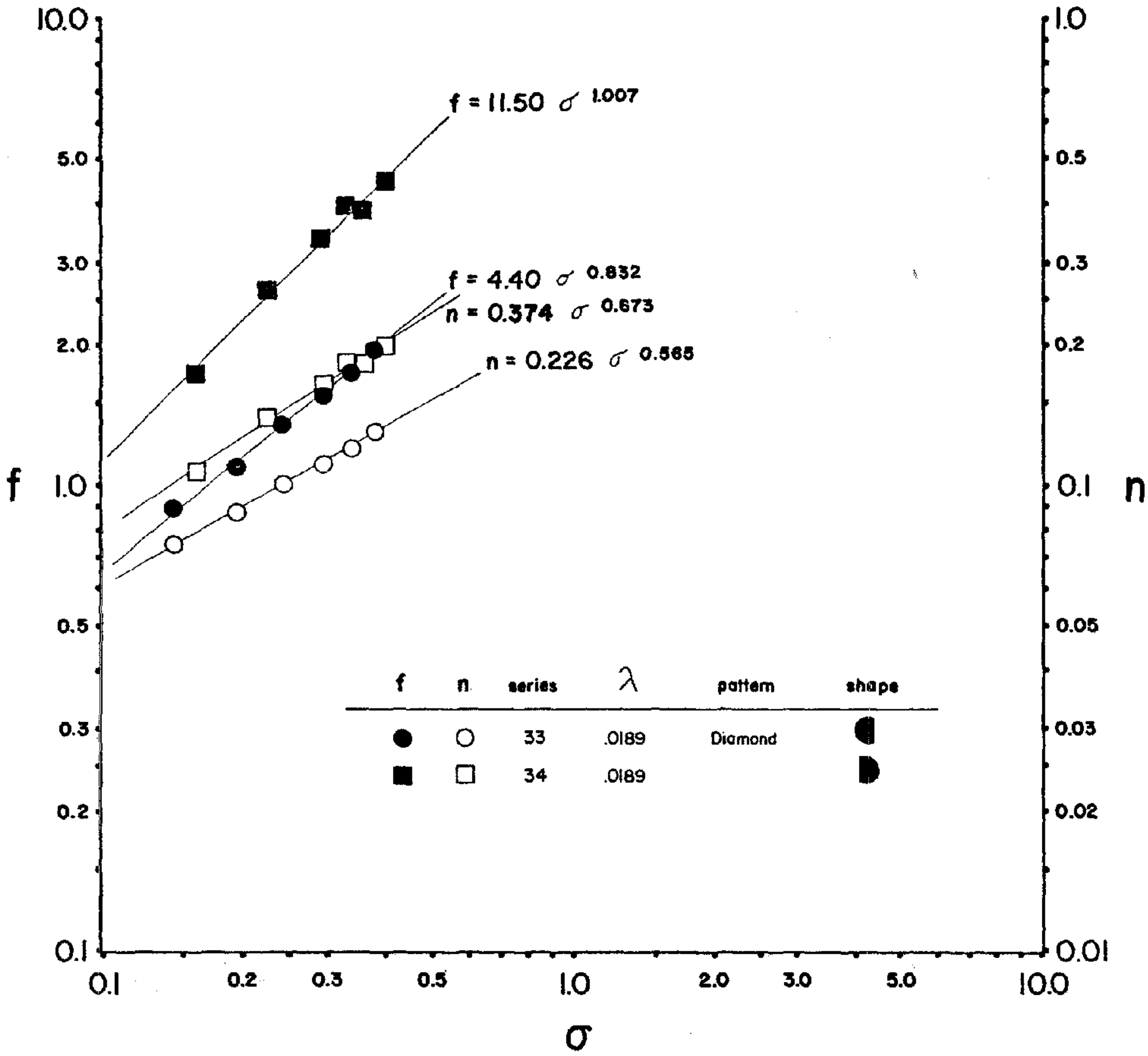

Figure 33. Functional Relationship of Resistance Coefficient to Roughness Concentration (0.08<F<0.21)

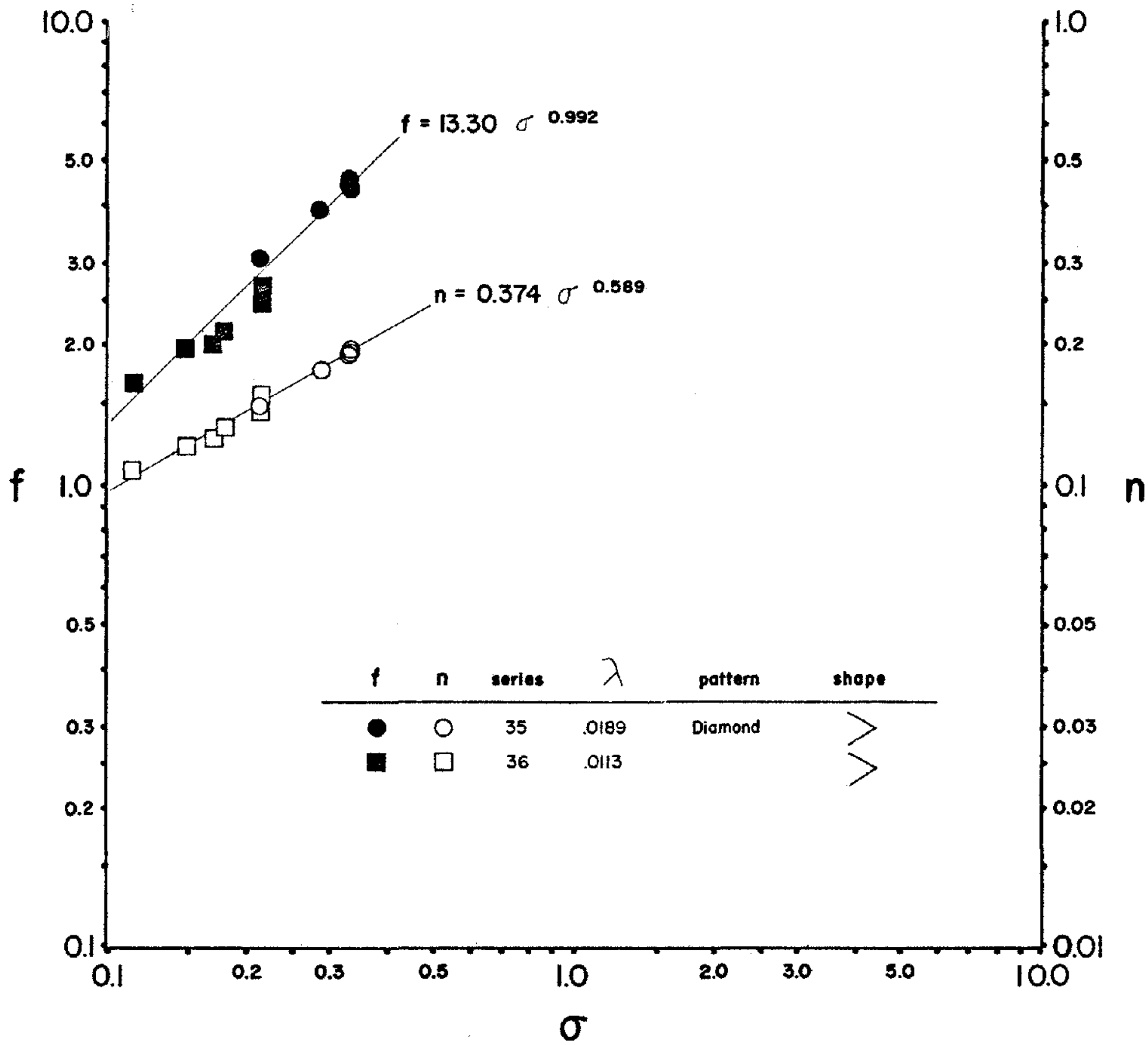

Figure 34. Functional Relationship of Resistance Coefficient to Roughness Concentration (0.08<F<0.21)

Table 2. Values of α, β, α_1 and β_1

Series No.	Roughness Pattern	α	β	α_1	β_1
5-14	Random	5.60	0.887	0.208	0.480
15-18	Rectangular	3.80	0.870	0.183	0.520
19-20	Diamond	5.10	1.045	0.210	0.602
25	Diamond	11.40	0.955	0.357	0.706
26	Diamond	7.60	0.941	0.275	0.635
27	Diamond	10.08	1.333	0.345	0.862
29	Rectangular	5.90	1.360	0.215	0.824
28&30	Diamond	6.03	0.980	0.238	0.603
31	Diamond	7.40	0.735	0.293	0.497
32	Diamond	4.80	0.897	0.247	0.598
33	Diamond	4.40	0.837	0.226	0.565
34	Diamond	11.50	1.007	0.374	0.673
35-36	Diamond	13.30	0.992	0.374	0.589

where $f = \alpha\ \sigma^{\beta}$, and

$n = \alpha_1\ \sigma^{\beta_1}$.

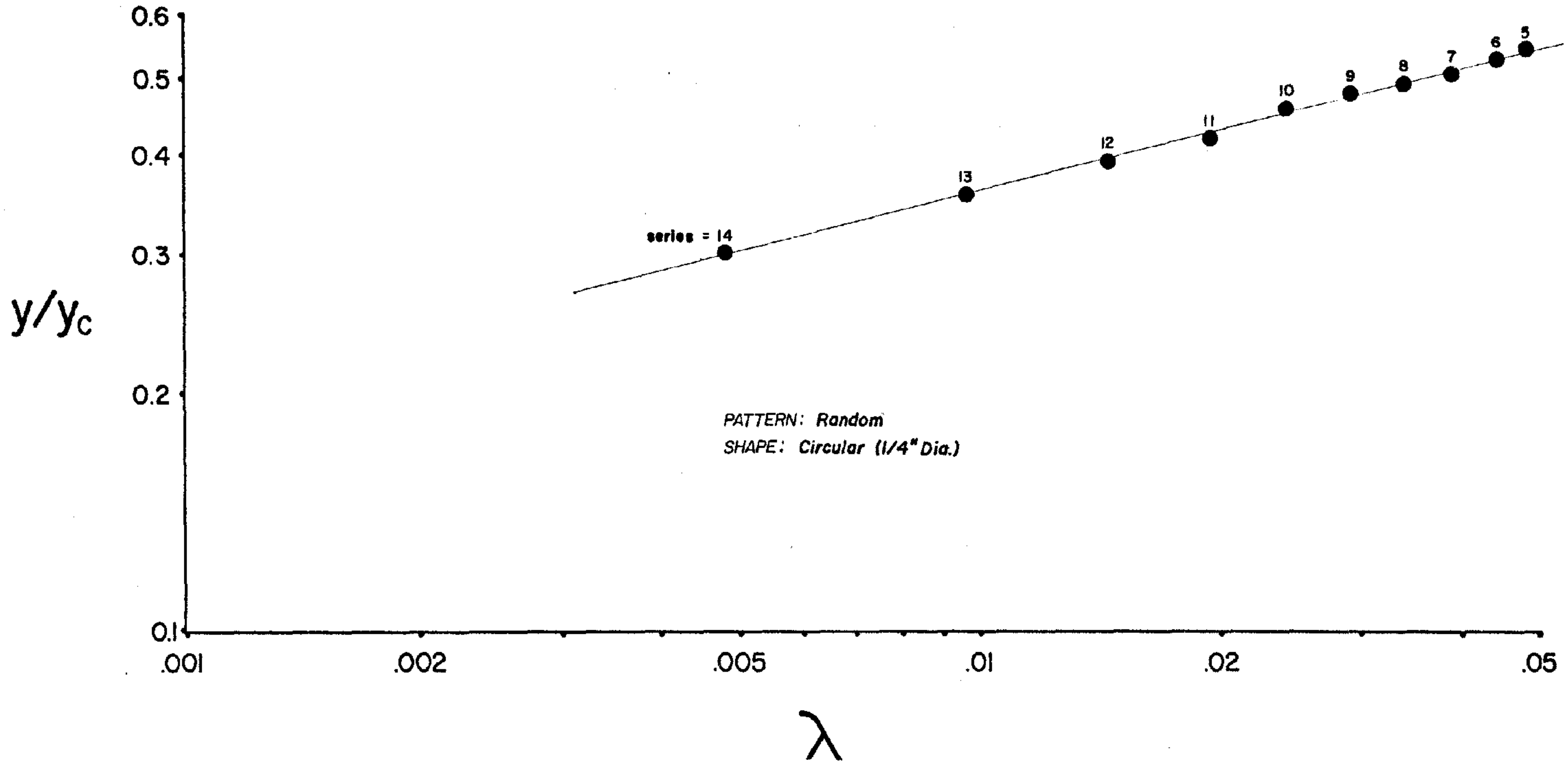

Figure 35. Variation of Depth with Roughness Density

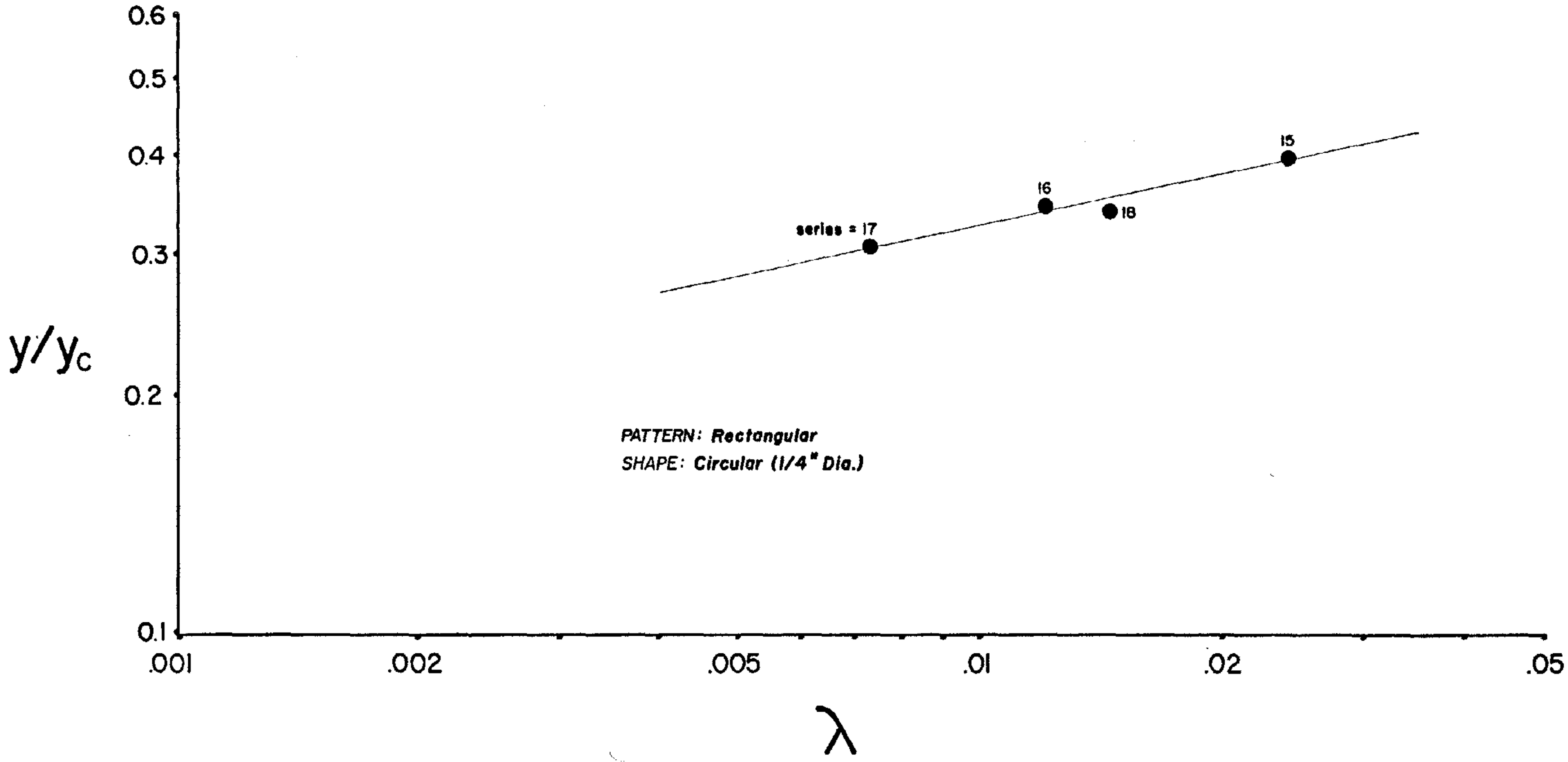

Figure 36. Variation of Depth with Roughness Density

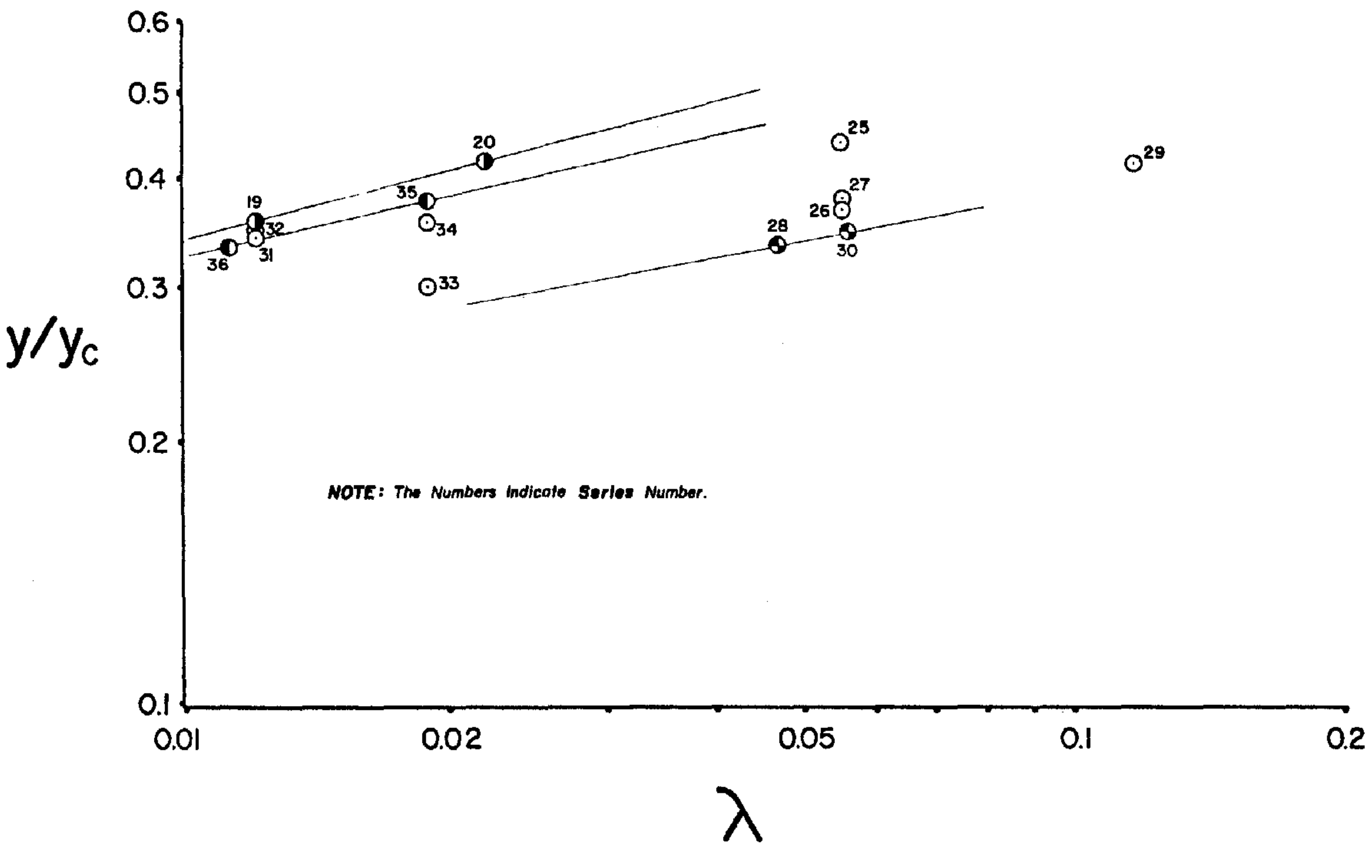

Figure 37. Variation of Depth with Roughness Density

DRAG COEFFICIENTS OF ROUGHNESS ELEMENTS

The drag coefficient of each roughness element is computed according to Equation 24,

$$C_d = \frac{S_f \, y}{\sigma \frac{V^2}{2g}}$$

Drag coefficients computed from the experimental data are presented in Appendix B. For circular cylindrical elements the values of C_d appear to vary with roughness pattern and size. Using data shown by Hoerner in Figure 126 of Reference 14, the calculated drag coefficients for a two-dimensional circular cylinder in the range of Reynolds number tested are between 1.0 to 1.20. This range is lower than that for the test data of this study. The logical explanation of this discrepancy is the occurrence of surface waves in the test flume which causes additional resistance over the data for submerged bodies available in the literature. Test results also show that for circular cylindrical roughness elements the value of C_d tends to increase with the size of the elements. This may be due to (1) a sidewall effect in the test data and/or (2) excessive surface wave generation by the roughness elements.

For the random pattern, C_d varies from 1.0 to 2.0 with an average of 1.40; for the rectangular pattern the average value of C_d is 1.10; and for the diamond pattern the average C_d is 1.25. The low average value of C_d associated with the rectangular pattern is obviously due to the wake interference between the rows. This is evident from a comparison of the data from Series 15 and 16 and from Series 17 and 18. For $\ell/b = 6$, $C_d = 1.0$, and for $\ell/b = 12$, $C_d = 1.25$. The high value of C_d associated with the random pattern appears to be due to the irregular variation in spacing of elements; thus it is not quite comparable to those values of C_d for rectangular and diamond patterns.

A comparison of the values of C_d from experimental data of this study with the data of Reference 14 for various element shapes is shown in Table 3. Note that the values of C_d in the present study are generally greater than those in Reference 14 by an order of 10 to 40 percent. This difference is probably due to the effect of the sidewall and of surface waves. Until other, similar experiments are conducted in a larger flume, however, one can only speculate on the sidewall effect and assume that surface waves are the principal factor in the greater value of C_d.

Table 3. Comparison of Drag Coefficients

Element Shape	Test Data of This Study		Existing Data	
	R	C_d	R	C_d
●	0.6 to 1×10^3	1.25	0.5×10^3	1.20
◆	6×10^3	2.0	10^4 to 10^6	1.55
◖	5×10^3	1.38	10^4 to 10^6	1.16
>	2.5×10^3	3.20	10^4 to 10^6	2.20

The values for C_d determined in this study may be used to compute the channel resistance using Equation 29. Such an alternative method is particularly useful in estimating the resistance field of forested flood plains once the roughness configuration is determined.

SELECTION OF ROUGHNESS PATTERN FOR LARGE FLUME BACKWATER EXPERIMENTS

As stated previously one of the objectives of this study is to determine the roughness patterns to be placed in a large test flume to produce sufficiently high resistance to characterize the flow field in heavily vegetated flood plains. The selection of such roughness patterns is generally governed by 1) ease of installing the roughness elements, 2) degree of roughness in the prototype flood plain, and 3) scale of the model.

Theoretically, when a scale model is used to study the flow characteristics of its prototype, the dynamic similarity must be maintained between the two. This condition requires that the Froude number and Reynolds number be the same in both model and prototype. Unfortunately, it is practically impossible to achieve a dynamically similar scale model if water is used in the model. Hence in practical application it is the normal practice to scale the gravity and adjust the viscous forces by increasing the roughness of the model over the roughness of the prototype. This increase is made by a trial and error process in which the depths and flows in the prototype are measured and the roughness of the model adjusted until the appropriate flows and depths in the prototype are reproduced in the model.

In dealing with river models, the situation is further complicated. Since the laboratory space is usually limited, the model depth is necessarily small, if the same scale is applied to both the horizontal and vertical dimensions. As a result of the shallow depth, the flow in the model may be laminar, the viscous effect becomes significant, and the Froudian model is no longer valid.

The viscous effect is commonly counteracted by the use of different scales for vertical and horizontal dimensions, a so-called distorted model. The vertical (depth) scale is exaggerated in relation to the horizontal (distance or width) scale so as to increase the velocity scale and produce turbulent flow in the model. A distorted model results in increased roughness over the scale model.

The bridge backwater experiments conducted in the large flume were not intended to represent the hydraulics of any site-specific case; rather, they cover a wide range of typical hydraulic characteristics of bridge crossing sites. The kind of roughness field to be installed in the large flume thus must provide sufficient range of variation to characterize the field conditions. Table 1 of Reference (15) shows a range of Manning's roughness coefficients between 0.03 to 0.2 for the flood plains.

The large test flume used in this study was 22 feet wide, 3 feet high and 184 feet long. The bottom slope of the flume was 0.022. The scales for this flume were based upon field data collected by the U. S. Geological Survey (15) for over one hundred streams in the States of Alabama, Louisiana and Mississippi. The scale ratios are:

$$Y_r = 1:12$$

$$X_r = 1:100$$

where Y_r = vertical scale ratio (model/prototype) and

X_r = horizontal scale ratio (model/prototype).

The above scale ratios and the field data of Manning's roughness coefficients, along with the derivations presented in Volume III of this project, give the range of Manning's roughness coefficients to be installed in the large test flume. This range of n is 0.06 - 0.4.

The range of n values required for the large test flume is then used to find a roughness pattern from the small flume test data which satisfies the selection factors given at the beginning of this section. The n vs. σ curves in Figures 23 through 32 are used to select the roughness pattern.[3] For a given value of n (in this case n = 0.4), that pattern is selected which gives least σ, and then for that value of σ, the smallest value of λ is chosen. The pattern thus selected gives the minimum number of roughness elements required to produce the specified roughness field.

In this manner it has been found that the v-shaped metal joists roughness elements in the diamond pattern (i.e., series 35 and 36) yield the best results, and are recommended for use in large flume experiments.

---

[3]For reasons given on page 48, the diamond pattern was selected over the rectangular pattern for the large flume test.

V. CONCLUSIONS

Six major conclusions regarding channel resistance for protruding large scale roughness elements may be drawn from an analysis of the experimental data collected during this study:

1. The Karman-Prandtl type of resistance equation is not applicable to determine the resistance of protruding large scale roughness elements.

2. The effect of Froude number on the channel resistance is not significant for the range of Froude numbers tested (i.e., $F = 0.08 - 0.205$) and the roughness concentration ($\sigma<2.3$) in this study.

3. The channel resistance is not a function of Reynolds number in the range of $10^4 - 10^5$, or the roughness concentration, $\sigma<2.3$.

4. The channel resistance is governed by the roughness pattern and the roughness concentration σ, where

$$\sigma = \frac{N\ b\ y}{B\ \Delta x} \tag{22}$$

5. The equation

$$f = \alpha\ \sigma^{\beta} \tag{50}$$

adequately describes the relationship between the resistance and the roughness concentration in horizontal channels.

6. The drag coefficients of roughness elements may be used to calculate the channel resistance for heavily forested flood plains as an alternative.

LIST OF REFERENCES

1. Keulegan, G. H., "Laws of Turbulent Flow in Open Channels," Research Paper RP-1151, National Bureau of Standards, Vol. 21, December 1938.

2. Prandtl, L., *Vier Abhandlungen zur Hydrodynamik und Aerodynamik,* Göttingen, 1927 (NACA TM 452-1928).

3. Karman, Theodor von, "Mechanische Ähnlichkeit und Turbulenz," *Proceedings, 3rd International Cong. for Applied Mechanics,* Stockholm, 1930.

4. Nikuradse, J., "Strömungsgesetze in Rauhen Röhren," *Forschungsarbeiten auf dem Gebiete des Ingenieur Wesens,* Heft 361, Vol. 4, Berlin, 1933.

5. Sayre, W. W., and M. L. Albertson, "Roughness Spacing in Rigid Open Channels," *J. Hydraulics Div., ASCE,* Vol. 87, No. HY3, May 1961.

6. Robinson, A. R., and M. L. Albertson, "Artificial Roughness Standard for Open Channels," *American Geophysical Union,* Vol. 31, No. 4, August 1950.

7. Einstein, H. A. and R. B. Banks, "Fluid Resistance of Composite Roughness," *Transactions, American Geophysical Union,* Vol. 31, No. 4, August 1950.

8. Barnes, H. H., Jr., "Roughness Characteristics of Natural Channels," U. S. Geological Survey Water Supply Paper 1849, U. S. Government Printing Office, 1967.

9. Chow, V. T., *Open-Channel Hydraulics* (New York: McGraw-Hill Book Co., 1959).

10. Herbich, J. B., and S. Schultis, "Large-Scale Roughness in Open-Channel Flow," *J. Hydraulics Div., ASCE,* Vol. 90, No. HY6, November 1964.

11. Hsieh, Tzeying, "Resistance of Cylindrical Piers in Open-Channel Flow," *J. Hydraulics Div., ASCE,* Vol. 90, No. HY1, January 1964.

Preceding page blank

12. *Standard Mathematical Tables*, The Chemical Rubber Company, 1964.

13. Rouse, Hunter, *Elementary Mechanics of Fluids* (New York: John Wiley & Sons, Inc., 1962), p. 211.

14. Hoerner, S. F., *Fluid-Dynamic Drag* (Self-Published at 2 King Lane, Brick Town, New Jersey, 08723, 1965).

15. Bradley, J. N., "Hydraulics of Bridge Waterways", Hydraulic Design Series No. 1, U. S. Department of Transportation, FHWA, Washington, D. C., 1970.

APPENDIX A

SUMMARY OF TEST DATA

Q = Flow (cfs)

DELX = ΔX = Length of test reach (ft)

B_1 = Channel width at upstream section (ft)

B_2 = Channel width at downstream section (ft)

D_1 = Depth at upstream section (ft)

D_2 = Depth at downstream section (ft)

V_1 = Velocity at upstream section (ft/sec)

V_2 = Velocity at downstream section (ft/sec)

H_1 = Total head at upstream section - referred to as arbitrary datum (ft)

H_2 = Total head at downstream section (ft)

NU = ν = Kinematic viscosity (ft^2/sec)

CONC = Roughness parameter = $\frac{\lambda}{b}$ $(\frac{1}{ft})$

WELM = Width of roughness elements perpendicular to flow direction

INPUT DATA

SERIES NO.	Q	DELX	B1	B2	D1	D2	V1	V2	H1	H2	NU	CONC	KELM
5	.2179	8.063	.771	.750	.765	.695	.369	.418	5.323	5.265	1.54	.1930	.25
5	.3669	8.063	.771	.750	1.076	.985	.442	.497	5.635	5.556	1.54	.1930	.25
5	.1017	8.063	.771	.750	.473	.430	.279	.315	5.030	4.999	1.54	.1930	.25
5	.1397	8.063	.771	.750	.577	.524	.314	.355	5.135	5.093	1.54	.1930	.25
5	.1260	8.063	.771	.750	.543	.496	.306	.344	5.100	5.065	1.54	.1930	.25
6	.3556	8.063	.771	.750	1.036	.948	.445	.500	5.596	5.521	1.57	.1737	.25
6	.3751	8.063	.771	.750	.989	.905	.492	.553	5.550	5.479	1.57	.1737	.25
6	.2631	8.063	.771	.750	.865	.788	.394	.445	5.424	5.360	1.57	.1737	.25
6	.1865	8.063	.771	.750	.709	.645	.345	.390	5.268	5.216	1.57	.1737	.25
6	.1261	8.063	.771	.750	.561	.507	.296	.337	5.119	5.078	1.57	.1737	.25
7	.4012	8.063	.771	.750	1.066	.975	.488	.549	5.627	5.549	1.57	.1544	.25
7	.3557	8.063	.771	.750	.995	.908	.464	.522	5.555	5.481	1.57	.1544	.25
7	.2530	8.063	.771	.750	.800	.726	.410	.463	5.360	5.300	1.57	.1544	.25
7	.1850	8.063	.771	.750	.658	.597	.365	.413	5.217	5.169	1.57	.1544	.25
7	.1315	8.063	.771	.750	.527	.476	.324	.368	5.086	5.047	1.57	.1544	.25

PAGE TWO

SERIES NO.	Q	DELX	B1	B2	D1	D2	V1	V2	H1	H2	NU	CONC	WELM
8	.4037	8.063	.771	.750	1.059	.966	.494	.557	5.620	5.540	1.59	.1351	.25
8	.3952	8.063	.771	.750	1.021	.934	.502	.564	5.582	5.506	1.59	.1351	.25
8	.2735	8.063	.771	.750	.812	.738	.437	.494	5.372	5.311	1.59	.1351	.25
8	.1979	8.063	.771	.750	.661	.598	.388	.441	5.220	5.170	1.59	.1351	.25
8	.1242	8.063	.771	.750	.494	.445	.326	.372	5.053	5.016	1.59	.1351	.25
9	.4270	8.063	.771	.750	1.044	.955	.530	.596	5.605	5.530	1.59	.1158	.25
9	.3080	8.063	.771	.750	.848	.773	.471	.531	5.408	5.346	1.59	.1158	.25
9	.2572	8.063	.771	.750	.758	.689	.440	.498	5.318	5.262	1.59	.1158	.25
9	.1789	8.063	.771	.750	.604	.546	.384	.437	5.163	5.116	1.59	.1158	.25
9	.1086	8.063	.771	.750	.452	.406	.312	.35[illegible]	5.011	4.977	1.59	.1158	.25
10	.4785	8.063	.771	.750	1.078	.988	.576	.646	5.640	5.563	1.54	.0965	.25
10	.3974	8.063	.771	.750	.956	.875	.539	.605	5.518	5.450	1.54	.0965	.25
10	.3308	8.063	.771	.750	.857	781	.501	.565	5.418	5.355	1.54	.0965	.25
10	.2542	8.063	.771	.750	.727	.660	.453	.513	5.267	5.233	1.54	.0965	.25
10	.1362	8.063	.771	.750	.490	.443	.361	.410	5.049	5.015	1.54	.0965	.25

PAGE THREE

SERIES NO.	Q	DELX	B1	B2	D1	D2	V1	V2	H1	H2	NU	CONC	WFLM
11	.4596	8.063	.771	.750	.972	.889	.613	.689	5.535	5.465	1.54	.0772	.25
11	.4061	8.063	.771	.750	.906	.829	.584	.656	5.468	5.405	1.54	.0772	.25
11	.3359	8.063	.771	.750	.796	.728	.547	.615	5.358	5.303	1.54	.0772	.25
11	.2413	8.063	.771	.750	.647	.589	.484	.546	5.208	5.163	1.54	.0772	.25
11	.1464	8.063	.771	.750	.476	.430	.399	.454	5.035	5.002	1.54	.0772	.25
12	.5149	8.063	.771	.750	.972	.892	.687	.770	5.536	5.470	1.46	.0579	.25
12	.4660	8.063	.771	.750	.918	.844	.658	.736	5.482	5.421	1.46	.0579	.25
12	.3885	8.063	.771	.750	.816	.749	.617	.692	5.379	5.325	1.46	.0579	.25
12	.2510	8.063	.771	.750	.619	.565	.526	.592	5.180	5.139	1.46	.0579	.25
12	.1279	8.063	.771	.750	.404	.365	.410	.467	4.964	4.937	1.46	.0579	.25
13	.5085	8.063	.771	.750	.877	.807	.752	.840	5.443	5.387	1.46	.0386	.25
13	.4569	8.063	.771	.750	.823	.760	.720	.802	5.368	5.335	1.46	.0386	.25
13	.3876	8.063	.771	.750	.750	.681	.670	.759	5.314	5.259	1.46	.0386	.25
13	.2520	8.063	.771	.750	.564	.515	.579	.652	5.126	5.091	1.46	.0386	.25
13	.1192	8.063	.771	.750	.354	.318	.437	.500	4.914	4.891	1.46	.0386	.25

PAGE FOUR

SERIES NO.	Q	DELX	B1	B2	D1	D2	V1	V2	H1	H2	NU	CONC	RELM
14	.5140	8.063	.771	.750	.750	.698	.869	.996	5.319	5.272	1.46	.0193	.25
14	.4415	8.063	.771	.750	.698	.638	.858	.964	5.266	5.221	1.46	.0193	.25
14	.3863	8.063	.771	.750	.623	.574	.804	.897	5.190	5.156	1.46	.0193	.25
14	.2477	8.063	.771	.750	.473	.433	.679	.763	5.037	5.011	1.46	.0193	.25
14	.1220	8.063	.771	.750	.306	.275	.517	.591	4.867	4.849	1.46	.0193	.25
15	.5107	8.600	.750	.760	.977	.913	.697	.736	5.549	5.471	1.52	.0966	.25
15	.4534	8.600	.750	.760	.907	.846	.667	.705	5.478	5.404	1.52	.0966	.25
15	.3864	8.600	.750	.760	.818	.766	.633	.667	5.368	5.323	1.52	.0966	.25
15	.2492	8.600	.750	.760	.609	.576	.546	.569	5.178	5.131	1.52	.0966	.25
15	.1232	8.600	.750	.760	.387	.372	.425	.436	4.954	4.925	1.52	.0966	.25
16	.5096	8.600	.750	.760	.638	.789	.811	.850	5.412	5.350	1.52	.0483	.25
16	.4619	8.600	.750	.760	.787	.741	.783	.820	5.361	5.301	1.52	.0483	.25
16	.3925	8.600	.750	.760	.709	.671	.735	.770	5.281	5.230	1.52	.0483	.25
16	.2475	8.600	.750	.760	.532	.505	.620	.645	5.102	5.061	1.52	.0483	.25
16	.1264	8.600	.750	.760	.341	.330	.494	.504	4.909	4.884	1.52	.0483	.25

PAGE FIVE

SERIES NO.	Q	CELX	B1	B2	D1	D2	V1	V2	H1	H2	NU	CONC	KELP
17	.5142	8.600	.750	.760	.726	.692	.944	.978	5.304	5.257	1.52	.0290	.25
17	.3606	8.600	.750	.760	.677	.646	.722	.747	5.249	5.205	1.52	.0290	.25
17	.3984	8.600	.750	.760	.608	.582	.874	.901	5.184	5.145	1.52	.0290	.25
17	.2460	8.600	.750	.760	.453	.437	.724	.741	5.025	4.996	1.52	.0290	.25
17	.1246	8.600	.750	.760	.296	.291	.561	.564	4.865	4.846	1.52	.0290	.25
18	.5128	8.600	.750	.760	.828	.784	.826	.861	5.403	5.346	1.52	.0580	.25
18	.4552	8.600	.750	.760	.775	.732	.783	.818	5.349	5.292	1.52	.0580	.25
18	.3917	8.600	.750	.760	.699	.663	.747	.777	5.272	5.222	1.52	.0580	.25
18	.2546	8.600	.750	.760	.533	.511	.637	.656	5.103	5.068	1.52	.0580	.25
18	.2091	8.600	.750	.760	.470	.450	.593	.611	5.039	5.006	1.52	.0580	.25
19	.5099	8.600	.750	.760	.829	.784	.820	.856	5.403	5.345	1.52	.0483	.25
19	.4565	8.600	.750	.760	.779	.735	.785	.821	5.353	5.295	1.52	.0483	.25
19	.3856	8.600	.750	.760	.702	.663	.732	.765	5.274	5.222	1.52	.0483	.25
19	.2348	8.600	.750	.760	.513	.490	.610	.631	5.083	5.046	1.52	.0483	.25
19	.0928	8.600	.750	.760	.334	.326	.371	.375	4.900	4.878	1.52	.0483	.25

SERIES NO.	Q	DELX	S1	S2	D1	D2	V1	V2	H1	H2	NU	CONC	KELM
20	.5108	8.600	.750	.760	1.039	.971	.663	.700	5.610	5.529	1.49	.0870	.25
20	.4706	8.600	.750	.760	.976	.913	.643	.678	5.546	5.470	1.49	.0870	.25
20	.3810	8.600	.750	.760	.856	.802	.593	.625	5.425	5.358	1.49	.0870	.25
20	.2999	8.600	.750	.760	.734	.691	.545	.571	5.303	5.246	1.49	.0870	.25
20	.1167	8.600	.750	.760	.395	.380	.394	.404	4.961	4.933	1.49	.0870	.25
25	.4550	8.198	.760	.760	1.013	.941	.591	.636	5.820	5.734	1.10	.0512	1.06
25	.4050	8.198	.760	.760	.930	.866	.573	.615	5.737	5.659	1.10	.0512	1.06
25	.3500	8.198	.760	.760	.835	.778	.552	.592	5.642	5.570	1.10	.0512	1.06
25	.2880	8.198	.760	.760	.730	.683	.519	.555	5.536	5.475	1.10	.0512	1.06
25	.1900	8.198	.760	.760	.570	.539	.436	.464	5.379	5.329	1.10	.0512	1.06
26	.6100	8.208	.760	.760	1.058	.943	.759	.851	5.855	5.758	1.10	.0512	1.06
26	.5520	8.208	.760	.760	.994	.884	.731	.822	5.790	5.698	1.10	.0512	1.06
26	.4550	8.208	.760	.760	.874	.775	.685	.772	5.669	5.588	1.10	.0512	1.06
26	.3500	8.208	.760	.760	.734	.646	.627	.713	5.528	5.458	1.10	.0512	1.06
26	.1900	8.208	.760	.760	.492	.428	.508	.584	5.264	5.237	1.10	.0512	1.06

PAGE SEVEN

SERIES NO.	Q	DELX	B1	B2	D1	D2	V1	V2	H1	H2	NU	CONC	RELM
27	.5520	8.208	.760	.760	1.008	.895	.721	.812	5.804	5.709	1.06	.0512	1.06
27	.4550	8.208	.760	.760	.936	.831	.640	.720	5.730	5.643	1.06	.0512	1.06
27	.4320	8.208	.760	.760	.855	.757	.665	.751	5.650	5.570	1.06	.0512	1.06
27	.3500	8.208	.760	.760	.748	.659	.616	.699	5.542	5.471	1.06	.0512	1.06
27	.2520	8.208	.760	.760	.592	.527	.560	.629	5.385	5.337	1.06	.0512	1.06
28	.6450	8.208	.760	.760	.996	.888	.852	.956	5.795	5.706	1.06	.0463	1.00
28	.5750	8.208	.760	.760	.920	.821	.822	.922	5.719	5.638	1.06	.0463	1.00
28	.5000	8.208	.760	.760	.837	.745	.786	.885	5.635	5.561	1.06	.0463	1.00
28	.4050	8.208	.760	.760	.734	.649	.726	.821	5.530	5.463	1.06	.0463	1.00
28	.2350	8.208	.760	.760	.579	.515	.648	.726	5.374	5.327	1.06	.0463	1.00
29	.4520	8.208	.760	.760	.988	.851	.602	.699	5.782	5.663	1.06	.1159	1.00
29	.4120	8.208	.760	.760	.917	.767	.591	.689	5.710	5.598	1.06	.1159	1.00
29	.3570	8.208	.760	.760	.836	.727	.561	.646	5.631	5.537	1.06	.1159	1.00
29	.2900	8.208	.760	.760	.734	.634	.520	.602	5.526	5.444	1.06	.1159	1.00
29	.1950	8.208	.760	.760	.581	.513	.442	.500	5.372	5.321	1.06	.1159	1.00

PAGE EIGHT

SERIES NO.	Q	DELX	B1	B2	D1	D2	V1	V2	H1	H2	NU	CONC	WELM
30	.5950	8,208	.760	.760	.975	.860	.803	.910	5.773	5.677	1.06	.0556	1.00
30	.5130	8.208	.760	.760	.873	.766	.773	.881	5.670	5.582	1.06	.0556	1.00
30	.4320	8.208	.760	.760	.780	.684	.729	.831	5.576	5.499	1.06	.0556	1.00
30	.3150	8.208	.760	.760	.629	.548	.659	.756	5.428	5.361	1.06	.0556	1.00
30	.0850	8.208	.760	.760	.296	.250	.378	.447	5.086	5.057	1.06	.0556	1.00
31	.6810	8.208	.760	.760	1.026	.927	.873	.967	5.812	5.732	1.12	.0242	.50
31	.5530	8.208	.760	.760	.896	.807	.812	.902	5.680	5.610	1.12	.0242	.50
31	.4490	8.208	.760	.760	.782	.701	.755	.843	5.565	5.502	1.12	.0242	.50
31	.3290	8.208	.760	.760	.652	.579	.664	.748	5.433	5.378	1.12	.0242	.50
31	.1950	8.208	.760	.760	.478	.421	.537	.609	5.256	5.217	1.12	.0242	.50
32	.9830	8.208	.760	.760	1.109	1.011	1.166	1.297	5.904	5.826	1.10	.0242	.50
32	.8190	8.208	.760	.760	.951	.904	1.087	1.192	5.783	5.716	1.10	.0242	.50
32	.6780	8.208	.760	.760	.878	.800	1.016	1.115	5.668	5.609	1.10	.0242	.50
32	.5090	8.208	.760	.760	.732	.668	.915	1.003	5.519	5.474	1.10	.0242	.50
32	.3610	8.208	.760	.760	.590	.532	.805	.893	5.374	5.334	1.10	.0242	.50
32	.2350	8.208	.760	.760	.454	.406	.681	.762	5.235	5.205	1.10	.0242	.50

PAGE NINE

SERIES NO.	Q	DELX	B1	B2	D1	D2	V1	V2	H1	H2	NU	CONC	WELM
33	.8990	8.208	.760	.760	1.066	.987	1.069	1.138	5.878	5.799	1.10	.0302	.63
33	.7560	8.208	.760	.760	.970	.880	1.028	1.133	5.760	5.690	1.10	.0302	.63
33	.6170	8.208	.760	.760	.852	.771	.953	1.053	5.640	5.578	1.10	.0302	.63
33	.4530	8.208	.760	.760	.706	.636	.844	.937	5.491	5.440	1.10	.0302	.63
33	.3210	8.208	.760	.760	.567	.508	.745	.831	5.350	5.309	1.10	.0302	.63
33	.1950	8.208	.760	.760	.418	.369	.614	.695	5.198	5.167	1.10	.0302	.63
34	.7520	8.208	.760	.760	1.169	1.046	.846	.946	5.954	5.850	1.08	.0302	.63
34	.6320	8.208	.760	.760	1.037	.928	.802	.896	5.821	5.730	1.08	.0302	.63
34	.5560	8.208	.760	.760	.970	.864	.754	.847	5.753	5.665	1.08	.0302	.63
34	.4570	8.208	.760	.760	.841	.745	.715	.807	5.623	5.545	1.08	.0302	.63
34	.3110	8.208	.760	.760	.661	.585	.619	.700	5.441	5.383	1.08	.0302	.63
34	.1870	8.208	.760	.760	.468	.410	.526	.600	5.246	5.206	1.08	.0302	.63

PAGE TEN

SERIES NO.	Q	DELX	B1	B2	D1	D2	V1	V2	H1	H2	NU	CONC	WELM
35	.5192	8.062	.760	.760	.960	.874	.712	.782	5.806	5.720	1.70	.0302	.63
35	.5256	8.062	.760	.760	.963	.877	.718	.789	5.809	5.724	1.70	.0302	.63
35	.5294	8.062	.760	.760	.968	.878	.720	.793	5.814	5.725	1.70	.0302	.63
35	.5192	8.062	.760	.760	.954	.866	.716	.789	5.800	5.713	1.70	.0302	.63
35	.4977	8.062	.760	.760	.921	.834	.697	.769	5.767	5.680	1.70	.0302	.63
35	.4108	8.062	.760	.760	.820	.744	.659	.726	5.665	5.589	1.70	.0302	.63
35	.2676	8.062	.760	.760	.618	.559	.570	.630	5.461	5.402	1.70	.0302	.63
36	.7712	8.062	.760	.760	1.039	.945	.977	1.074	5.841	5.751	1.70	.0181	.63
36	.7639	8.062	.760	.760	1.028	.942	.978	1.067	5.830	5.748	1.70	.0181	.63
36	.5764	8.062	.760	.760	.858	.783	.884	.969	5.657	5.586	1.70	.0181	.63
36	.5342	8.062	.760	.760	.817	.746	.860	.940	5.615	5.550	1.70	.0181	.63
36	.4291	8.062	.760	.760	.713	.647	.792	.873	5.510	5.447	1.70	.0181	.63
36	.2684	8.062	.760	.760	.548	.500	.645	.706	5.341	5.296	1.70	.0181	.63

APPENDIX B

SUMMARY OF TEST RESULTS

The following notations are used in this Appendix:

FR = Froude Number ($\mathbf{F}$) = $\dfrac{V}{\sqrt{gy}}$

RE = Reynolds Number ($\mathbf{R}$) = $\dfrac{VY}{\nu}$

REB = Reynolds Number of element = $\dfrac{Vb}{\nu}$

SIGMA = σ = roughness concentration = $\dfrac{\lambda y}{b}$

$\dfrac{D}{B}$ = Depth-width ratio = $\dfrac{y}{B}$

CD = C_d = Drag coefficient of elements

1/SQRTF = $1/\sqrt{f}$

CHEZYC = Chezy's C

N = Manning's n

D/W = y/b

LAMBDA = = $\dfrac{Nb^2}{B\Delta X}$

D/Yc = y/Yc

Preceding page blank

SUMMARY OF DATA ANALYSIS

SERIES NO.	FR	HF	HEB	SIGMA	D/B	F	CD	1/SQRTF	CHEZY C	W	D/W	LAMBDA	D/YC
5	.051	.75	.53	1.691	.960	8.736	1.292	.338	5.430	.260	35.040	.0482	5.344
5	.082	1.26	.64	2.387	1.355	11.799	1.236	.291	4.672	.320	49.464	.0482	5.330
5	.078	.35	.40	1.046	.594	5.069	1.212	.444	7.128	.183	21.672	.0482	5.493
5	.079	.48	.45	1.275	.724	6.602	1.295	.389	6.247	.216	26.424	.0482	5.420
5	.079	.44	.44	1.203	.683	5.500	1.143	.426	6.644	.195	24.936	.0482	5.422
6	.084	1.19	.63	2.068	1.304	10.647	1.287	.306	4.919	.303	47.616	.0434	5.239
6	.095	1.26	.69	1.974	1.245	7.868	.997	.356	5.722	.258	45.456	.0434	4.826
6	.081	.88	.56	1.723	1.087	9.603	1.394	.323	5.179	.279	39.672	.0434	5.336
6	.079	.63	.49	1.411	.890	8.328	1.475	.347	5.562	.251	32.496	.0434	5.458
6	.076	.43	.42	1.113	.702	6.963	1.568	.378	6.074	.221	25.632	.0434	5.570
7	.090	1.35	.69	1.891	1.342	9.459	1.251	.325	5.218	.286	48.984	.0386	4.973
7	.089	1.20	.65	1.763	1.251	9.255	1.312	.329	5.276	.280	45.672	.0386	5.024
7	.088	.85	.58	1.416	1.005	7.666	1.358	.361	5.789	.246	36.672	.0386	5.062
7	.087	.62	.52	1.163	.825	6.359	1.367	.397	6.365	.217	30.120	.0386	5.123
7	.066	.44	.46	.929	.659	5.220	1.404	.438	7.025	.189	24.072	.0386	5.140

PAGE TWO

SERIES NO.	FR	RE	REO	SIGMA	D/B	F	CD	1/SQRTF	CHEZY C	N	D/W	LAMBDA	D/YC
8	.092	1.34	.69	1.641	1.331	9.371	1.427	.327	5.243	.285	48.600	.0338	4.913
8	.095	1.31	.70	1.565	1.285	8.135	1.283	.351	5.627	.264	46.920	.0338	4.811
8	.093	.91	.61	1.256	1.019	6.970	1.387	.379	6.079	.235	37.200	.0338	4.875
8	.092	.66	.54	1.021	.828	5.853	1.434	.413	6.634	.208	30.216	.0338	4.913
8	.090	.41	.46	.761	.617	4.557	1.497	.468	7.519	.175	22.536	.0338	4.999
9	.099	1.42	.74	1.389	1.314	7.556	1.360	.364	5.839	.255	47.976	.0290	4.672
9	.098	1.02	.66	1.126	1.066	6.396	1.420	.395	6.346	.227	38.904	.0290	4.711
9	.097	.85	.61	1.005	.951	5.865	1.463	.412	6.616	.213	34.728	.0290	4.742
9	.095	.59	.54	.799	.756	4.906	1.535	.451	7.246	.188	27.600	.0290	4.800
9	.090	.36	.44	.596	.564	4.165	1.747	.490	7.865	.165	20.592	.0290	4.996
10	.106	1.64	.83	1.196	1.358	6.807	1.423	.383	6.152	.244	49.584	.0241	4.476
10	.105	1.36	.77	1.060	1.204	6.079	1.433	.406	6.510	.226	43.944	.0241	4.489
10	.104	1.13	.72	.948	1.077	5.803	1.530	.415	6.663	.216	39.312	.0241	4.539
10	.102	.87	.65	.803	.912	5.129	1.597	.442	7.087	.198	33.288	.0241	4.581
10	.099	.47	.52	.540	.613	3.410	1.578	.542	8.692	.151	22.392	.0241	4.671

PAGE THREE

SERIES NO.	FR	RE	REM	SIGMA	D/B	F	CD	1/SQRTF	CHEZY C	N	D/W	LAMBDA	D/YC
11	.119	1.57	.88	.862	1.224	4.910	1.424	.451	7.243	.203	44.664	.0193	4.141
11	.117	1.40	.84	.804	1.141	4.542	1.413	.469	7.531	.193	41.640	.0193	4.179
11	.117	1.15	.79	.706	1.002	3.967	1.405	.502	8.059	.177	36.576	.0193	4.180
11	.115	.83	.70	.573	.613	3.350	1.463	.546	8.769	.157	29.664	.0193	4.226
11	.112	.50	.56	.420	.596	2.626	1.564	.617	9.905	.132	21.744	.0193	4.323
12	.133	1.66	1.04	.648	1.226	3.703	1.430	.520	8.341	.177	44.736	.0145	3.645
12	.131	1.68	.99	.612	1.158	3.534	1.443	.532	8.537	.171	42.286	.0145	3.685
12	.130	1.40	.93	.544	1.029	3.151	1.449	.563	9.041	.158	37.560	.0145	3.696
12	.126	.91	.80	.411	.778	2.482	1.508	.635	10.188	.134	26.416	.0145	3.944
12	.125	.46	.63	.267	.506	1.725	1.614	.761	12.220	.104	18.456	.0145	4.015
13	.153	1.84	1.14	.390	1.107	2.378	1.524	.649	10.409	.139	40.416	.0096	3.503
13	.151	1.65	1.09	.367	1.041	2.314	1.578	.657	10.550	.136	37.992	.0096	3.537
13	.149	1.40	1.02	.331	.941	2.463	1.856	.637	10.227	.138	34.344	.0096	3.568
13	.148	.91	.88	.250	.709	1.592	1.593	.792	12.719	.106	25.896	.0096	3.584
13	.142	.43	.67	.156	.442	1.125	1.607	.943	15.133	.082	16.128	.0096	3.677

PAGE FOUR

SERIES NO.	FR	RE	REB	SIGMA	D/P	F	CD	1/SQRTF	CHEZY C	N	D/W	LAMBDA	D/YC
14	.176	1.86	1.34	.167	.905	1.215	1.825	.907	14.558	.097	34.512	.0048	2.970
14	.196	1.67	1.30	.155	.878	1.157	1.870	.930	14.920	.093	32.064	.0048	2.965
14	.194	1.39	1.21	.139	.787	.899	1.621	1.055	16.930	.081	26.728	.0048	2.991
14	.189	.89	1.03	.105	.596	.724	1.725	1.175	18.865	.069	21.744	.0048	3.044
14	.181	.44	.79	.067	.382	.544	2.023	1.355	21.754	.056	13.944	.0048	3.130
15	.130	1.76	.98	1.095	1.252	4.301	.982	.482	7.739	.191	45.360	.0242	3.902
15	.129	1.58	.94	1.016	1.161	4.128	1.016	.492	7.899	.185	42.072	.0242	3.916
15	.129	1.35	.89	.918	1.049	3.650	.994	.523	8.401	.171	38.016	.0242	3.925
15	.126	.87	.76	.687	.785	2.684	.977	.610	9.797	.139	28.440	.0242	3.947
15	.123	.43	.59	.440	.503	1.779	1.011	.750	12.034	.105	18.216	.0242	4.043
16	.162	1.78	1.14	.472	1.077	2.190	1.161	.676	10.845	.133	39.048	.0121	3.363
16	.162	1.61	1.10	.443	1.012	2.137	1.207	.684	10.976	.130	36.672	.0121	3.373
16	.160	1.37	1.03	.400	.914	1.854	1.159	.734	11.787	.119	33.120	.0121	3.395
16	.155	.86	.87	.301	.687	1.592	1.324	.793	12.722	.105	24.658	.0121	3.470
16	.152	.44	.66	.194	.444	1.009	1.297	.996	15.978	.078	16.104	.0121	3.514

PAGE FIVE

SERIES NO.	FR	RE	REB	SIGMA	D/P	F	CD	1/SQRTF	CHEZY C	N	D/W	LAMBDA	U/YC
17	.201	1.79	1.32	.247	.939	1.081	1.095	.962	15.438	.091	34.032	.0073	2.914
17	.159	1.26	1.01	.230	.676	1.615	1.755	.787	12.626	.110	31.752	.0073	3.407
17	.203	1.39	1.22	.207	.786	.862	1.065	1.065	17.085	.080	28.560	.0073	2.899
17	.194	.56	1.00	.155	.589	.720	1.163	1.178	18.909	.069	21.360	.0073	2.990
17	.183	.43	.77	.102	.389	.528	1.292	1.376	22.090	.055	14.088	.0073	3.103
18	.166	1.79	1.16	.501	1.068	1.934	.862	.719	11.541	.125	38.688	.0145	3.319
18	.163	1.59	1.10	.524	.998	2.008	.957	.706	11.327	.125	36.168	.0145	3.359
18	.163	1.37	1.04	.474	.902	1.757	.926	.755	12.110	.115	32.688	.0145	3.356
18	.158	.89	.89	.363	.691	1.309	.901	.874	14.026	.095	25.056	.0145	3.428
18	.156	.73	.83	.320	.609	1.255	.980	.893	14.329	.091	22.080	.0145	3.444
19	.164	1.76	1.15	.467	1.068	1.995	1.067	.708	11.363	.127	38.712	.0121	3.333
19	.163	1.60	1.10	.439	1.003	2.040	1.162	.700	11.238	.127	36.336	.0121	3.358
19	.160	1.34	1.03	.396	.904	1.897	1.199	.726	11.652	.120	32.760	.0121	3.398
19	.154	.82	.85	.291	.664	1.444	1.242	.832	13.358	.099	24.072	.0121	3.476
19	.114	.32	.51	.191	.437	1.563	2.003	.800	12.838	.096	15.840	.0121	4.247

PAGE SIX

SERIES NO.	FR	RE	RED	SIGMA	D/B	F	CD	1/SQRTF	CHEZY C	N	D/K	LAMBDA	D/YC
20	.120	1.84	.95	1.049	1.331	5.250	1.251	.436	7.005	.213	46.240	.0218	4.117
20	.120	1.67	.92	.986	1.251	4.929	1.250	.450	7.230	.204	45.336	.0218	4.118
20	.118	1.36	.65	.865	1.098	4.486	1.296	.472	7.578	.191	39.792	.0218	4.161
20	.116	1.07	.78	.744	.944	3.907	1.313	.506	8.120	.173	34.200	.0218	4.195
20	.113	.42	.56	.405	.513	2.041	1.262	.700	11.233	.113	18.600	.0218	4.280
25	.109	2.16	4.93	.600	1.286	7.015	2.921	.378	6.060	.245	11.060	.0543	4.376
25	.110	1.94	4.77	.552	1.182	6.238	2.626	.400	6.426	.226	10.166	.0543	4.346
25	.112	1.68	4.59	.496	1.061	5.577	2.814	.423	6.796	.212	9.130	.0543	4.302
25	.113	1.38	4.31	.434	.930	4.696	2.705	.461	7.406	.190	7.998	.0543	4.292
25	.106	.91	3.61	.342	.732	4.318	3.157	.481	7.724	.175	6.300	.0543	4.461
26	.142	2.93	6.46	.615	1.316	4.700	1.912	.461	7.403	.201	11.326	.0543	3.685
26	.141	2.65	6.24	.577	1.236	4.497	1.949	.472	7.569	.195	10.630	.0543	3.697
26	.141	2.18	5.65	.507	1.085	3.949	1.949	.503	8.076	.179	9.334	.0543	3.693
26	.142	1.68	5.38	.424	.908	3.377	1.991	.544	8.734	.160	7.811	.0543	3.681
26	.142	.91	4.38	.283	.605	2.276	2.013	.663	10.639	.123	5.208	.0543	3.688

PAGE SIX

SERIES NO.	FR	RE	RED	SIGMA	D/B	F	CD	1/SQRTF	CHEZY C	N	D/K	LAMBDA	D/YC
20	.120	1.84	.95	1.049	1.331	5.250	1.251	.436	7.005	.213	46.240	.0218	4.117
20	.120	1.67	.92	.966	1.251	4.929	1.250	.450	7.230	.204	45.336	.0218	4.118
20	.118	1.36	.85	.865	1.098	4.486	1.296	.472	7.578	.191	39.792	.0218	4.161
20	.116	1.07	.78	.744	.944	3.907	1.313	.506	8.120	.173	34.200	.0218	4.195
20	.113	.42	.56	.405	.513	2.041	1.262	.700	11.233	.113	18.600	.0218	4.280
25	.109	2.16	4.93	.600	1.286	7.015	2.921	.378	6.060	.245	11.060	.0543	4.376
25	.110	1.94	4.77	.552	1.182	6.238	2.626	.400	6.426	.228	10.166	.0543	4.346
25	.112	1.66	4.59	.496	1.061	5.577	2.814	.423	6.796	.212	9.130	.0543	4.302
25	.113	1.38	4.31	.436	.930	4.696	2.705	.461	7.406	.190	7.998	.0543	4.292
25	.106	.91	[illegible]	.342	.732	4.318	3.157	.481	7.724	.175	6.300	.0543	4.461
26	.142	2.93	6.45	.615	1.316	4.700	1.912	.461	7.403	.201	11.326	.0543	3.685
26	.141	2.65	6.24	.577	1.236	4.497	1.949	.472	7.569	.195	10.630	.0543	3.697
26	.141	2.16	5.85	.507	1.085	3.949	1.949	.503	8.076	.179	9.334	.0543	3.693
26	.142	1.68	5.38	.424	.908	3.377	1.991	.544	8.734	.160	7.811	.0543	3.681
26	.142	.91	4.38	.283	.605	2.276	2.013	.663	10.639	.123	5.208	.0543	3.688

PAGE SEVEN

SERIES NO.	FR	RE	REB	SIGMA	D/B	F	CD	1/SQRTF	CHEZY C	N	D/K	LAMBDA	D/YC
27	.138	2.75	6.34	.565	1.252	4.829	2.065	.455	7.304	.202	10.772	.0543	3.746
27	.127	2.27	5.67	.543	1.162	5.217	2.403	.438	7.027	.208	10.002	.0543	3.957
27	.139	2.15	5.90	.495	1.061	4.037	2.036	.496	7.488	.180	9.125	.0543	3.737
27	.136	1.75	5.46	.432	.926	3.626	2.097	.525	8.429	.167	7.964	.0543	3.753
27	.140	1.26	4.95	.344	.736	2.365	1.734	.648	10.393	.130	6.334	.0543	3.716
28	.164	3.21	7.11	.523	1.239	3.220	1.538	.557	8.945	.165	11.304	.0463	3.343
28	.165	2.86	6.86	.480	1.145	2.910	1.504	.566	9.408	.155	10.446	.0463	3.335
28	.165	2.49	6.56	.439	1.041	2.638	1.501	.616	9.682	.145	9.492	.0463	3.327
28	.164	2.02	6.08	.384	.910	2.430	1.581	.641	10.295	.136	8.298	.0463	3.347
28	.164	1.42	5.41	.304	.720	1.705	1.402	.766	12.293	.110	6.564	.0463	3.346
29	.120	2.26	5.11	1.279	1.210	8.115	1.586	.351	5.634	.261	11.034	.1159	4.136
29	.122	2.06	5.03	1.185	1.121	7.311	1.543	.370	5.936	.244	10.224	.1159	4.077
29	120	1.78	4.74	1.088	1.030	6.338	1.456	.397	6.375	.224	9.390	.1159	4.120
29	120	1.45	4.41	.951	.900	5.593	1.470	.423	6.787	.206	8.208	.1159	4.136
29	.112	.97	3.70	.761	.720	3.947	1.297	.503	8.079	.167	6.564	.1159	4.310

PAGE EIGHT

SERIES NO.	FR	RE	REH	SIGMA	D/H	F	CD	1/SQRTF	CHEZY C	N	D/K	LAMBDA	D/YC
30	.158	2.97	6.73	.612	1.207	3.768	1.539	.515	8.268	.178	11.010	.0556	3.436
30	.161	2.56	6.50	.547	1.078	3.309	1.513	.550	8.823	.163	9.834	.0556	3.358
30	.161	2.15	6.13	.468	.963	2.908	1.488	.586	9.413	.150	8.784	.0556	3.394
30	.163	1.57	5.56	.393	.774	2.325	1.480	.656	10.527	.130	7.062	.0556	3.368
30	.139	.42	3.24	.162	.359	1.460	2.004	.828	13.282	.090	3.276	.0556	3.741
31	.164	3.21	3.42	.284	1.285	2.897	2.554	.588	9.430	.157	23.436	.0121	3.342
31	.164	2.61	3.19	.247	1.120	2.547	2.575	.627	10.057	.144	20.436	.0121	3.349
31	.164	2.12	2.97	.215	.976	2.297	2.666	.660	10.591	.134	17.796	.0121	3.350
31	.159	1.55	2.63	.179	.810	2.132	2.981	.685	10.993	.125	14.772	.0121	3.422
31	.151	.92	2.13	.131	.591	1.676	3.209	.773	12.399	.105	10.768	.0121	3.542
32	.211	4.75	4.66	.308	1.395	1.711	1.390	.765	12.270	.123	25.440	.0121	2.841
32	.206	3.93	4.32	.275	1.247	1.534	1.394	.807	12.957	.114	22.740	.0121	2.866
32	.205	3.25	4.04	.244	1.104	1.368	1.404	.855	13.720	.105	20.136	.0121	2.880
32	.202	2.44	3.63	.203	.921	1.075	1.322	.965	15.480	.091	16.800	.0121	2.909
32	.200	1.73	3.22	.163	.738	.977	1.499	1.012	16.237	.083	13.464	.0121	2.932
32	.194	1.13	2.73	.125	.566	.778	1.557	1.134	18.200	.071	10.320	.0121	2.992

PAGE NINE

SERIES NO.	FR	RE	REB	SIGMA	D/R	F	CR	1/SQRTF	CHEZY C	N	D/W	LAMBDA	D/YC
33	.198	4.31	5.41	.375	1.364	1.965	1.508	.713	11.449	.131	19.901	.0189	2.948
33	.195	3.63	5.12	.335	1.217	1.741	1.295	.758	12.165	.121	17.760	.0189	2.948
33	.196	2.90	4.75	.294	1.068	1.570	1.334	.798	12.811	.112	15.581	.0189	2.967
33	.192	2.17	4.22	.243	.883	1.354	1.392	.859	13.791	.101	12.883	.0189	3.014
33	.189	1.54	3.73	.195	.707	1.114	1.430	.948	15.208	.088	10.320	.0189	3.038
33	.184	.94	3.10	.143	.518	.894	1.567	1.058	16.978	.075	7.555	.0189	3.100
34	.150	3.66	4.32	.401	1.457	4.503	2.805	.471	7.564	.200	21.264	.0189	3.548
34	.151	3.49	4.09	.356	1.293	3.893	2.733	.507	8.135	.183	16.864	.0189	3.535
34	.147	2.72	3.86	.332	1.207	3.952	2.973	.503	8.073	.182	17.606	.0189	3.593
34	.151	2.24	3.67	.267	1.043	3.352	2.916	.546	8.766	.164	15.226	.0189	3.541
34	.147	1.52	3.16	.226	.820	2.607	2.687	.619	9.940	.139	11.962	.0189	3.596
34	.150	.92	2.72	.159	.578	1.739	2.732	.758	12.172	.107	8.429	.0189	3.557

PAGE TEN

SERIES NO.	FR	RE	REB	SIGMA	D/B	F	CD	1/SQRTF	CHEZY C	N	D/W	LAMBDA	D/YC
35	.137	1.61	2.29	.332	1.207	4.516	3.397	.471	7.553	.194	17.606	.0189	3.761
35	.138	1.63	2.31	.333	1.211	4.401	3.300	.477	7.651	.192	17.664	.0189	3.743
35	.139	1.64	2.32	.334	1.214	4.586	3.426	.467	7.494	.196	17.722	.0189	3.737
35	.139	1.61	2.31	.330	1.197	4.467	3.387	.473	7.594	.193	17.472	.0189	3.732
35	.138	1.51	2.25	.319	1.155	4.540	3.569	.469	7.533	.194	16.848	.0189	3.752
35	.138	1.27	2.12	.283	1.029	3.960	3.493	.503	8.065	.177	15.014	.0189	3.749
35	.138	.83	1.84	.213	.774	3.082	3.612	.570	9.143	.149	11.299	.0189	3.755
36	.191	2.39	3.14	.215	1.305	2.713	3.147	.607	9.745	.153	19.046	.0113	3.125
36	.192	2.37	3.13	.214	1.296	2.468	2.884	.636	10.216	.145	18.912	.0113	3.123
36	.180	1.79	2.84	.178	1.080	2.168	3.042	.679	10.899	.132	15.754	.0113	3.139
36	.179	1.66	2.76	.170	1.030	2.006	2.951	.706	11.331	.126	15.024	.0113	3.149
36	.176	1.33	2.55	.148	.895	1.975	3.343	.712	11.420	.122	13.056	.0113	3.167
36	.164	.83	2.07	.114	.689	1.651	3.627	.778	12.490	.107	10.061	.0113	3.337

APPENDIX C

NOTATION USED IN THIS REPORT

B Width of flume

b Width of element perpendicular to flow

C Chezy coefficient

C_d Drag coefficient of roughness element

C_f Loss coefficient due to form drag

C_s Loss coefficient due to surface resistance

C_w Loss coefficient due to surface wave

d Mean depth

F Force

F Froude number

F_f Form resistance

F_s Surface resistance

F_w Wave resistance

f Darcy-Weisbach resistance coefficient

f_e Modified friction factor from Darcy-Weisbach f, defined by

$$f_e = \frac{4R\ S_f}{V^2/2g}$$

g Gravitational constant

H Total head

k Length of element parallel to flow

ℓ Element spacing parameter, see Figure 4

N Number of elements

n Manning's roughness coefficient

P Wetted perimeter

Q Flow rate

R Hydraulic radius

$\mathbf{R}$ Reynolds number

S_f Energy gradient

S_o Slope of channel

s Element spacing parameter

s Element offsetting parameter

t Height of element

V Mean velocity of flow

x Distance in direction of flow

y Depth

y_c Critical depth

y_n Normal depth

Z_o Elevation of channel floor

α Coefficient

α_1 Coefficient

β Coefficient

β_1 Coefficient

γ Specific weight

ε y/y_c

ζ Channel plan factor

η Cross sectional shape factor

θ Channel profile factor

λ Density of roughness elements

μ Dynamic viscosity

ν Kinematic viscosity

ξ Roughness element shape factor

ρ Fluid density

σ Concentration of roughness elements

τ_d Shear stress due to drag

ϕ "Function of"

χ A roughness parameter dependent on size, shape and spacing of elements

GPO 891-522

FHWA

R&D